NOVEL INNERVATION PATHWAYS IN THE REGULATION OF BASAL FOREBRAIN NEURONS

Ph.D. Thesis

Zsuzsanna Bardóczi

János Szentágothai Doctoral School of Neuroscience

Semmelweis University

Supervisor:	Imre Kalló, M.D., Ph.D.
Official reviewers:	István Ábrahám, Ph.D., D.Sc., Habil Zsuzsanna Várnainé Tóth, Ph.D.
Head of the Final Examination Committee:	András Csillag, M.D., Ph.D., D.Sc.
Members of the Final Examination Committee:	Ádám Dénes, M.D., Ph.D. Dobolyi Árpád, Ph.D., D.Sc., Habil

Budapest
2018

TABLE OF CONTENTS

List of abbreviations

ACh - Acetylcholine

AChR - Acetylcholine receptor

AD - Alzheimer's disease

AHA - anterior hypothalamic area

Arc - arcuate nucleus

AVPV - anteroventral periventricular nucleus

BF - basal forebrain

BLA - basolateral nucleus of the amygdala

cAMP - cyclic adenosine monophosphate

ChAT - choline acetyltransferase

CNS - central nervous system

CTB - cholera toxin B

DA - dopamine

DAB - diaminobenzidine

DBB - diagonal band of Broca

Dyn - dynorphin

E2 - 17β-estradiol

EA - extended amygdala

EC - entorhinal cortex

EGFP - enhanced green fluorescent protein

ERα - estrogen receptor alpha

ERβ - estrogen receptor beta

FSH - follicle-stimulating hormone

GABA - gamma-aminobutyric acid

GABA-A - gamma-aminobutyric acid A receptor

GABA-B - gamma-aminobutyric acid B receptor

GlyR - Glycine receptor

GLYT1 - glycine transporter, type 1

GLYT2 - glycine transporter, type 2

GnRH - gonadotropin-releasing hormone

GP - globus pallidus

HDB - horizontal limb of the diagonal band of Broca

HPG - Hypothalamo-pituitary-gonadal

icv - intracerebroventricular

INF - Infundibular nucleus

InfS - Infundibular stalk

IR - immunoreactive

Kiss1R - Kisspeptin receptor

KNDy - Kisspeptin/Neurokinin B/Dynorphin

KP - Kisspeptin

LC - locus coeruleus

LDT - laterodorsal tegmental nuclei

LH - luteinizing hormone

LHA - lateral hypothalamus

LTP - long term potentiation

mAChRs - muscarinic acetylcholine receptor

MBH - mediobasal hypothalamus

MCH - melanin-concentrating hormone

MCPO - magnocellular preoptic nucleus

MPA - medial preoptic area

MS - medial septum

nAChRs - nicotinic acetylcholine receptor

NBM - nucleus basalis of Meynert

Ni-DAB - nickel-diaminobenzidine

NK3R - neurokinin B receptor

NKB - neurokinin B

NMDA - N-methyl-D-aspartate

NREM - non-rapid eye movement

OB - olfactory bulb

OVLT - organum vasculosum of the lamina terminalis

OVX - ovariectomized

PBS - phosphate buffered saline

PFA - paraformaldehyde

PFC - prefrontal cortex

PHDA - periventricular hypophysial dopaminergic

PPT - pedunculopontine

REM - rapid eye movement

RMg - raphe magnus nucleus

RP3V - rostral periventricular area of the third ventricle

POA - preoptic area

SCN - suprachiasmatic nucleus

SFO - subfornical organs

SGI-NiDAB - silver gold intesified nickel-diaminobenzidine

Si - substantia innominata

TH - tyrosine hydroxylase

THDA - tuberohypophysial dopaminergic

TIDA - tuberoinfundibular dopaminergic

TMN - tuberomammillary nucleus

VAChT - vesicular acetylcholine transporter

VDB - vertical limb of the diagonal band of Broca

VIP - vasoactive intestinal peptide

VLPO - ventrolateral preoptic nucleus

VP - ventral pallidum

ZT - zeitgeber time

1. Introduction

1.1. Organization of basal forebrain (BF)

The BF is located close to the medial and ventral surfaces of the cerebral hemispheres, to the front of and below the striatum. The main regions of the BF are: medial septum (MS), ventral pallidum (VP), diagonal band nuclei, substantia innominata (Si)/extended amygdala (EA), nucleus basalis of Meynert (NBM) and peripallidal regions. The BF contains a heterogeneous mixture of cell types: neuropeptide containing neurons [1] such as Gonadotropin-releasing hormone (GnRH)-immunreactive (IR) neurons, a heterogeneous collection of cholinergic, gamma-aminobutyric acid (GABA)-ergic, glutamatergic projection neurons, and various interneurons [2]. This highly complex brain region has been implicated in the regulation of reproduction, cortical activation, attention, motivation, memory, and neuropsychiatric disorders (i.e. Alzheimer's disease (AD), Parkinson's disease, schizophrenia, drug abuse) [3-11].

GnRH neurons form a unique cell population in the BF in that they are born in the olfactory placod and migrate during the embryonic development into the hypothalamus and BF areas [12]. In contrast, the BF cholinergic projection neurons and the other cell types, including GABAergic projection neurons and subsets of cortical and striatal GABAergic interneurons originate within the primordium of the ventral telencephalon (subpallium) [13].

According to the classical concept of the ascending arousal system [14], a major branch of the complex pathways from the rostral pons and caudal midbrain reaches the hypothalamus and the BF to activate these brain regions. The possible existence of an ascending inhibitory (glycinergic) pathway and local action of glycine in the BF have been indicated in previous studies from our laboratory [15, 16]; the expression of the glycine receptor (GlyR) alpha 1 subunit in GnRH neurons strongly suggests that glycine can directly influence GnRH neurons via GlyR. Also, we have confirmed the presence of membrane glycine transporter type 1 (GLYT1) and glycine transporter type 2 (GLYT2) in the BF regions indicating a role for glycine in the regulation of local neuronal populations.

The first part of my Ph.D. thesis addresses the issue of whether the GnRH and/or cholinergic neurons are targets of glycine signaling in the BF.

1.2. Cholinergic neurons in the BF

1.2.1. Distribution and projection of cholinergic neurons in the BF

Acetylcholine (ACh) is synthesized in nerve terminals from choline and acetyl coenzyme A by the cytoplasmic enzyme choline acetyltransferase [17] and transported into synaptic vesicles by the vesicular acetylcholine transporter (VAChT) [18]. Using antisera against ChAT represents a reliable marker for the study of cholinergic neurons in the central and peripheral nervous systems. Five main neuronal groups that contain the majority of central cholinergic neurons have been identified.

These include: (i) the efferent cranial nerve nuclei and motoneurons of the spinal cord; (ii) the parabrachial complex; (iii) the brainstem reticular complex; (iv) the neostriatal complex; and (v) the medial basal forebrain [19]. In my Ph.D. thesis, the focus is on the input of the BF cholinergic neurons.

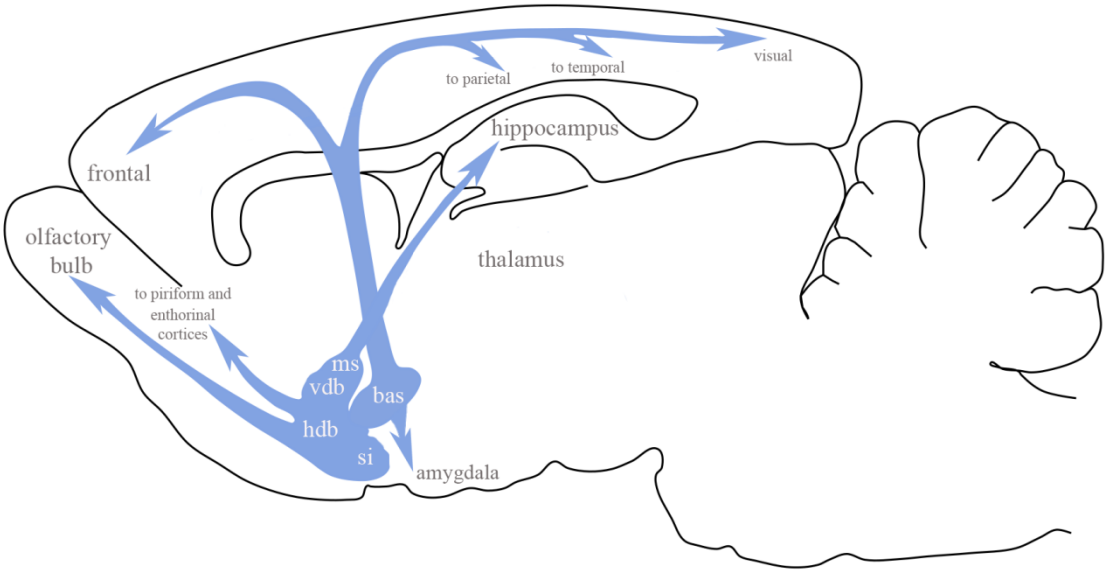

Fig. 1. *Schematic representation of the basal forebrain cholinergic neurons and their projection areas. bas=nucleus basalis; ms=medial septum; vdb=vertical diagonal band nucleus; hdb=horizontal diagonal band nucleus; si=substantia innominate. Modified from [20].*

Mesulam and his colleagues subdivided the BF cholinergic neurons into four major subgroups, which they designated Chl-Ch4. Ch1 subgroup consist of the medial septal cholinergic neurons. Ch2 subgroup contain the cholinergic neurons, which are located

in the vertical limb of the diagonal band (VDB). The Chl and Ch2 groups collectively provide the major cholinergic innervation of the hippocampus. The group of cholinergic neurons in the horizontal limb of the diagonal band (HDB) and magnocellular preoptic nucleus (MCPO) are termed as Ch3 subgroup of cholinergic neurons. The neurons from the Ch3 mainly project to the olfactory bulb, piriform, and entorhinal cortices. Cholinergic neurons within the VP, Si/EA, globus pallidus (GP), internal capsule, and nucleus ansa lenticularis, collectively termed the Ch4 subgroup, project to the basolateral amygdala, and innervate the entire neocortex according to a rough medio-lateral and antero-posterior topography (**Fig.1.**) [1, 21]. Cholinergic neurons in the MS/VDB, HDB and MCPO also innervate the orexin/hypocretin neurons in the lateral hypothalamus [22, 23].

1.2.2. Basic operation modes of BF cholinergic neurons

In the central nervous system (CNS), the BF cholinergic neurons release acethylcholine (ACh), which binds to the appropriate receptors on the postsynaptic target cells. The ACh effects depend on the presence of the AChR subtype(s) on the target, the cellular localization of the AChRs and the multiplicity of downstream signaling cascades that can be activated. AChRs are categorized based on their sensitivity to plant alkaloids and their binding capacity for muscarine or nicotine (mAChRs & nAChRs). Muscarinic AChRs are metabotropic receptors that bind ACh and transduce their signaling via activation of heterotrimeric G proteins that, in turn, affect the opening, closing, and kinetics of (primarily) K^+, Ca^{2+} and non-selective cation channels. In contrast to ACh interactions with mAChRs, binding of ACh to nicotinic AChRs results in the direct gating of non-selective cation channels. Twelve different types of nAChR subunits have been identified in the brain (α2–10 and β2–β4) [24].

Based on previous studies, ACh release is characterized classically as slow and tonic [25]. The anatomically diffuse cholinergic system and early microdialysis experiments that documented ambient levels of ACh at micromolar concentrations in brain tissue [25] suggest the “volume” mode of transmission.

This hypothesis has now been substantially revised by Sarter & colleagues [26]. Using more rapid assays for ACh release and new approaches for selective activation of

cholinergic neurons and their terminal fields, they find evidence for a faster and more focal ACh release and downstream signaling than previously considered [27, 28].

Záborszky and his colleagues supported these findings with a detailed electrophysiological characterization of the cholinergic neurons in the NBM. They identified two populations: a more excitable, early firing population that show spike frequency adaptation and a less excitable, late firing population that could maintain low frequency tonic firing [29]. The two phenotypes of cholinergic neurons may provide the cellular basis for two different modes of signaling: fast and focal and slow and paracrine. Taken together, it appears that these modes of ACh release play important roles in different aspects of information processing [28, 30].

1.2.3. BF cholinergic neurons as major targets of ascending reticular activating system (ARAS)

Forebrain activation and cortical arousal/waking behavior are thought to be critically influenced by ascending pathways deriving from the brainstem [31-38]. The role of the upper brainstem in forebrain arousal was demonstrated fifty years ago by Moruzzi and Magoun [39]. However, the specific structures that activate the forebrain have only been described recently.

The ascending arousal system has two major branches. One pathway originates from cholinergic cell groups in the upper pons, the pedunculopontine (PPT) and laterodorsal tegmental nuclei (LDT) and reaches the thalamus where it activates the thalamic relay neurons that are crucial for transmission of information to the cerebral cortex. The neurons in the PPT/LDT show most rapid firing during wakefulness and rapid eye movement (REM) sleep; the REM stage is characterized by concomitant cortical activation, loss of muscle tone in the body and active dreams [40]. These cholinergic cells are much silent during non-REM (NREM) sleep, when cortical activity is slow.

The other branch circumvents the thalamus and activates the cerebral cortex to facilitate the processing of inputs from the thalamus. This pathway originates from various monoaminergic cell groups, including the tuberomammillary nucleus (TMN) containing histamine, the A10 cell group containing dopamine (DA), the dorsal and median raphe nuclei containing serotonin, and the locus coeruleus (LC) containing noradrenaline. The input to the cerebral cortex is enhanced by lateral hypothalamic peptidergic neurons

(containing melanin-concentrating hormone (MCH) or orexin/hypocretin), and BF neurons (containing ACh or GABA). The monoaminergic neurons, which are part of this pathway, increase their firing rate during wakefulness, decrease firing activity during NREM sleep and stop altogether during REM sleep [41-43]. Orexin neurons in the LHA are, similarly, most active during wakefulness [44-46], whereas MCH neurons are active during REM sleep [47]. Many BF neurons, including most cholinergic neurons, are active during both wake and REM sleep [48].

However, other pathways also exist which, in turn, promote sleep. During the 1980s and 1990s, investigators found that a group of neurons located in the ventrolateral preoptic nucleus (VLPO) send outputs to all of the major cell groups in the hypothalamus and brainstem that participate in arousal [49]. The VLPO neurons are primarily active during sleep, and contain the inhibitory neurotransmitters, galanin and GABA [50-52]. They send output to monoaminergic neurons in the TMN, the A10 cell group, the raphe cell groups and the locus coeruleus LC. They also innervate the LHA, including the perifornical (PeF) orexin neurons, and interneurons of the brainstem cholinergic cell groups, the (PPT) and (LDT). The LC and DR play an important role in gating REM sleep [47, 53]. The VLPO neurons also innervate the histaminergic neurons, which are involved in the transitions between arousal and NREM sleep [53-55].

1.2.4. Potential role of cholinergic output to forebrain centers

ACh is reponsible for attention [56, 57], arousal [58-60], learning and memory [61, 62] and the sleep-wake cycle [60, 63, 64]. It is thought that the effect of ACh depends on its target areas [56, 65].

In rats, cholinergic neurons that project to the cerebral cortex are dispersed throughout the BF within the nuclei of the diagonal band of Broca (DBB), MCPO, Si and GP [66, 67]. They compose the extrathalamic relay from the brainstem activating system to the cerebral cortex [39, 68], where they potently excite cortical neurons and stimulate cortical activation [69-71]. Release of ACh is in close association with cortical activation during the states of waking and paradoxical sleep [72-75]. The cholinergic neurons are more active during wakefulness and REM sleep (wake/REM active) than during NREM sleep, as are the glutamatergic and parvalbumin-positive GABAergic neurons, which are also distributed in the BF. Optogenetic activation of these neurons rapidly induces

wakefulness, contrasting with somatostatin-positive GABAergic neurons, the stimulation of which promotes NREM sleep [76]. However, chemogenetic activation of BF cholinergic or glutamatergic neurons in behaving mice has no effect on total wakefulness. In contrast, similar chemogenetic activation of BF GABAergic neurons produces sustained wakefulness and high frequency cortical rhythms [77].

The cholinergic neurons, which are located in the NBM and DBB, project to the prefrontal cortex (PFC) [78-80]. The PFC is an integral node in circuits underlying attention and ACh modulates these processes. Attention consists of two separate processing streams: goal or cue driven attention is known "top down" while sensory driven attention is known "bottom up" [81, 82]. Basically, top down attention is considered as voluntary, or "feed-back" driven, thus incoming sensory information is processed by higher cortical areas. However, bottom up attention is considered as involuntary, or "feedforward", thus sensory information is fed forward and up to the cortex [81, 82]. Enzyme selective microelectrode studies confirmed that ACh in the PFC modulates the cue detection and cue triggered changes in goal-oriented behavior [83, 84]. Taken together, both the beginning and the end of the attention loop are mediated by ACh and initiate the top down control over downstream sensory cortical areas.

Cholinergic neurons also modulate the sensory cortex related to attention. During the attentional performance of a behavioral task, ACh decorrelates intracortical noise in sensory cortices, which is often measured as "desynchronization" or decreased power of low frequency local field potential (LFP). Decorrelation increases the response reliability of sensory cortex neurons to the appropriate stimuli [85, 86].

Cholinergic innervation from the MS and DBB to the hippocampus plays an important role in the formation of spatial memories: elevated ACh level have been confirmed by microdialysis in the hippocampus during performance of various memory tasks [87-89]. At the circuit level, several lines of studies of memory suggest that ACh, acting via both nicotinic and muscarinic AChRs (nAChRs and mAChRs), is important for the initiation of long-term potentiation (LTP), a synaptic substrate of memory. In the hippocampus cholinergic signaling both promotes LTP and regulates cognition associated oscillatory activity. Theta rhythm phase can both regulate the possibility that LTP is initiated and determine whether stimulation will generate synaptic potentiation or depression [90]. Oscillations are known to isolate the signal of encoding from retrieval actions, the

differentiation that is crucial for memory as the status of these oscillations at the onset of a behavioral task presumes learning success [91].

The medial septal cholinergic neurons also send axons to the entorhinal cortex (EC). The EC plays an important role in processing and conveying spatial information to the hippocampus. Optogenetic studies revealed that the septal cholinergic neurons modulate EC neurons in layer specific manner, via nAChRs and mAChRs. Selective lesions of septal cholinergic neurons or their optogenetic activation have indicated that ACh plays an important role in regulating theta rhythmic activity in the hippocampus, thereby augmenting the dynamics of memory encoding [92-95].

Furthermore, a dense projection of the BF cholinergic neurons reaches the basolateral nucleus of the amygdala (BLA), which is a subcortical limbic structure [2]. While ACh mediates the spatial memory in the hippocampus, it consolidates the emotionally salient memories in the amygdala [20, 96]. Optogenetically stimulated cholinergic neurons in the amygdala enhance emotionally salient memories, and optogenetic inhibition decreases them: both nAChRs and mAChRs play a role in these processes [97].

Cholinergic neurons, which are lying in the HDB, innervate the olfactory bulb (OB) [98, 99]. The layered architecture of the OB, and its function as a relay between odor input and higher cortical processing, make it possible to examine how sensory information is processed at synaptic and circuit levels. The OB receives also strong neuromodulatory inputs, in part from BF cholinergic system. Cholinergic axons regulate the activity of various cells and synapses within the OB, especially the numerous dendro dendritic synapses, resulting in highly variable responses of OB neurons to odor input that is dependent on the behavioural state of the animal. Behavioral, electrophysiological, anatomical, and computational studies provide evidence for the involvement of mAChRs and nAChRs in the actions of ACh in the OB [100].

Taken together, BF cholinergic neurons represent a heterogeneous cell population (Ch1-Ch4; [21]) with different projection areas, and they have been implicated in arousal, sleep-wake cycle, attention, memory and olfactory processes. Thus, it is very important to define which BF cholinergic subgoups are regulated by glycine.

1.3. GnRH neurons in the BF

1.3.1. General morphology of the GnRH neurons

GnRH is synthesized and secreted from a relatively small population of neurons, the majority of which is located in mice and rats in the preoptic area (POA) of the hypothalamus; these cells represent the central regulators of reproductive functions and fertility. GnRH neurons do not develop from the neural tube; they originate from the nasal placodes and migrate prenatally along the olfactory sensory axons to the cribriform plate (E13.5) and then, to the BF areas (E16.5). From birth through adulthood, these neurons do not form a well-defined nucleus, but are scattered from the rostral POA to the caudal hypothalamus [12].

The number of GnRH neurons in mice is low (~800) [101]. Most GnRH neurons exhibit a fusiform, bipolar morphology with two processes, which originate from opposite sides of the soma. Unipolar or multipolar morphology also appear in a smaller percentage [102]. Furthermore, the GnRH processes have also dendritic spines, filopodium-like structures and cilia. Campbell and colleagues examined 45 biocytin-filled GnRH neurons in mice and they observed the highest density of dendritic spines on the proximal part (mostly on the first 50 μm) of the dendrite, which likely indicates the location of the majority of excitatory synaptic inputs [102-104]. Recently, a relatively high density of afferents were detected on distal processes of GnRH neurons in the vicinity of median eminence [105]. Approximately half of the GnRH neurons have filopodia, which are involved in synaptogenesis by locating and guiding appropriate axons back to the dendrite [102, 106-108]. GnRH neurons possess also multiple cilia [109, 110], which contain signaling molecules, including certain G protein-coupled receptors (GPCRs); these receptors may sense different neuromodulators in the extracellular space. The cilia of GnRH neurons express Kisspeptin receptor (Kiss1R), suggesting that the cilia may also play a role in kisspeptin (KP)-mediated increases in GnRH neuron firing rate [111].

GnRH neurons have long processes (over 1000 μm), which mostly project to the ME. Between 50% and 70% of all GnRH neurons throughout the BF project to the median eminence [112-114]. Interestingly, these processes have a spike initiation site and conduct action potentials to the median eminence. They also receive simultaneously and integrate synaptic inputs along the complete length of the processes, thus regulating the

excitability of the neuron. These processes have axon- and dendrite-like properties, thus nowadays they are termed as „dendrons" [115].

Varicose axons, in addition to these dendrons, have also been observed [116]. Often they emanate from the thick dendron-like processes, and form synapses in the rostral periventricular area of the third ventricle (RP3V) and arcuate nucleus (Arc) as we have shown [117].

1.3.2. Distribution of GnRH cell bodies

The GnRH neurons are distributed from the olfactory bulbs to the medial septal nuclei and POA, ventral aspects of the anterior hypothalamic area (AHA) and mediobasal hypothalamus (MBH). The pattern of the distribution forms an inverted "Y": the rostral-most midline GnRH cell bodies in the MS dividing at the beginning of the third ventricle within the rostral POA to form the two arms of the inverted "Y" that extend back into the ventral AHA and MBH. Although this continuum can be found in all mammals, there are species differences in the distribution of GnRH neurons along this pathway [109]. In rats, one group of the GnRH neurons is distributed in septal areas as well as in the medial septal nucleus, and in the vertical and horizontal limbs of the diagonal band of Broca and near to the organum vasculosum of the lamina terminalis (OVLT). Another group of GnRH-neurons is found in the medial preoptic area. Furthermore, fewer GnRH neurons are located in the periventricular portion of the preoptic nucleus, in the bed nucleus of the stria terminalis and in the lateral preoptic area. Caudal to the septal-preoptic area, GnRH perikarya are observed in the anterior and ventrolateral hypothalamus, but absent from the medial basal hypothalamus/Arc. Some can be found also in different parts of the hippocampus (indusium griseum, CA3 and CA1 fields of Ammon's horn) and in the piriform cortex [116].

In human and monkeys, GnRH cell bodies reside more caudally, as they are most concentrated in the ventral and basal hypothalamus. They extend their processes ventrally to the median eminence and infundibular stalk and caudally to the mammillary complex [118].

1.3.3. Hypothalamo-pituitary-gonadal (HPG) axis

Most of the GnRH processes terminate in the external zone of median eminence, where GnRH is secreted in the hypothalamo-hypophysial portal bloodstream, which carries it to the anterior pituitary gland. GnRH acts on the GnRH receptors, which are present on the gonadotrope cells and stimulates the release of luteinizing hormone (LH) and follicles stimulating hormone (FSH).

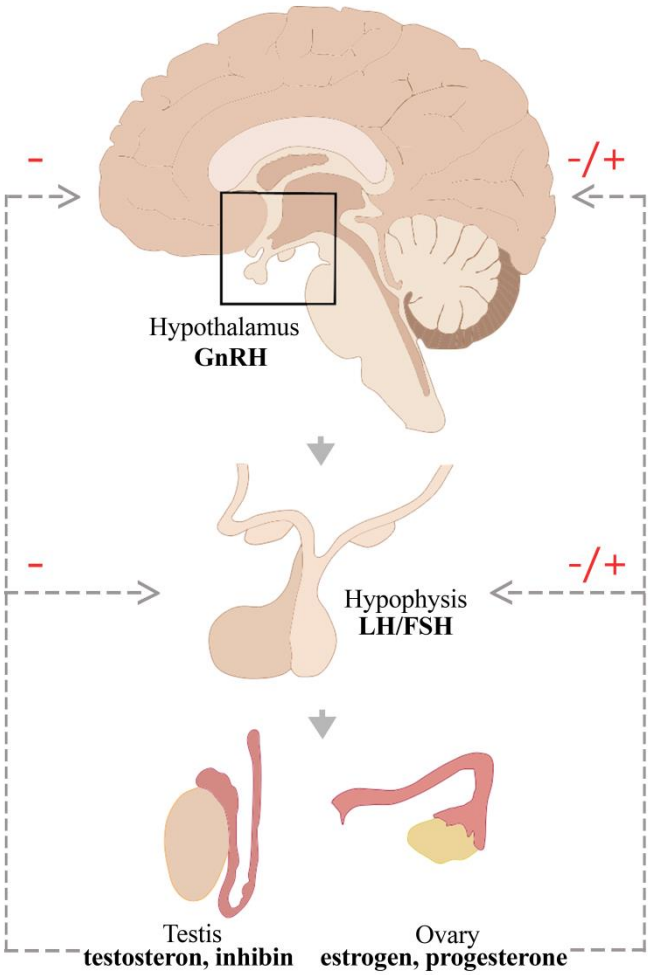

Fig. 2. *The schematic drawing of the HPG axis. Hypophysiotropic GnRH is released by the hypothalamus and stimulates the secretion of gonadotropins (LH and FSH) from the hypophysis. LH and FSH act on the gonads and the gonadal steroids and peptides regulate the functions of the HPG axis by negative (in males and females) and positive (only in females) feedback mechanisms. (FSH: follicle stimulating hormone, GnRH: gonadotropin-releasing hormone, LH: luteinizing hormone). Modified from [119].*

Low-frequency pulses of GnRH result in release of FSH, whereas high-frequency pulses of GnRH preferentially trigger LH release [120]. Thus, the gonadotropes convert the hypothalamic signal (GnRH) to a systemic response (the release of FSH and LH) regulating fertility. LH and FSH are released into the systemic circulation and act on the gonads. In males, LH stimulates testosterone production from Leydig cells, whereas FSH stimulates the spermatogenesis in the Sertolli cells, which produce inhibin. In females, LH promotes the ovulation as well as corpus luteum formation and function, whereas FSH triggers ovarian follicle formation as well as estrogen secretion. The gonadal steroids (estrogen, progesterone and testosterone) and the peptide hormone (inhibin) exert feedback effects, acting centrally to influence GnRH secretion and at the pituitary to influence gonadotrope responsiveness to GnRH (**Fig. 2.**) [121]. In both males and females, the gonadal steroids exert negative feedback effects on the hypothalamo-pituitary unit. In reproductively active females, preceding the time of ovulation, estradiol feedback switches from negative to positive action, triggering the LH surge.

1.3.3.1. Operation modes (pulsatile and surge) of the GnRH neurons and the underlying electrophysiological events in GnRH neurons

In humans, the reproductive cycle, called the menstrual cycle, lasts approximately 28 days, while in rodents this cycle, called the estrous cycle, lasts approximately 4-5 days. The estrous cycle in mice and rats can be divided into 4 stages: proestrus, estrus, metestrus and diestrus [122].

For most of the cycle (during estrus, metestrus and diestrus), the secretion pattern of GnRH is pulsatile characterized by small amplitude and hourly release. The plasma circulation of LH and FSH and plasma concentration of estradiol (E2) are low [123]. The pulsatility of GnRH release is essential for the synthesis and secretion of pituitary gonadotropins and hence the maintenance of normal reproductive function in mammals [124]. Preceding the time of ovulation, at the end of the follicular phase (in proestrus), this pattern turns into a non-pulsatile surge with large amplitude, a few hours lasting release [125-128]. The GnRH surge in turn, evokes the pituitary LH surge that subsequently initiates ovulation. Similarly, in various laboratory animal species, the

secretion pattern of GnRH correlates with the pulsatile secretion of LH in the peripheral blood [129-132].

A subpopulation of GnRH neurons exhibit burst firing in acute brain slice preparations. Another population is silent, whereas a further smaller cell group exhibits continuous activity [133, 134]. Bursts are comprised of two to several action potential spikes and intraburst frequency varied from ~2–25 Hz. Interburst period varies from a few to many seconds both within and among cells [134-138]. These patterns are observed in gonadectomized as well as intact male and female mice throughout the estrous cycle [133, 134, 139]. During burst firing GnRH neurons use typical combinations of T-type calcium currents (IT), calcium-activated potassium currents of the afterhyperpolarization (IKCa), persistent sodium currents and sodium currents of the afterdepolarization (IsADP) and hyperpolarization-activated non-specific cation currents (Ih) [130, 140-142].

During the positive and negative feedback effects of estradiol, synaptic and intrinsic changes are observed in the GnRH neurons. Using the ovariectomized (OVX) and estradiol (E2) treated model, Moenter and her colleagues have shown that during negative feedback, the GnRH neuron activity is suppressed, with reduced GABAergic and glutamatergic transmission and reduced whole-cell calcium current in the background [143-145]. In contrast, during positive feedback, GnRH neuron activity is increased together with the GABAergic transmission and whole-cell calcium currents [143, 144].

1.3.3.2. The "GnRH Pulse generator" – Intrinsic vs. extrinsic features of the network

The pulsatile release of GnRH is essential for normal reproductive function and fertility. The term 'GnRH pulse generator' has been used to describe the central neuroendocrine oscillator since the 1980s. Since the Arc contains the largest population of GnRH neurons in primates it was postulated that the network of GnRH neurons establish the endogenous pulse-generating mechanism [146-148]. Studies on immortalized GnRH neurons [149-152] also supported this view by revealing that cultured GnRH cells are capable of synchronized oscillation of intracellular calcium ion concentrations ($[Ca^{2+}]i$) at a frequency similar to that of pulsatile GnRH release [153, 154]. However, the

evidence for inherent pulsatility of GnRH neurons does not necessarily exclude the hypothesis for the existence of an external GnRH pulse generator.

Results of several rodent experiments employing deafferentations and lesions indicated that the GnRH pulse generator is localized in the Arc [155-158]. This was rather suprising since no or very few GnRH cells are located in the rat or mouse Arc. Ohkura and his colleagues examined the effect of various types of hypothalamic deafferentation on the LH secretion in ovariectomized rats. They found that anterior, anterolateral or complete hypothalamic deafferentation did not affect the frequency of LH pulses. However, when these investigators cut off the anterior part of the Arc from the MBH, the LH pulses became irregular, indicating that an extrinsic GnRH pulse generator is located in the MBH [159].

The discovery of the role of KP and its receptor, Kiss1R, in hypogonadotropic hypogonadism [17, 160] attracted the attention of the neuroendocrinologist to study the exact role of the KP system in the function of GnRH neurons. There are two major populations of KP neurons located in the POA occupying the anteroventral periventricular nucleus (AVPV) and the Pe (recently called as the rostral periventricular area of the third ventricle; RP3V) and the Arc (see more details in the next chapter), respectively. Despite the evidence that GnRH neurons can synchronize their activity autonomously, the fact that Kiss1R mutations impair reproductive function suggest that GnRH neurons are not the only players. Similarly to the Arc lesions [158], the intra-Arc infusion of a Kiss1R antagonist [161] can also interrupt the pulsatile secretion of LH suggesting that KP neurons, constitute at least a part of the neural substrate of the GnRH pulse generator.

Although GnRH neurons are likely able to independently generate a synchronous rhythm, a GnRH pulse generator existing within the Arc is responsible for fine-tuning the oscillatory activity of GnRH neurons in response to diverse regulatory signals [124, 162, 163].

1.3.3.3. The surge mode of GnRH secretion – Integration of estrogen- and circadian signals in the regulation of GnRH secretion

In rodents, interaction of the estradiol and circadian inputs triggers the LH surge. The LH surge is timed to specific hours of the day, it occurs late afternoon (beginning 1.5 h

before the lights off and lasts between 16.00-19.00) in nocturnal species [125, 164, 165]. Using OVX+E2 models, electrophysiological recordings in the afternoon (4–7:30 p.m.) have shown an increased mean firing rate and instantaneous firing frequency of GnRH neurons compared with cells recorded in the morning (from 10 a.m. to 1:30 p.m.). OVX alone caused no time-of-day differences. These findings provide evidence that the estradiol and circadian inputs act together on LH release and differences in pattern of GnRH neuron firing may reflect the switch in estradiol action and underlie GnRH surge generation [125].

While nocturnal rodents have their LH surge in the afternoon of proestrus, humans exhibit the LH surge in the early morning. In both species, this coincides with the beginning of the active phase [166].

The circadian information is conveyed by the suprachiasmatic nucleus (SCN). The ventrolateral part of the SCN sends vasoactive intestinal peptide (VIP)-positive afferents to GnRH neurons [167-169] and ~40% of GnRH neurons express the VIP receptor (VPAC2) [170]. It is important to note that electrophysiological examinations have shown that VIP neurons have a time-of-day- and estradiol-dependent excitatory effect on a subpopulation of GnRH neurons; the mean firing rates of approximately half of GnRH neurons are increased by VIP from ovariectomized, estradiol-treated female mice but only when recorded between 14:00 and 16:00 h [171]. In addition, the SCN delivers the circadian information to the GnRH neurons via an indirect pathway. The SCN afferents innervate the AVPV neurons, which express ERα [167, 172] and the cyclic adenosine monophosphate (cAMP) levels within the AVPV neurons change with the circadian rhythm in rat [173]. Using tract tracing and anatomical studies, Vida and her colleagues identified vasopressin-containing axons of SCN origin in apposition to KP-immunoreactive (IR) neurons in the RP3V [174]. As RP3V KP neurons express ERα, they may integrate both the circadian and the estrogenic signals, and convey these information to GnRH neurons.

For most of the cycle estradiol has a suppressive, negative feedback effect on gonadotropin secretion. However, in proestrus, this negative effect switches to a positive feedback, which induces the GnRH surge. Estrogens' feedback actions are mediated predominantly via ERα [175-180], since null mutant mice for these receptors do not show normal regulation of the GnRH/LH axis or LH surges [181] and are infertile [182].

ERα is absent from the GnRH neurons [183]. Therefore, the ERα- signal to GnRH neurons is likely indirect and mediated by ERα positive afferents. Such afferent neurons are located in RP3V [184], as well as within the MBH [180]. The phenotypes of these ER-expressing cells in the RP3V may be GABA [185, 186], glutamate [187] or both amino acid transmitters[188] as well as neuropeptides such as neurotensin [189] or KP [190-192].

The absence of ERα from GnRH neurons, however, does not exclude the possibility for estogens to influence directly the function of GnRH neurons. They express functional ERβ receptors (ERβ mRNA [193, 194] and protein [195, 196] as it was shown for rats and mice [194]). ERβ in these cells was implicated in rapid nongenomic estrogen effects on intracellular signaling [197-199]. Studies have shown that estradiol rapidly phosphorylates cAMP response element binding protein (CREB) [200], increases intracellular calcium concentrations [201] and changes the firing rate [201-203] the inhibitory or excitatory effects reported was dependent upon the dose of estradiol applied [202].

1.3.4. Kisspeptin (KP) neurons forming a major input to GnRH neurons

Since its discovery in 2003, there is a growing number of studies about the role of KP in regulation of GnRH function. Kiss1R can directly regulate GnRH neurons and complete KP- or Kiss1R deletion in transgenic mice results in infertility associated with hypogonadotropism and absence of puberty and ovarian cyclicity in adulthood [17, 160, 191, 204-206]. As mentioned in the previous chapter, their major subpopulations are located in the Arc and the RP3V. More than 90% of KP neurons in both the RP3V and Arc express ERα, [207], which suggests that they play important roles in estradiol feedback regulation of GnRH release.

1.3.4.1. KP neurons in the rostral periventricular area of the third ventricle (RP3V) – role in surge generation

Estradiol differentially regulates KP expression of the two KP cell populations; in the RP3V [208-212] ovariectomy reduces and estradiol-replacement increases KP expression. KP neurons exhibit estradiol-regulated currents determining their intrinsic excitability [213]. On the basis of cFos expression, RP3V KP neurons are activated at

the time of surge onset in parallel with that of the GnRH neurons [190-192]. Furthermore, the RP3V KP neurons send projections that innervate GnRH-IR neurons [214, 215] thus, they have the capacity to convey critically important estrogen-dependent signals to GnRH neurons. It has been hypothesized that the RP3V KP cell population mediates the positive-feedback effect of estrogen on GnRH neurons and thereby contributes to the generation of the GnRH surge [177, 180, 190, 191, 216-218]. These areas also contain tyrosine hydroxylase immunoreactive (TH-IR) neurons, which play location-specific roles in the neuroendocrine control of both the luteinizing hormone and prolactin secretion, as well as in sexually motivated behaviors. Furthermore, in the RP3V, KP neurons co-localize with TH. The presence of TH in this neuronal population indicates dopamine synthesis in these neurons [219-221].

1.3.4.2. KP neurons in the arcuate nucleus (Arc) – the extrinsic pulse generator

In contrast to the RP3V, in the Arc ovariectomy increases and estradiol reduces KP expression [208-212]. Investigations have shown that the postovariectomy increase in LH secretion is blunted in GPR54 knockout mice [222] as well as in rats in which KP neurons of the Arc have been deleted nucleus-specifically with saporin [223]. Based on these observations, it was speculated that KP neurons in the Arc mediate the negative feedback of estrogen on GnRH secretion [223] and influence the episodic release of GnRH.

In addition, KP cells co-express NKB and Dyn in the Arc; therefore, they were named ‘KNDy’ neurons (Kisspeptin/Neurokinin B/Dynorphin) [224, 225]. Recent studies suggested that KNDy neurons in the Arc play an important role in driving episodic GnRH secretion. More than 90% of these neurons receive input from other KNDy neurons, thus forming an interconnected network which enables them to fire synchronously [163, 226]. KNDy neurons communicate with each other via NKB and its receptor (NK3R), and also Dyn and its receptor (Dyn/κ-opioid receptor), whereas they do not express Kiss1R. KNDy neurons contain NK3R and administration of an NK3R agonist increased multiple-unit activity [47] [163]. In contrast to NKB, Dyn dampens and eventually terminates KNDy neural activity and thus, GnRH pulse. KNDy axons directly innervate the perikaryon and dendrites of GnRH neurons [214] and

communicate primarily via KP/Kiss1R signaling. Indeed, the majority of GnRH neurons express Kiss1R [227-229] and respond to KP with increased neuronal activity [230]. The optogenetic activation of Arc KP neurons in male and in diestrous and ovariectomized mice, evokes LH pulses [231].

The hypothalamic dopaminergic neurons maintain an inhibitory control on prolactin-secreting cells in the hypophysis [232]; this tonic effect is important for the pulsatile secretion of GnRH, since a reduction of dopamine secretion during lactation results in an increased prolactin level, and consequently, suspension of the pulsatile secretion of GnRH [233, 234]. In contrast to the RP3V KP neurons, the Arc KP and TH cells appear to form completely distinct subpopulations. The preoptic TH-IR neurons termed as the A14-15 dopaminergic cell groups whereas dopaminergic neurons in the Arc form the A12 cell group. These dopaminergic neuron populations establish local connections, as well as distinct terminal fields in the pituitary gland. Based on the rostro-caudal distribution of the dopaminergic perikarya and their terminal fields, three anatomically and functionally different systems (i.e. tuberoinfundibular dopaminergic (TIDA), tuberohypophysial dopaminergic (THDA) and periventricular hypophysial dopaminergic (PHDA) are distinguished. TIDA neurons are located mostly in the dorsomedial part of the Arc (A12) and project to the external zone of the median eminence where dopamine is released into the perivascular space surrounding the capillary loops of the pituitary portal system. THDA neurons are found in the rostral Arc (A12) between the previous two cell groups and project to both the intermediate and the neural lobe of the pituitary gland. The PHDA neurons (A14-A15) are located in the AVPV and the Pe and terminate in the intermediate lobe. Furthermore, in the Arc, the KP neurons receive a massive innervation from TH cells (and vice versa), which may contribute to the suspension of the pulse generator during lactation [235, 236].

1.3.5. Projection areas of GnRH neurons - neuronal output to preoptic/hypothalamic centers

GnRH neurons form the final common pathway for the hypothalamic neuronal circuitry that regulates gonadal functions. However, GnRH not only drives the anterior pituitary gland functions that govern ovarian steroidogenesis, follicular maturation and ovulation, but also acts as a neuromodulator within the brain [118, 237].

The majority of the axons originating from the GnRH cells in the medial septal and preoptic-suprachiasmatic regions form the septo-preoptico-infundibular tracts. These axons terminate mainly in the median eminence to control pituitary release of gonadotropins. Furthermore, approximately 20% of all rostral POA GnRH neurons project to the OVLT and 85% of these projections may be involved in the GnRH surge mechanism (**Fig.3. A**-**B**) [238]. Thus, the majority of the GnRH processes project beyond the blood–brain barrier and sense the blood constituents such as hormones, glucose or other metabolic substrates [239]. Besides the GnRH processes, the OVLT receives dense innervation from axons containing several other different neuropeptides and neurotransmitter, such as thyrotropin-releasing hormone, somatostatin, dopamine, norepinephrine, serotonin, ACh, oxytocin and vasopressin [240]. It is possible that the GnRH neurons match fertility levels in the OVLT to the homeostatic status of the individual [241, 242]. However, the exact role of GnRH-IR fibers in the OVLT remains to be clarified.

The GnRH neurons send also processes to the subfornical organs (SFO), which is another circumventricular organ [238]. The SFO is located in the roof of the third ventricle below the fornix. It is known to be a critical regulator of fluid homeostasis and also contributes to blood pressure regulation [243-245]. However, the exact role of GnRH processes in the SFO is unknown.

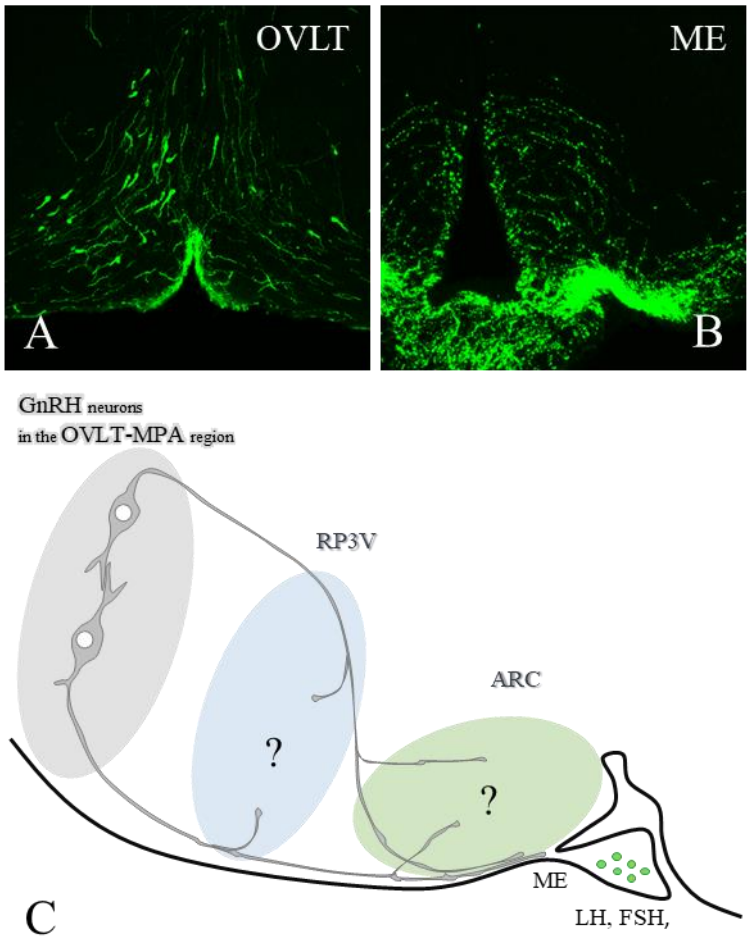

Fig.3. *Distribution and projection of GnRH neurons in mouse brain. The GnRH cell bodies are mainly located in OVLT-medial preoptic area [246] region (**A**) and send processes to the main terminal fields, the OVLT and the external zone of median eminence (ME) (**B**). Schematic drawing illustrates that the GnRH neurons, from the OVLT-MPA region, project to the median eminence and send axonal branches to the RP3V and Arc forming putative synaptic connections with neuronal populations (**C**). Modified from [247].*

In the medial septal-preoptic regions, the GnRH cells send fibers in dorsal direction, gives off collaterals and returns to its own or to other perikarya apparently to form axosomatic connections. This observation may provide the morphological basis for a connected syncytium, which might help synchronize the GnRH neuron population.
Furthermore, the GnRH neurons, from the septal-preoptic and suprachiasmatic regions, project also through classical efferent pathways such as the stria terminalis, stria

medullaris thalami, stria longitudinalis medialis and lateralis, fimbria hippocampi, fasciculus retroflexus, medial forebrain bundle, and posterior commissure and target several other brain regions. Fibers from the medial septal and preoptic regions pass through the dorsomedial hypothalamus and compose a periventricular subependymal GnRH network that serves as the origin of the extrahypothalamic projections. Fibers pass through the Arc, as well [248]. In my studies, we focused on these fibers forming synaptic contacts on different target cell population in the RP3V and Arc (**Fig.3. C**). Scattered GnRH fibers are seen in the mammillary complex, raphe nuclei, medial nucleus of the amygdala, medial habenular nuclei, and ventral tegmental area. In addition to these nuclei, the GnRH processes make up a dense plexus around the aqueductus cerebri in the mesencephalic central gray. Moreover, GnRH neurons from the MS, the nucleus of diagonal band, the olfactory tubercle and the medial surface of the hemispheres reach the medial layers of the olfactory bulb. GnRH neurons also send axons to several areas outside the nervous tissue such as the subarachnoidal space or the ventricular lumen [248].

There is evidence that central administration of GnRH can inhibit the reproductive axis in sheep [249, 250] and rats [251, 252]. Electrophysiological recording of spontaneously active neurons of the Arc revealed that GnRH (10 nM-10 pM) administered adjacent to the infundibular recess significantly altered the firing frequency of unidentified neurons. Predominantly excitatory responses were detected [253]. Results of these previous studies suggest that the GnRH neurons can influence directly the function of certain neurons in the AVPV and the Arc.

Previous anatomical studies have identified putative sites for central actions of GnRH. GnRH-IR axon projections are detected in the preoptic area (i.e. AVPV) [116, 118, 254] and in the MBH [118, 254], including the Arc (**Fig.3. C**).

These previous findings prompted us to study, whether GnRH neurons project to the KP- and TH-IR cells and form synaptic connections with them. Using a correlated light- and electron microscopic immunohistochemical approach, we examined the putative connections between GnRH processes and KP- and TH-IR neurons in both the RP3V and the Arc.

1.4. Potential role of a glycinergic input to BF neurons

In the central nervous system, the two main inhibitory amino acids are glycine and γ-aminobutyric acid (GABA). These neurotransmitters activate the strychnine sensitive glycine receptors and GABAA receptors, respectively, which permit chloride influx through the postsynaptic membrane to hyperpolarize postsynaptic neurons. GABAergic neurotransmission is almost ubiquitous in the mammalian CNS, whereas glycinergic neurons are mainly restricted to the spinal cord and brainstem [255, 256]. It is therefore not surprising that our knowledge on the contribution of GABAergic neurons to defined neuronal circuits is much more detailed than the available information about glycinergic neurons. This has changed when the glycin transporter transgenic animals have been generated [257]. GLYTs, depending on their location, have distinct functions at glycinergic synapses. GLYT2 provides glycine for the refilling of presynaptic vesicles of glycinergic neurons [258], whereas GLYT1 ensures the removal of glycine from the synaptic cleft into glial cells, leading to the termination of glycine-mediated neurotransmission. In addition, GLYT1 is also present in certain glutamatergic neurons and regulates the concentration of glycine at excitatory synapses containing NMDA receptors, which are known to require glycine as a coagonist [259]. Using the GLYT2-GFP mice and immunohistochemistry, we detected the presence of membrane GLYT1 and GLYT2 in the mouse BF, suggesting a potential role for glycine in this region [15].

Only the use specific antisera against GLYT2, which is a reliable marker for glycinergic neurons in the CNS [260] and is concentrated primarily in the glycinergic fibers, has made it possible to visualize the projections. Zeilhofer and his colleagues generated the bacterial artificial chromosome (BAC) transgenic mice that express enhanced green fluorescent protein (EGFP) specifically in glycinergic neurons under the control of the GLYT2 promoter [257]. This transgenic mouse line made the mapping of the cell bodies, thus the source of glycinergic projections to BF areas, possible.

Glycine has a complex role in the central nervous system. Glycine acts on strychnine-sensitive glycine receptors (GlyRs), which mostly cause Cl^- influx, hyperpolarizing thereby the neuron to inhibit its activity.

Glycine is also able to act as an excitatory neurotransmitter. On the one hand, in the developing CNS, the intracellular Cl^- concentration is high compared to the extracellular space. Binding to the GlyRs causes Cl^- to spill out from the cell, causing a strong depo-

larization and neurotransmitter release, instead of hyperpolarization [261]. Studies have shown that, this phenomenon exists also in mature neurons [22, 262]. Glycine binding to the GlyR generates depolarizing response instead of hyperpolarization due to the increased intracellular Cl^- concentration [263]. On the other hand, glycine also acts on the N-methyl-D-aspartate (NMDA) receptor as a coagonist and, as such, facilitates excitatory neurotransmission [264].

Our previous studies confirmed the presence of the GlyR alpha 1 subunit mRNA in GnRH neurons by microarray examinations [16]. Furthermore, GnRH neurons express functional ionotropic GABA-A receptors [265-269] and GABA-B [270] receptors, but the response of GnRH neurons to activation of GABA receptors is controversial. Mature GnRH neurons maintain high intracellular chloride concentrations, which can result in excitatory responses to GABA-A-R activation in adult mice [265, 267] and rats [271, 272]. However, many studies suggest that GABA exerts an inhibitory effect on GnRH/LH release [273-275]. Most GnRH neurons (about 80-100%) express α-amino-3-hydroxy-5-methyl-4-isoxazolepropionic acid [246] receptors, whereas only a small subpopulation (∼20%) have NMDA receptors [136, 268, 276, 277].

The BF cholinergic neurons receive GABAergic input [278] and they are inhibited by GABA via GABA-A receptors [279]. Furthermore, the cholinergic neurons also contain NMDA receptor subunits [280].

Taken together, these observations raise the possibility that glycine acts directly on GnRH and cholinergic neurons. One of the possible effects is, depolarization or hyperpolarization via GlyR (depending on the intracellular Cl^- concentrations). The other possibility is that, glycine binds to NMDA receptors as coagonist and excites the GnRH and cholinergic neurons.

Thus, using immunohistochemistry we addressed whether the GnRH and cholinergic neurons contain the GlyR and receive direct input from GLYT2-IR fibers. We examined the presence of GLYT1-IR profiles in the vicinity of GnRH and cholinergic neurons and we also tested the direct effect of glycine on these neurons by electrophysiological recordings.

2. Aims:

2.1. Investigating potential target cells of glycine in the BF

2.1.1. GlyR in GnRH and cholinergic neurons

2.1.2. GLYT2-IR afferents to GnRH and cholinergic neurons

2.1.3. Source of glycinergic fibers in the BF

2.1.4. GLYT1-IR astrocytic processes in the vicinity of GnRH and cholinergic neurons.

2.1.5. Membrane potential properties of GnRH and cholinergic neurons in the presence of glycine

2.2. Characterization of GnRH efferents and their target cells in mice and humans

2.2.1. Ultrastructural features of GnRH processes in mice

2.2.2. KP-KP contacts in mice and human

2.2.2. Effects of circadian, hormonal and lactation-related changes on the GnRH input to KP- and TH-IR neurons in mice

3. Materials and Methods

3.1. Mouse brain samples

3.1.1. Brain tissue collected for immunohistochemical processing

Wild-type (CD1, Charles River) and transgenic mice (1–3 month-old, 25–30 g body weight) were housed under controlled lighting (12 h light/dark cycle; lights on at 7:00 A.M.), and temperature (22°C) conditions with access to food and water ad libitum. The list of animal models used in the different experiments is summarized in **Table I.** below. Five to six virgin animals were kept in a single cage, whereas pregnant and postpartum mothers were individually housed. A group of animals were ovariectomized (OVX, day 0) and 7 days later (day 7) implanted subcutaneously with a capsule (ID 1.57 mm, OD 3.18 mm) containing either 17β-estradiol (0.625 μg in 20 μl sunflower oil; OVX+E2) or vehicle (OVX+Oil) [125]. Three days after implantation (day 10), mice were colchicine-treated (intracerebroventricularly 40 μg in 4 μl 0.9% saline) and 24 h later (day 11) they were sacrificed at either zeitgeber time [281] 4–5 or ZT11–12; these times include, respectively, the negative and positive feedback phases of oestrogen's effects on LH release [125]. Surgery was performed on animals under deep anesthesia induced by an intraperitoneally injected cocktail of ketamine (25 mg/kg body weight), Xylavet (5 mg/kg body weight), and Pipolphen (2.5 mg/kg body weight) in saline. All studies were performed with permission from the Animal Welfare Committee of the Institute of Experimental Medicine (No. 2285/003), the Debrecen University (No. 6/2011/DE MÁB and 5/2015/DEMÁB), the Eötvös Loránd University (PEI/001/37-4/2015) and in accordance with legal requirements of the European Community (Decree 86/609/EEC).

3.1.2. Mouse models used in the different experiments

For our experiments, we used different mouse models and surgeries, which are summarized in **Table I.** below.

Table I. *Mouse models, surgeries and their experiments.*

Strain and Genotype /Sex	***Age and Number***	***Sugery/Treatment***	***Used in Experiment/ Results***
CD1 WT/♂♀	1-3 month-old, n=69	∅	(4.1.2.); (4.1.4.); (4.2.6.)
CD1 WT ♀	1-3 month-old, n=10	OVX + oil	(4.2.1.); (4.2.4.); (4.2.6.)
CD1 WT ♀	1-3 month-old, n=10	OVX + E2/EB	(4.2.1.); (4.2.2.); (4.2.4.); (4.2.5.); (4.2.6.)
C57BL/6J GnRH-GFP ♀	1-3 month-old, n=3	∅	(4.1.1.)
C57BL/6J ChAT-GFP ♂	1-3 month-old, n=3	∅	(4.1.1.)
C57BL/6J GLYT2-GFP ♂	1-3 month-old, n=12	Cholera toxin B (CTB) and Fluoro-Gold injection	(4.1.3.)

3.1.3. Acute slices collected for electrophysiological examination

For electrophysiological experiments, we used two mouse line. The technical details are summarized in **Table II**. below.

Table II. *The mouse acute brain slices.*

Strain and Genotype/Sex	***Age and Number***	***Surgery/ Treatment***	***Used in Experiment/Results***
C57BL/6J GnRH-GFP pro-estrus ♀	1-3 month-old, n=3	∅	(4.1.5.)
C57BL/6J ChAT-GFP ♂	1-3 month-old, n=26	∅	(4.1.5.)

3.2. Human brain tissue samples

Human hypothalami were collected at autopsy from the 1st Department of Pathology and Experimental Cancer Research, Semmelweis University, Budapest, Hungary, and the Department of Pathology, Saint Borbála Hospital, Tatabánya. Three-four hours after death, the brains were removed from the skull of a 77-year-old (SKO5) and a 71-year-old (SKO8) female subject and a 55-year-old male individual (SKO7) who died from causes not linked to brain diseases (SKO5, SKO8: heart failure; SKO7: pulmonary embolism). Ethic permissions were obtained from the Hungarian Medical Research Council /ETT TUKEB 33268-1/2015/ EKU (0248/15) and 31443/2011/EKU (518/PI/11)/ and from the Regional and Institutional Committee of Science and Research Ethics of Semmelweis University (SE-TUKEB 251/2016), in accordance with the Hungarian Law (1997 CLIV and 18/1998/XII.27. EÜM Decree/).

3.3. Preparation of mouse and human sections for light microscopic studies

The mice to be used for light- and confocal microscopic studies, were perfused transcardially, first with phosphate buffered saline (PBS) solution (10 ml 0.1M PBS; pH 7.4) and then with PBS containing 4% paraformaldehyde [237] (100 ml 4% PFA in 0.1M PBS). The brains were post-fixed in 2% PFA/PBS solution for 24h at 4 °C, cryoprotected overnight in 25% sucrose. Serial 30-μm thick coronal sections were cut with a Leica SM 2000R freezing microtome (Leica Microsystems, Nussloch Gmbh, Germany). The sections were divided into three sequential pools and stored in antifreeze solution (30% ethylene glycol; 25% glycerol; 0.05 M phosphate buffer; pH 7.4) at –20 °C until use.

Hypothalamic tissue blocks were dissected from the brain of three postmenopausal women (aged 53-88) within 24 h after death. The subjects had no history of neurological or endocrine disorders. The tissues were rinsed briefly with running tap water and then, immersion-fixed with 4% PFA in 0.1 M PBS (PBS; pH 7.4) for 10 days. The tissue blocks were infiltrated with 20% sucrose and cut serially either at 30 or at 100 μm thickness with a freezing microtome.

After the endogenous peroxidase activity had been quenched with 0.5% H_2O_2 (10 min), sections were permeabilized with 0.5% Triton X-100 (catalog #23,472-9, Sigma-Aldrich; 20 min). Finally, 2% normal horse serum (NHS) was applied (for 20 min) to reduce nonspecific antibody binding. Subsequent treatments and interim rinses in PBS

(3X for 5 min) were performed at room temperature, except for the incubations in the primary antibody or fluorochrome conjugates, which took place at 4°C.

3.4. Preparation of mouse and human sections for electron microscopic studies

Mice were perfused first with PBS (10 ml, 0.1M; pH 7.4), then a mixture of 2% PFA and 4% acrolein. Brains were postfixed in 2% PFA/PBS solution for 24h at 4 °C. 30-µm thick coronal sections were cut with a Leica VTS-1000 Vibratome (Leica Microsystems, Wetzlar, Germany) and treated with 1% sodium borohydride (30 min), 0.5% H_2O_2 (15 min) and permeabilized with three freeze-thaw cycles, as described previously [174].

Human tissue samples from elderly subjects were shown previously to contain high levels of KP immunoreactivities ((Hrabovszky, 2014; Rometo, Krajewski, Lou Voytko, & Rance, 2007). The internal carotid and vertebral arteries were cannulated, and the brains were perfused first with physiological saline (1.5 L for 30 min) containing 5 mL Na-heparin (5000 U/mL), followed by a fixative solution (3–4 L for 2.0–2.5 h) containing 4% PFA, 0.05% glutaraldehyde, and 0.2% picric acid in 0.1 M phosphate buffer (PB; pH = 7.4). The hypothalami were dissected out and postfixed overnight in 4% PFA without glutaraldehyde. Fifty-micrometer-thick coronal sections were prepared from the hypothalami with a Leica VTS-1000 Vibratome (Leica Microsystems, Wetzlar, Germany).

2% normal horse serum (NHS) was applied (for 20 min) to reduce nonspecific antibody binding. Subsequent treatments and interim rinses in PBS (3X for 5 min) were performed at room temperature, except for incubation in the primary antibody which took place at 4°C.

After immunohistochemical detection of tissue antigens, the labelled mice and human sections were treated with 1% osmium tetroxide (1 h) and 2% uranyl acetate (in 70% ethanol; 40 min), dehydrated in an ascending series of ethanol and acetonitrile, and flat-embedded in TAAB 812 medium epoxy resin between glass microscope slides precoated with a liquid release agent (#70880; Electron Microscopy Sciences, Fort Washington, Pa., USA). The resin was allowed to polymerize at 56 °C for 2 days.

3.5. Single- and multiple labeling of tissue antigens for confocal analyses

Sections of mice or humans were incubated for 72 h in a single primary antibody or a cocktail of two or three primary antibodies (KP, GlyR, GFP, CTB, GnRH, TH). The antigen-antibody complexes were detected by incubating the sections in corresponding FITC-, CY3-, or CY5-conjugated secondary antibodies (12h). In the case of GlyR, the signal was amplified by using biotinylated tyramide (BT) and Alexa Fluor 594 fluorochrome bound to streptavidin in the immunohistochemical procedure. For studying KP contacts in the human INF, FITC-tyramide was employed to amplify the signal. The immunofluorescent sections were mounted onto glass slides from 0.1 M Tris–HCl buffer (pH 7.6) and cover slipped with an aqueous mounting media, Mowiol (M1289 Sigma, [282]. Technical details are summarized in **Table III.** below.

Table III. *Details of single- and multiple labeling for confocal microscopic analysis.*

Used in Experiment/Results	***Primary Antibodies used***	***Secondary Antibodies used***	***Signal Amplification employed***
(4.2.3.)	sheep anti-KP (GQ2)	Biot-Dk-anti-sheep IgG (Jackson, 1:1,000)	ABC/FITC-tyramide
(4.1.1.)	guinea pig anti-GlyR (#105-136aa) and rabbit anti-GFP (#AB10145)	Biot-Dk-anti-gp IgG (Jackson, 1:1,000) and Biot-Dk-anti-rabbit IgG (Jackson, 1:1,000)	ABC/BT/STA-Alexa Fluor 594
(4.1.3.)	goat anti-CTB (#103) and rabbit anti-GFP (#AB10145)	CY3-Dk anti-goat IgG (Jackson, 1:2,000) and FITC-Dk anti-rabbit IgG (Jackson, 1:1,000)	∅
(4.2.6.)	guinea-pig anti-GnRH (#1018), rabbit anti-KP (#566) IgG and chicken anti-TH (#TYH)	FITC-Dk anti-guinea pig IgG (Jackson, 1:1,000), CY3-Dk anti-rabbit IgG (Jackson, 1:2,000) and CY5-Dk anti-chicken IgG (Jackson, 1:1,000)	∅

3.6. Single- and dual labeling for light- and electron microscopy

Sections of mice or humans were single or double labelled for light- and electron microscopic examinations. The sections were incubated (72 hours) concurrently in the primary antibodies. This was followed by visualization of the KP-, GlyR-, GnRH-, GLYT2-, GLYT1-IR structures by incubating the sections sequentially in appropriate biotinylated secondary antibody (12 h) and then Vectastain ABC Elite solution (1: 1,000, 1.5 h). The peroxidase reaction was carried out in the presence of H_2O_2 and nickel-diaminobenzidine (NiDAB), and post-intensified with silver-gold (SGI-NiDAB) [196]. After this reaction, the KP-, TH-, GnRH-, ChAT-IR structures were detected by incubating sections sequentially in appropriate biotinylated secondary antibody (1 day) and then, Vectastain ABC Elite solution (1: 1,000; 1.5 h) and the peroxidase reaction was carried out in the presence of H_2O_2 and diaminobenzidine (DAB) alone. For light-microscopic examinations, the sections were mounted onto glass slides and cover slipped with Depex mounting medium (EMS Cat. #13514,[283]). For electron microscopic examinations, the sections were dehydrated and embedded in epoxy resin (see above). The technical details are summarized is **Table IV**. and **Table V**. below.

Table IV. *Details of single- and dual labeling for light- and electron microscopic analysis.*

Used in Experiment/Results	***Primary Antibodies used***	***Secondary Antibodies used***	***Visualization***
(4.2.3.)	sheep anti-KP (GQ2)	Biot-Dk-anti-sheep IgG (Jack-son, 1:1,000)	SGI-NiDAB
(4.1.1)	guinea-pig anti-GlyR (#105-136aa)	Biot-Dk-anti-gp IgG (Jackson, 1:1,000)	SGI-NiDAB
(4.2.5.)	guinea-pig anti-GnRH (#1018) and rabbit anti-KP (#566)	Biot-Dk-anti-gp IgG (Jackson, 1:1,000) and Biot-Dk-anti-rabbit IgG (Jackson, 1:1,000)	SGI-NiDAB and DAB
(4.2.5.)	guinea-pig anti-GnRH (#1018) and chicken anti-TH (#TYH)	Biot-Dk-anti-gp IgG (Jackson, 1:1,000) and Biot-Dk-anti-chicken IgG (Jackson, 1:1,000)	SGI-NiDAB and DAB
(4.1.2.)	rabbit anti-GLYT2 (#N30aa) and guinea-pig anti-GnRH (#1018)	Biot-Dk-anti-rabbit IgG (Jackson, 1:1,000) and Biot-Dk-anti-gp IgG (Jackson, 1:1,000)	SGI-NiDAB and DAB
(4.1.2.)	rabbit anti-GLYT2 (#N30aa) and goat anti-ChAT (#AB144P)	Biot-Dk-anti-rabbit IgG (Jackson, 1:1,000) and Biot-Dk-anti-goat IgG (Jackson, 1:1,000)	SGI-NiDAB and DAB
(4.1.4.)	goat anti-GLYT1 (#AB1770) and guinea-pig anti-GnRH (#1018)	Biot-Dk-anti-goat IgG (Jackson, 1:1,000) and Biot-Dk-anti-gp IgG (Jackson, 1:1,000)	SGI-NiDAB and DAB
(4.1.4.)	goat anti-GLYT1 (#AB1770) and goat anti-ChAT (#AB144P)	Biot-Dk-anti-goat IgG (Jackson, 1:1,000) and Biot-Dk-anti-goat IgG (Jackson, 1:1,000)	SGI-NiDAB and DAB

Table V. *List of Primary antibodies used for single- and multiple-labeling of tissue antigens.*

Antiserum used	***Host species***	***Working Dilution***	***Source***
anti-KP antibody	sheep	1: 20,000	GQ2, [284]
anti-KP antibody	rabbit	1:100,000	#566, from Alan Caraty [285]
anti-GnRH antibody	guinea-pig	1:600,000	#1018, from Erik Hrabovszky, [286]
anti-TH antibody	chicken	1:1,000	#TYH, (Aves Laboratories Inc.)
anti-GLYT2 antibody	rabbit	1 mg/ml	#N30aa, from Masahiko Watanabe, [287]
anti-ChAT antibody	goat	1:1,1500	#AB144P-1ML, (Millipore)
anti-GLYT1 antibody	goat	1:10,000	#AB1770, (Millipore)
anti-GFP antibody	rabbit	1:2,500	#AB10145, (Millipore)
anti-GlyR antibody	guinea-pig	1 mg/ml	#105-136aa, from Masahiko Watanabe, [287]
anti-CTB antibody	goat	1:2,000	#103, List Biological Lab.

3.7. Tract-tracing to identify glycinergic afferents to BF neurons

The tract-tracing experiments are summarized in **Table VI.** below.

Table VI. *Detalis of tract-tracing experiments.*

Tracer used	***Injection parameters***	***Visualization of antigen-antibody complexes/Dilution***
CTB (0,5% solution)	The following stereotaxic coordinates were used, respectively, with reference to the bregma (B) planes: MS: anteroposterior, +0.61 mm; mediolateral, +0.0 mm; dorsoventral, -4 mm; HDB: anteroposterior, +0.37 or +0.02 mm; mediolateral, +0.80 or +1.40 mm; dorsoventral, -4.90 or -5.00 mm (Paxinos, 2013); and VP/SI: anteroposterior, +0.13 mm; mediolateral, +1.20 mm; dorsoventral, -4.25 mm. CTB was injected via unilateral iontophoresis (5 μA, 7 s on-off) into the BF for 20 min.	FITC-conjugated donkey anti-rabbit IgG (Jackson, 1:1,1000)
Fluoro-Gold (2.5–5.0%)	The following stereotaxic coordinates were used, respectively, with reference to the bregma (B) planes: MS: anteroposterior, +0.61 mm; mediolateral, +0.0 mm; dorsoventral, -4 mm; HDB: anteroposterior, +0.37 or +0.02 mm; mediolateral, +0.80 or +1.40 mm; dorsoventral, -4.90 or -5.00 mm (Paxinos, 2013); and VP/SI: anteroposterior, +0.13 mm; mediolateral, +1.20 mm; dorsoventral, -4.25 mm. Fluoro-Gold was injected via unilateral iontophoresis (5 μA, 7 s on-off) into the BF for 20 min.	-

3.8. Immunohistochemical controls

The specificities of the ChAT, GLYT1, GLYT2, GlyR primary antisera have been reported previously, thus controls included preabsorption of the ChAT antibody with the corresponding protein antigen [288], immunoblot confirmation of GLYT2 and GlyR bands at the expected molecular weight in samples of transfected cells and mouse brain tissue [287], and detection of GLYT1 mRNA signal in brain sections in comparative distribution to GLYT1 immunoreactivity [289].

The ChAT and GLYT2 antibody labeling did not reveal structures other than those detected by transgenic eGFP fluorescence expressed under the promoter of ChAT or GLYT2. The specific binding of the panαGlyR antibody to the glycine receptors was confirmed by a second, α2 subunit specific antiserum (Santa Cruz Biotechnology Cat# sc-17279 Lot# RRID: AB_2110230) detected in the same distribution in the BF. Increasing dilutions of the primary antisera resulted in a commensurate decrease and eventual disappearance of the immunostaining; omission of the primary antibodies or their preabsorption with corresponding peptide antigens resulted in complete loss of the immunostaining. The secondary antibodies employed here were designed for multiple labeling and pre-absorbed by the manufacturer with immunoglobulins from several species, including the one in which the other primary antibody had been raised.

The specificities of the GnRH, TH and KP primary antisera were reported previously [284, 285, 290, 291]. Negative controls included the use of increasing dilutions of the primary antisera, which resulted in a commensurate decrease and eventual disappearance of the immunostaining. Omission of the primary antibodies or their preabsorption with corresponding peptide antigens ((1 μM KP10 (NeoMPS, Strasbourg, France) for #566 antiserum [285], 5μg/ml KP54 (Phoenix Pharmaceuticals, Inc., Burlingame, CA) for GQ2 [292] resulted in complete loss of the immunostaining. Besides negative controls, positive controls were also carried out (by employing well-characterized reference antibodies) to validate the staining patterns generated by the GnRH, TH and KP antibodies. Thus, three sets of sections were dual-immunolabeled by using the guinea pig anti-GnRH, the chicken anti-TH and the sheep anti-KP antisera with the following reference antibodies: rabbit anti-GnRH (LR1 from R.A. Benoit), mouse anti-TH (#22941 from Immunostar) and rabbit anti-KP (#566 from A. Caraty), respectively. By employing two different fluorochromes, the test antisera generated overlapping signals with the

reference antibodies for each antigen. Secondary antibodies were designed for multiple labeling and pre-absorbed by the manufacturer with immunoglobulins from several species, including the one in which the other primary antibody had been raised.
In the case of GQ2 KP antiserum, in control experiments, combined use of the sheep GQ2 KP antiserum and one of two reference KP antibodies (KISS1 AAS26420C or KISS1 AAS27420C; Antibody Verify) raised in rabbits resulted in dual labeling of nearly all KP-IR structures, serving as proof for the specificity of the KP signal [293].

3.9. Microscopy and data analysis

3.9.1. Correlated light- and electron microscopy

The flat-embedded sections were initially investigated by light microscopy at 60x magnification. The black color of SGI/Ni-DAB-labeled structures were easily distinguishable from the brown, DAB-labeled structures and made the selection of potential contact sites possible in flat-embedded sections. Areas exhibiting appositions of GLYT1-, GLYT2- or GnRH-IR processes on the somatodendritic region of ChAT-, GnRH-, KP- or TH-IR neurons were further processed. Semithin (1 μm) and ultrathin (50–60 nm) sections were cut with a Leica Microsystems ultracut UCT ultramicrotome. The ultrathin sections were collected in ribbons onto Formvar-coated single slot grids, contrasted with 2% lead citrate and examined with a Jeol 100 C Transmission Electron Microscope. The contact sites were identified in serial ultrathin sections. The two distinct electron dense markers enabled also the electron microscopic identification of pre- and postsynaptic elements.

3.9.2. Confocal laser microscopy

Regions of interest (ROI; 50589 μm^2) containing TH-IR neurons in the periventricular regions of the POA (3-6 ROI/Bregma levels to cover the entire area) and Arc (3-7 ROI/Bregma levels) were scanned (to a depth of 19-20 μm) in one side of the selected three sections of the POA or Arc regions. Each perikaryon showing TH- and/or KP-immunoreactivities and receiving GnRH afferent(s) has been recorded. Appositions (defined by the absence of any visible gap between the juxtaposed profiles in at least one optical slice) and immunoreactive perikarya were numbered. Both perikaryal and

dendritic appositions were counted; dendrites were considered only if their connections to the perikaryon was traceable. To avoid double counting of perikarya or appositions, immunoreactive profiles appearing repeatedly in the overlapping parts of neighboring Z-stacks or neighboring optical slices of the Z-stacks were identified and encoded with the same number.

3.9.3. Mapping and quantification

KP-immunopositive or KP-immunonegative TH-IR cell populations, and TH-immunonegative KP-IR neurons were distinguished in the POA and named as KP^-/TH^+, KP^+/TH^+, KP^+/TH^-, respectively. In accordance with previous studies, the TH-IR neurons in the Arc were immunonegative for KP. The percentage of neurons immunoreactive either for TH or KP, or for both TH and KP, and the percentage of GnRH appositions on each of these neurons in the POA were determined and comparisons made for the different models by means of one-way ANOVA, with the post hoc Tukey HSD test. The mean number of GnRH appositions on the different phenotype of cells were also determined. This approach made comparisons between the preoptic and arcuate TH-IR cell populations possible by using two-way ANOVA, with the post hoc Tukey HSD. Statistical significance was defined at $p<0.05$.

To identify the source of glycinergic input to the BF, the retrograde tracers CTB or Fluoro-Gold were injected into the MS, HDB, VP and SI of mice expressing GFP under the control of GLYT2 promoter. Although the distribution of retrogradely labeled GFP-positive neurons varied from brain to brain depending on the exact location and size of injection sites, there were brainstem areas and nuclei commonly labeled for the tracer.

4. Results

4.1. Examination of glycinergic input to BF neurons

4.1.1. Subnucleus and cell-specific appearance of glycine receptors (GlyRs) in the BF

Using a pan-GlyR antibody, immunoreactive puncta were detected in all subdivisions of BF and septal-preoptic area. The VP showed the weakest pan-GlyR immunoreactivity; no obvious difference could be observed in the intensity of staining in the MS, VDB/ HDB, SI, NBM and septal-preoptic area. The deposited immunohistochemical reaction product often delineated cellular borders even in weakly labeled areas (**Fig. 4. A–C**).

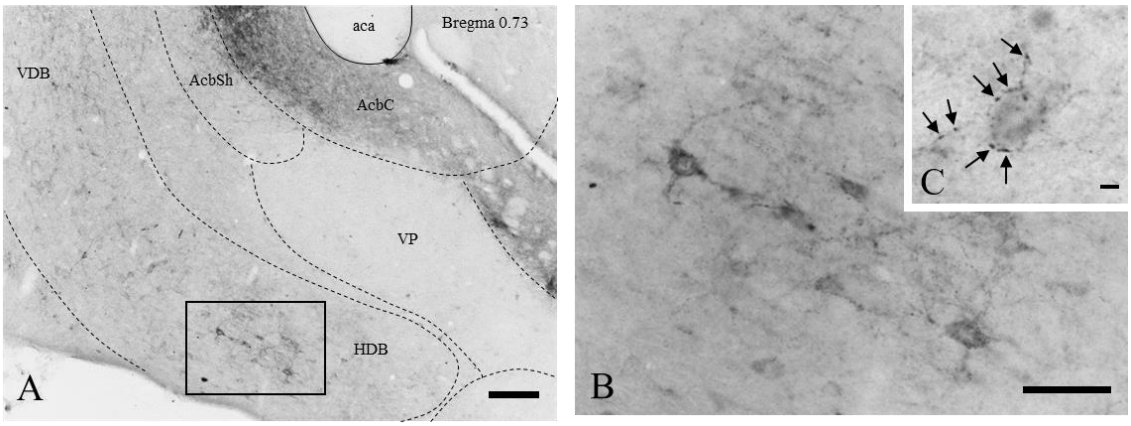

Fig. 4. *Distribution of GlyR-IR sites in the basal forebrain detected by a pan-GlyR antibody (**A**). The punctate appearance of GlyR-immunoreactivity (revealed by NiDAB) often delineates cellular borders in the strongly labeled accumbens core, in the medium labeled HDB, as well as in the weakly labeled VP (Bregma level, 0.73). The boxed area of HDB is further magnified in (**B**) showing GlyR immunoreactivity in the perikaryon as well as in the processes of cells. (**C**) A high-power photograph of a single cell, with GlyR-IR sites primarily distributed at the periphery of the cell (arrows). aca, Anterior commissure, anterior part; AcbC, accumbens nucleus, core region; AcbSh, accumbens nucleus, shell region. Scale bars; A, B, 100 μm; C, 5 μm.*

Although many neurons in the septal-preoptic area were immunopositive for GlyR subunits, double-labeling revealed no clear evidence for the presence of this receptor in GnRH neurons (**Fig. 5. A-C**). Contrasting the GnRH neurons, confocal microscopic

analyses of double-labeled sections identified GlyR-IR sites in strong association with most cholinergic neurons (**Fig. 5. D-E**), suggesting that glycine can directly influence BF cholinergic functions.

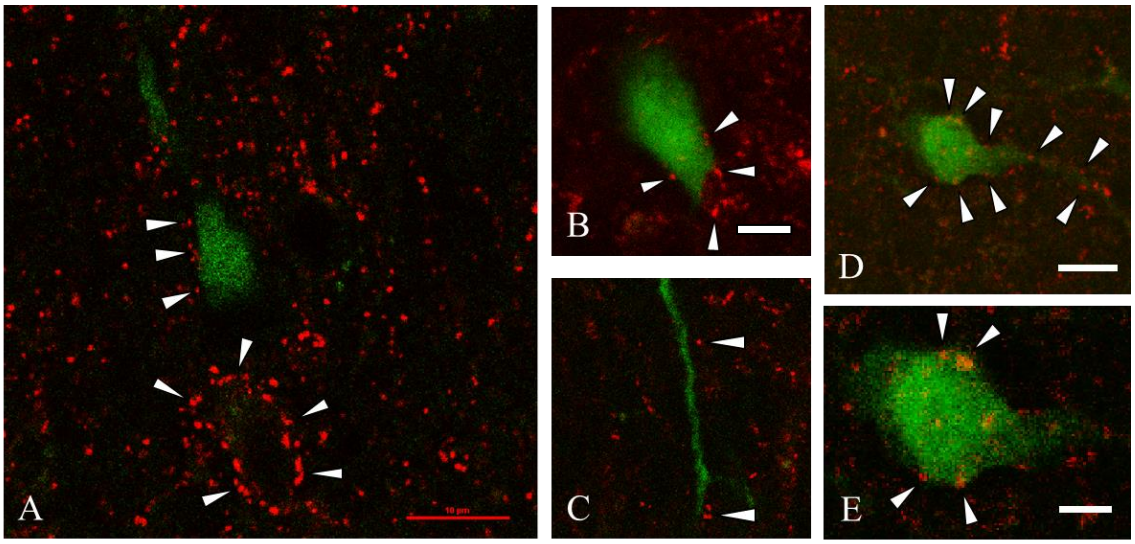

Fig. 5. *Confocal microscopic analysis of GlyR-immunoreactivities in sections also labeled for GnRH or ChAT cells. (**A**) Medium intensity of GlyR labeling are seen in MPA, where most of the GnRH neurons are located. The high power images show some GlyR-IR sites (white arrowheads) in the close vicinity of GnRH-IR soma (**B**) and processes (**C**). However, gaps are seen in most cases between the GlyR- and GnRH-IR structures. GlyR-IR varicosities seem to rather delineate non-GnRH neurons (**A**). A ChAT-eGFP neuron exhibiting GlyR-IR sites (**D-E**) at the contour of the cell (arrows). Scale bars: A, 10 µm; B, 5 µm; D, 10 µm; E, 5 µm. Contrast and brightness were adjusted with the 'Curves' function of Adobe Photoshop.*

4.1.2. Distribution of glycinergic (GLYT2-IR) fibers in the BF and their appositions to GnRH and cholinergic neurons

The location of glycinergic cell bodies is mainly restricted to the spinal cord and the brainstem. However, the axonal projections of these cells reach most of the forebrain regions, including the BF and the septo-preoptico-hypothalamic region.

By immunohistochemical labeling of GLYT2, we detected a high density of glycinergic (GLYT2-IR) axons in the mouse BF and septo-preoptico-hypothalamic region, including the areas where GnRH- and ChAT-IR neurons are distributed [i.e., GLYT2-IR

fibers were observed in the MS, VDB, HDB, LDB, VP, SI, and the EA; **Fig. 6. A–C**]. Light microscopy analyses of GLYT2-IR fibers and GnRH- or ChAT-IR neurons in the BF areas demonstrated several axo-somatic and axo-dendritic contacts between them (**Fig. 6. D-F**). Analysis of high-power light microscopic images often revealed GLYT2-IR fiber varicosities, with a central non-labeled area indicating embedded processes of target cells and concave joined surfaces (**Fig. 6. F, inset**) indicating axo-spinous connections.

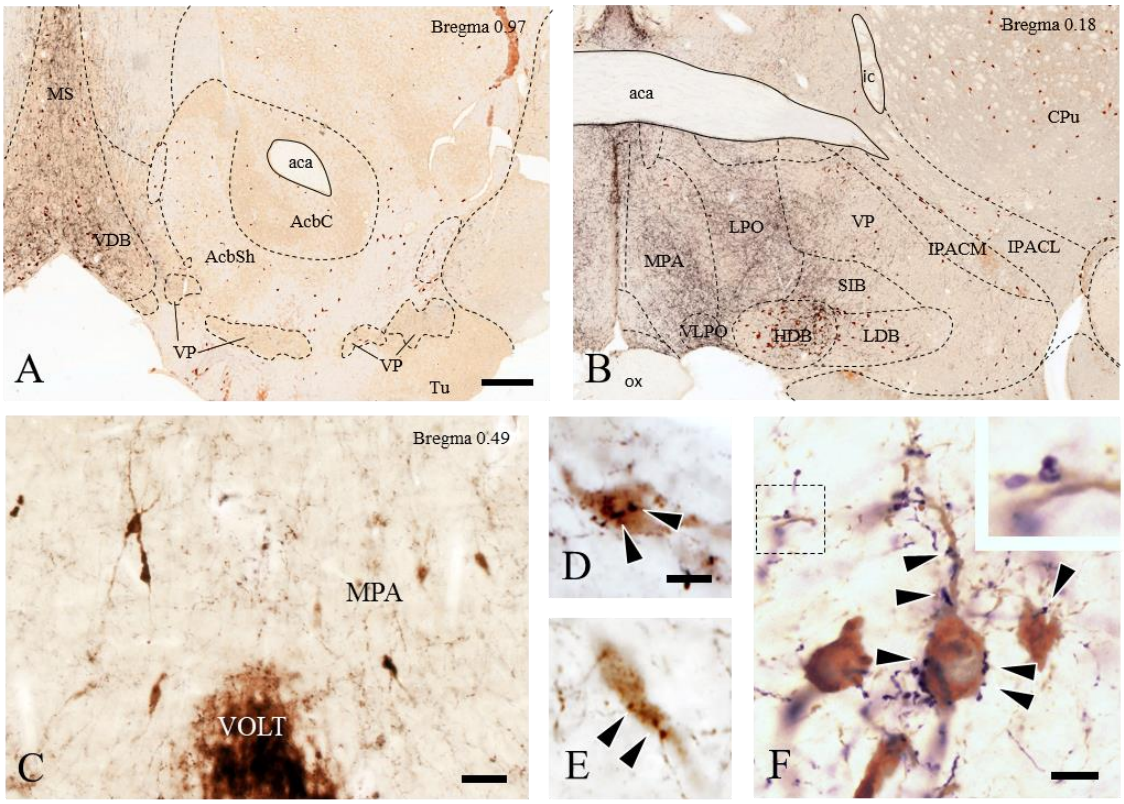

Fig. 6. *Dual immunohistochemical labeling to identify the relationship between GLYT2-IR fibers and GnRH- or ChAT-IR neurons in the basal forebrain. Distribution of GLYT2/ChAT-IR cellular profiles in the basal forebrain shown in coronal sections at two different rostrocaudal levels. (**A-B**). GnRH-IR neurons are embedded in a rich network of the GLYT2-IR axons in the MPA (**C**). High magnification images of GnRH neurons in close relationship with GLYT2-IR fibers (arrowheads) (**D, E**). Varicose GLYT2-IR axons establish axo-somatic and axo-dendritic connections (arrowheads) with ChAT-IR neurons in the basal nucleus (**F**). The axon varicosities often surround or embed neural profiles, as demonstrated by the insets, showing central lighter areas in cer-*

*tain axon varicosities (**F and inset**). The rostrocaudal levels are given in millimeters from the bregma, based upon the mouse brain atlas (Paxinos, 2013). aca, anterior commissure, anterior part; AcbC, accumbens nucleus, core region; AcbSh, accumbens nucleus, shell region Cpu, caudate-putamen (striatum ic, internal capsule; IPACL, interstitial nucleus of the posterior limb of the anterior commissure, lateral part; IPACM, interstitial nucleus of the posterior limb of the anterior commissure, medial part; LPO, lateral preoptic area; LDB, lateral nucleus of the diagonal band; MPA, medial preoptic area; MS, medial septal nucleus; och, optic chiasm; SIB, SI, basal part; Tu, olfactory tubercle; VLPO, ventrolateral preoptic nucleus; VOLT, vascular organ of the lamina terminalis. Scale bars: A–B, 500 µm; C, 250 µm; D-F, 10 µm. Contrast and brightness were adjusted using the Curves function of Adobe Photoshop.*

These contacts were further investigated at the ultrastructural level. In the case of GnRH neurons, in spite of the relatively frequent appositions seen at light microscopy levels, EM analysis of serial ultrathin sections failed to detect synapses at the contact sites (n= 54 investigated) (**Fig. 7. A-D**).

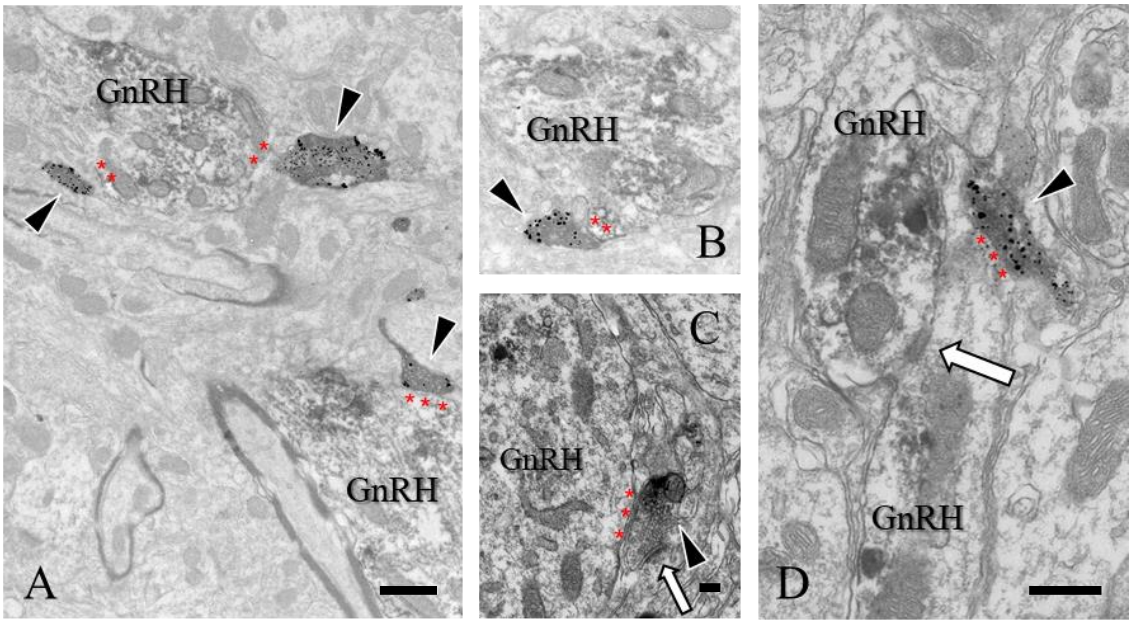

Fig. 7. *Preembedding dual-label immunohistochemistry for GLYT2 and GnRH. Electron microscopic images show that GLYT2-IR terminals (arrowheads) contact GnRH cells (**A-D**). Frequently however, they don't establish synaptic connections (red stars*

*sign the missing synaptic contact). GLYT2-IR terminals form symmetric synapse with a non-labeled neurons (white thick arrow on **C**), while GnRH neurons contact each other (white thick arrow on **D**). Scale bars: A, 1 μm; C, 250 nm; D, 500 nm.*

In contrast to the GnRH neurons, 32 synapses were identified with cholinergic profiles at the ultrastructural level. GLYT2-IR axon terminals were found to surround smaller-diameter as well as larger-diameter ChAT-IR dendrites (**Fig. 8. A**) and formed symmetric synapses with dendritic shafts (**Fig. 8. A**; n=20) and perikarya (**Fig. 8. B**; n=1).

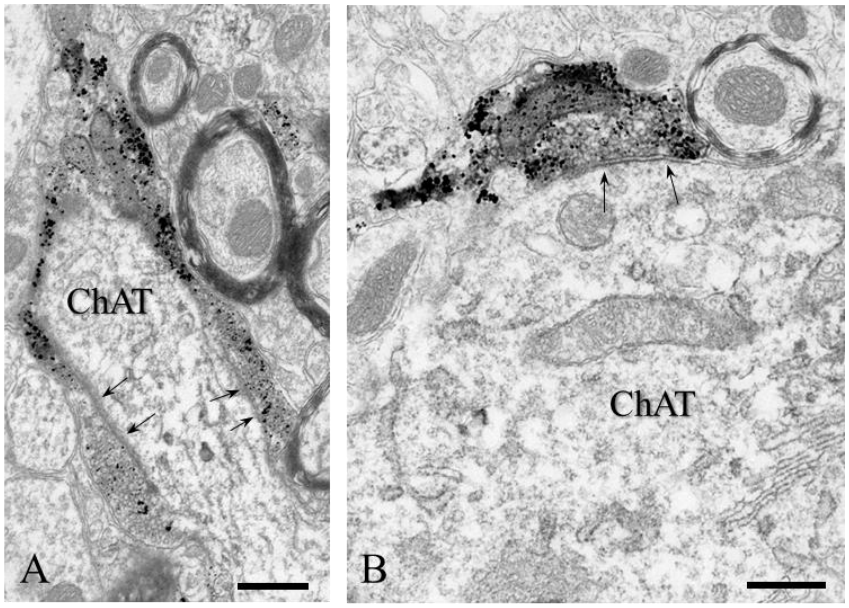

Fig. 8. *Electron microscopic images of GLYT2-IR fibers in apposition to ChAT-IR neurons of the basal forebrain. The appositions between GLYT2-IR axons and ChAT-IR dendrites (**A**) or soma (**B**) often proved to be synaptic connections (black arrows) showing characteristics of the symmetric types. Scale bars: A-B, 500 nm.*

In addition, the correlated bright-field and electron microscopic (**Fig. 9.**) approach and analysis of serial ultrathin sections also revealed axo-spinous connections on somatic (**Fig. 9. C', C"**; n =2) and dendritic spines (**Fig. 9. D'-D""**; n= 9).

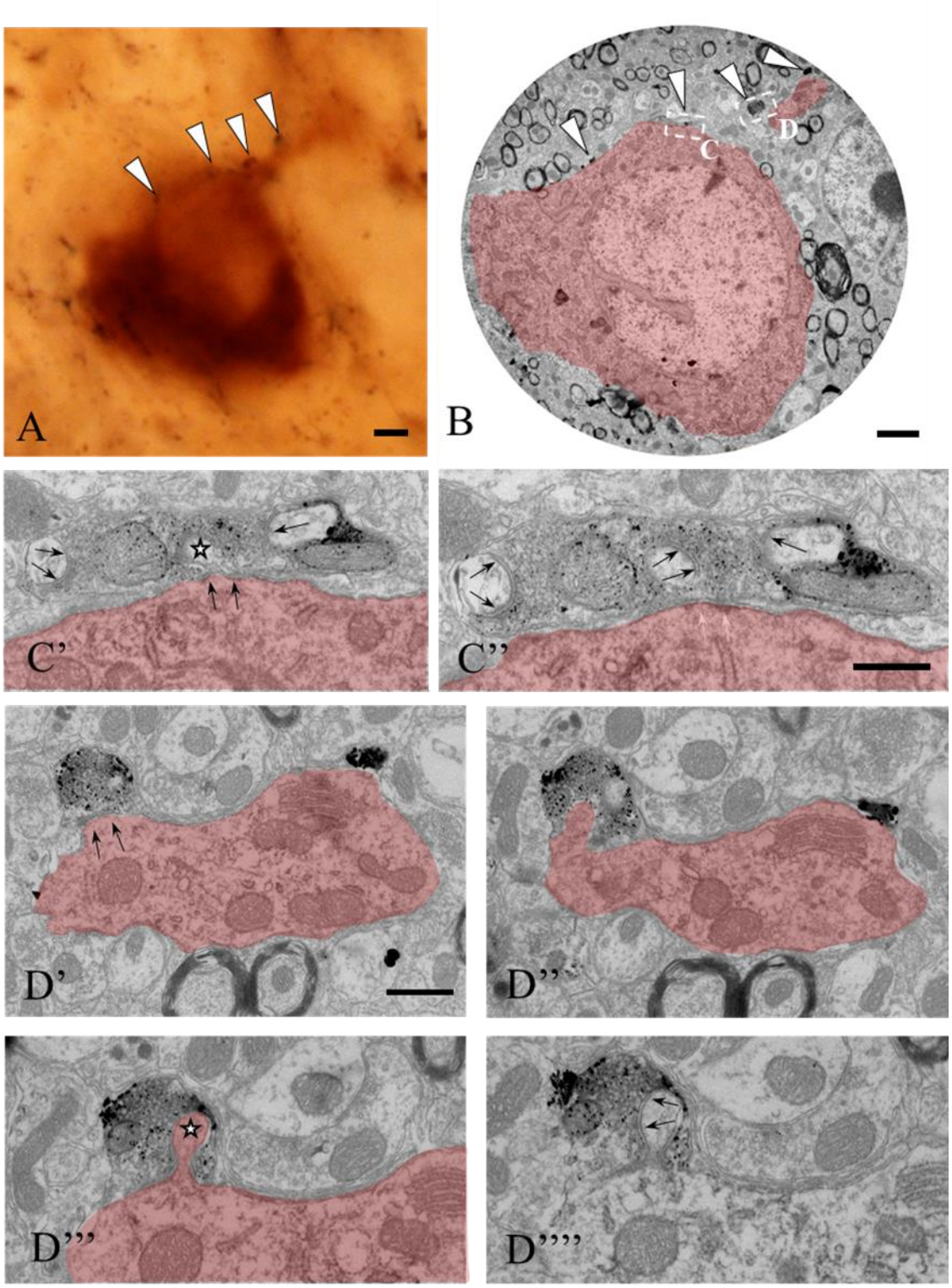

Fig. 9. *GLYT2-IR axon terminals synapse with somatic (**C'-C''**) and dendritic (**D'-D''''**) spines of cholinergic neurons in the HDB. (**A**), High-power micrograph of the immuno-histochemically double labeled and epoxy-embedded section shows multiple contacts (arrowheads) between GLYT2-IR axon varicosities and a ChAT-IR neurons (highlighted*

*in red). (**B**), The outlined areas (labeled with **C** and **D**) of the low-power electron micrograph are shown in further magnified images of consecutive ultrathin sections (**C'-D""**). Dendritic spines are embedded in and synapsing (black arrows) with GLYT2-IR axon terminals; the spine neck identifies the dendritic spine (stars) in connection with the ChAT-IR neuron. Scale bars: A, 5µm; B, 2µm; C–D, 500 nm.*

4.1.3. Localization of glycinergic neurons projecting to the BF

To identify the source of glycinergic input to the BF, the retrograde tracers CTB or Fluoro-Gold were injected into the MS, HDB, VP, and SI (**Fig. 10. A–D**) of mice expressing GFP under the control of GLYT2 promoter. We did not inject tracer into the MPA region because of the missing evidence for connection between glycinergic fibers and GnRH neurons. Although the distribution of retrogradely labeled GFP-positive neurons varied from brain to brain depending on the exact locations and sizes of injection sites, there were brainstem areas and nuclei commonly labeled for the tracer (**Fig. 10. E**). The highest number of double-labeled neurons were in the raphe magnus (RMg) (**Fig. 10. E–H**; 25 7.4% of all GFP neurons, n =6). Retrogradely labeled GFP-positive neurons were also commonly present in the different parts of the pontine reticular nucleus and the gigantocellular reticular nucleus. A few cells could also be detected in the periaqueductal gray (**Fig. 10. E**).

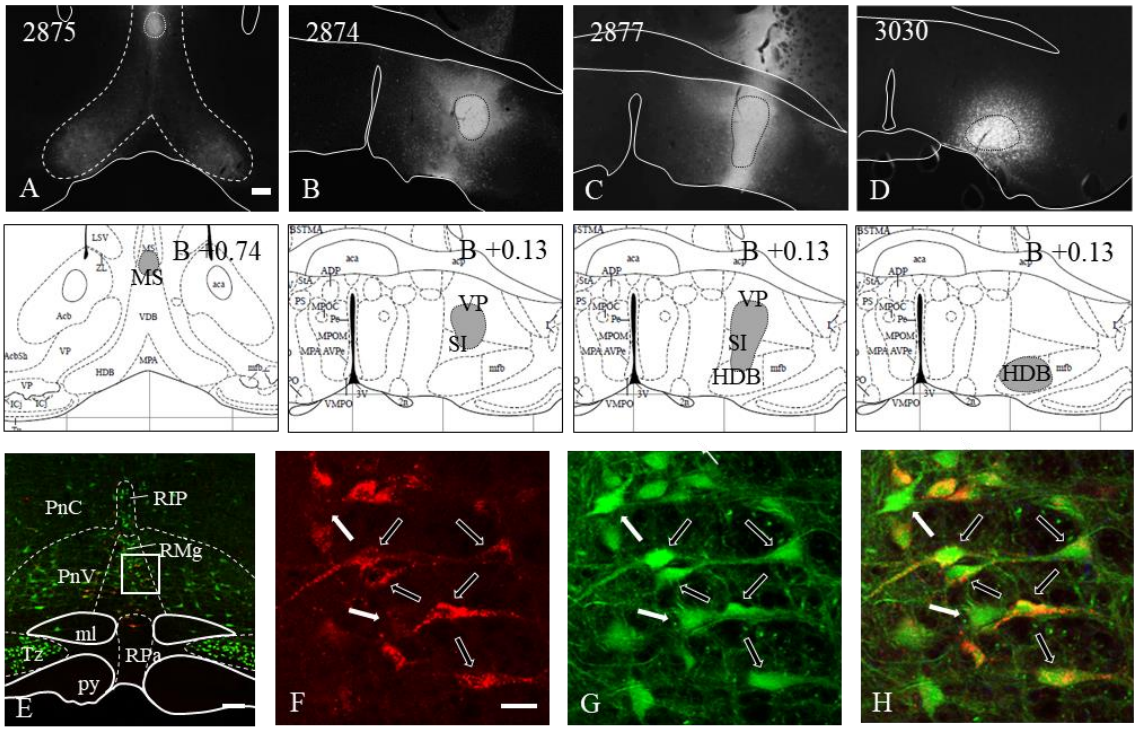

Fig. 10. *Location of basal forebrain-projecting glycinergic neurons revealed by iontophoretic injection of the retrograde tracer CTB or Fluoro-Gold into different subdivisions of the BF.* ***A–D****, Representative CTB-IR (#2875, #2874, and #2877) and Fluoro-Gold (#3030) injection sites plotted in basal forebrain section images and the corresponding atlas figures (based on Paxinos, 2013).* ***E****, Retrogradely labeled cells detected in the pons, containing GLYT2-GFP-expressing cells in the RMg, pontine reticular nucleus ventral part (PnV) and caudal part (PnC), and raphe interpositus nucleus (RIP). The outlined area is further magnified in* ***F–H*** *to demonstrate double-labeled neurons projecting to the BF.* ***F–H****, The single-labeled (white arrow) and double-labeled cells (black arrows) are shown in corresponding single- (****F, G****) and dual- (****H****) color images. Gi, Gigantocellular reticular nucleus; GiA, gigantocellular reticular nucleus part; GiV, gigantocellular reticular nucleus, ventral; PnO, pontine reticular nucleus, oral part; py, pyramidal tract; Rpa, raphe pallidus nucleus; Tz, nucleus of the trapezoid body. Scale bars: A, E, 100 μm; F, 25 μm.*

4.1.4. GLYT1-IR astroglial processes in the vicinity of GnRH and cholinergic neurons

Contrasting the dorsal forebrain areas, GLYT1-immunoreactivity in the BF is very strong, in the major regions populated by GnRH neurons and/or cholinergic neurons i.e. MS, VDB, MPA, VOLT, HDB, VP, Si. GLYT-1 immunoreactivity appears as confluent patches (**Fig. 11. A–B**). Immunohistochemical colabeling with the astroglial marker glutamine synthetase revealed that GLYT1 is primarily present in astrocytes (data not shown). Light microscopic studies revealed that the GnRH and cholinergic neurons were embedded in GLYT1-IR astrocytic microenvironment of the BF (**Fig. 11. C-E**). At the ultrastructural level, the presence of GLYT1 immunoreactivity in thin glial processes was confirmed, often adjacent to axon terminals establishing asymmetric or symmetric synapse with the GnRH and cholinergic neurons (**Fig. 12. A–D**).

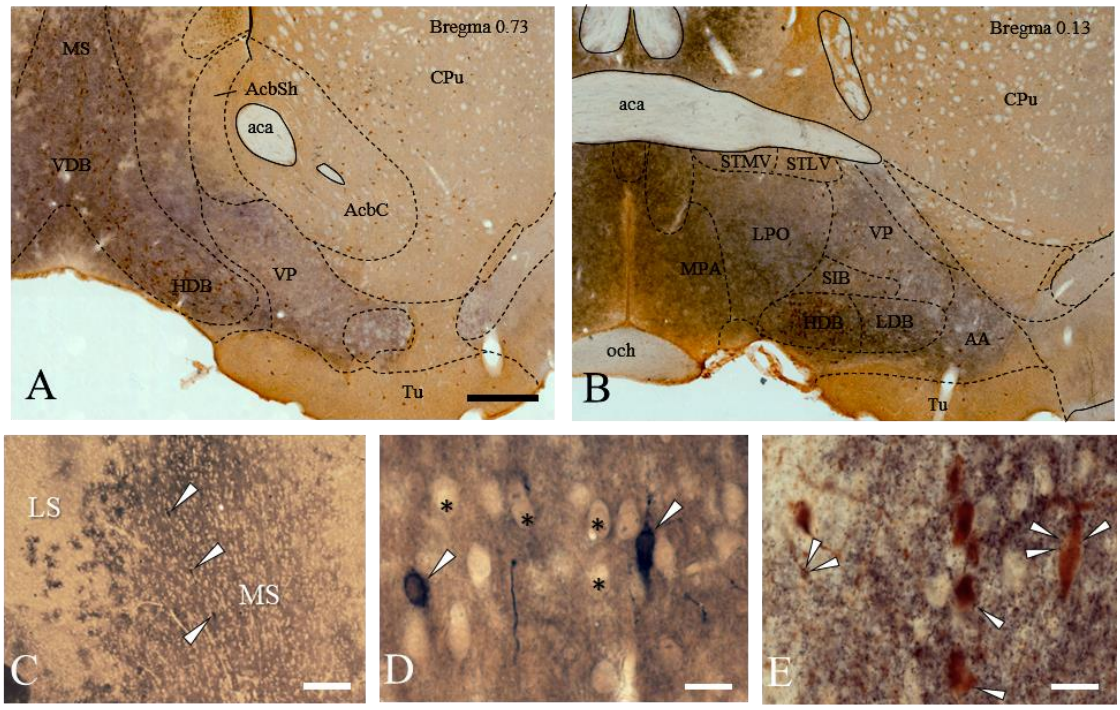

Fig. 11. *Preembedding immunohistochemical detection of GLYT1 and GnRH or ChAT neurons in the basal forebrain. Distribution of GLYT1 immunoreactivity (labeled by the black SGI-NiDAB) in the basal forebrain shown in coronal sections at two different rostrocaudal levels (**A-B**). The GnRH-IR neurons (labeled by the brown DAB; arrows) are scattered in the septo-preoptic area, which is also heavily labeled for GLYT1 (**C**). The GLYT1-immunoreactivity was found adjacent to non-labeled neurons (asterisks), as*

*well as neurons labeled for GnRH (arrows) (**D**). Medium power image reveals GLYT1-IR puncta occasionally in clear patchy arrangement resembling the shape of astrocytes. Many immunoreactiv (IR) puncta are in close vicinity to ChAT-IR neurons (arrow-heads) (**E**). The rostrocaudal levels are given in millimeters from the bregma, based upon the mouse brain atlas (Paxinos, 2013). st, Stria terminalis; STLP, bed nucleus of the stria terminalis, lateral division, posterior part; STLV, bed nucleus of the stria terminalis, lateral division, ventral part; STMV, bed nucleus of the stria terminalis, medial division, ventral part. Scale bars: A, 500 μm; C, 250 μm; D-E 50 μm. Contrast and brightness were adjusted by the Curves function of Adobe Photoshop 5.1.*

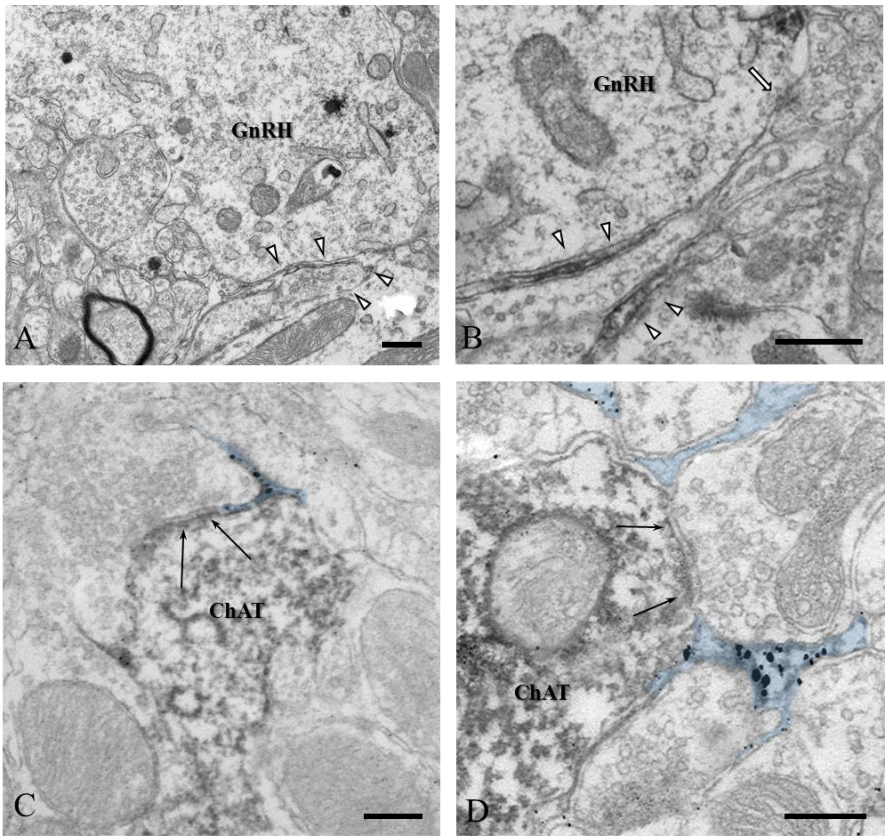

Fig. 12. *Dual-labeling for GLYT1 positive astrocytes and GnRH or ChAT neurons. Electron microscopic images of GLYT1-IR processes (labeled with silver-gold particles) (arrowheads) were found adjacent to neurons labeled for GnRH (labeled with DAB) (arrows) (**A, B**). High power image shows that the astrocytic processes appear also in the vicinity of synapses (thick arrow) established on GnRH-IR cells (**B**). The GLYT1-IR processes (highlighted in blue) appear adjacent to nonlabeled axon terminals synapsing (arrows) with a ChAT-IR dendrite (**C, D**). Scale bars, A-B, 500 nm; C–D, 250 nm.*

4.1.5. Collaborative studies on the membrane effects of glycine in GnRH- and cholinergic neurons

GnRH and cholinergic neurons were tested for direct effects of glycine in the BF by using electrophysiological approaches. In the case of GnRH neurons, whole cell recordings revealed that glycine (4 μM) had no significant effect on the frequency of action potential firing on GnRH neurons of proestrous mice (**Fig. 13**.). The neurons were injected with three current step pulses in current clamp mode (length: 900 ms, amplitudes: -30 pA, 0 pA, +30 pA). Current steps were applied before the administration of glycine (control recordings) and then in the first, third, fifth and tenth minutes after the administration of glycine.

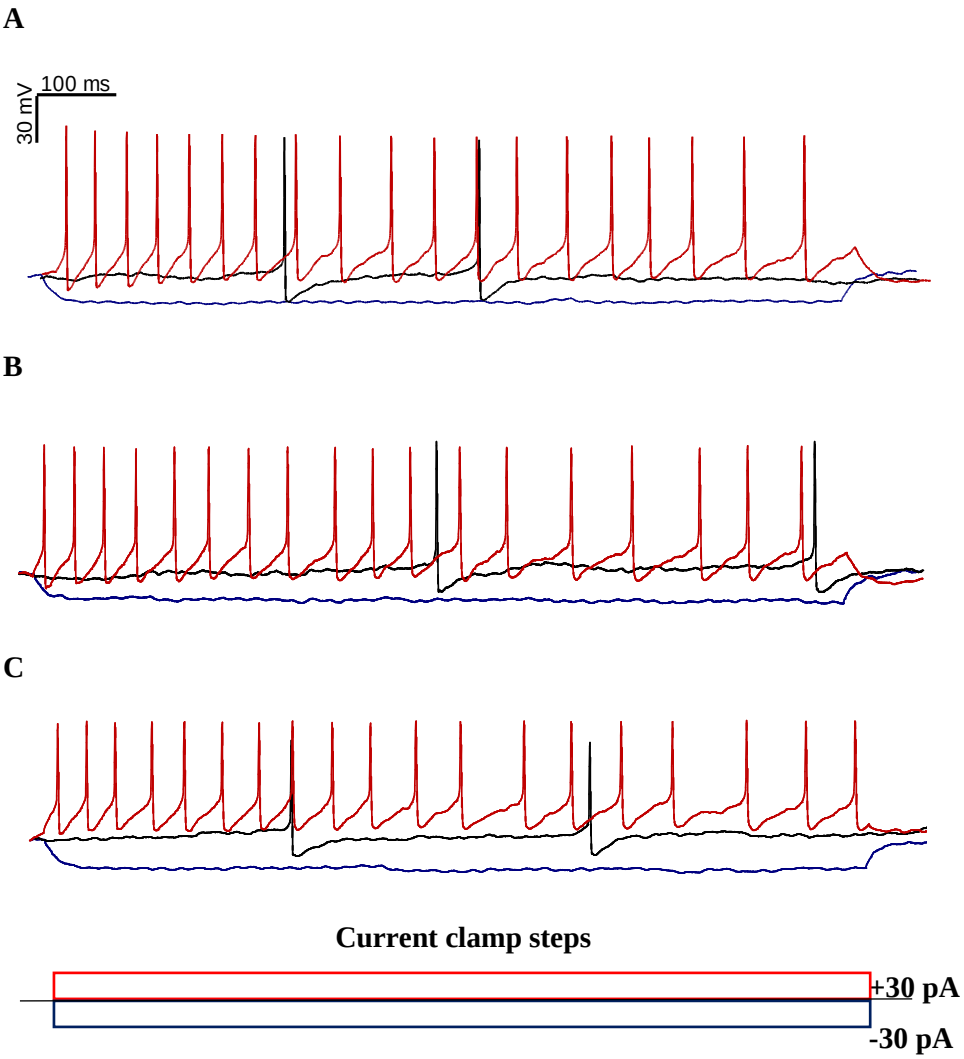

Fig. 13. *Absence of effect of glycine on firing of GnRH neurons of proestrous mice. Glycine did not alter the frequency of the action potentials at any time. (**A**) action potential firing without glycine, (**B**) one minute and (**C**) five minutes after glycine*

treatment. Blue line: hyperpolarizing step, black line: resting condition, red line: depolarizing step.

In contrast to GnRH neurons, electrophysiological recordings support a substantial glycinergic input to cholinergic neurons in all subdivisions of the BF. Approximately 80% of the recorded neurons, selected randomly from the medial septal nucleus, HDB, VP, Si, and the lateral nucleus of the diagonal band, displayed bicuculline-resistant, strychnine-sensitive spontaneous IPSCs (**Fig. 14. A, B, C**). Based on the reversal potential calculations of the events, these IPSCs were very likely chloride currents, as they were clearly distinguished from potassium currents and mixed cationic conductances. Although a slight difference in the frequency range of IPSCs could be observed in dorsomedially versus ventro laterally distributed cells (**Fig. 14. D**), the frequent appearance of cholinergic neurons showing pan-GlyR immunoreactivity or a close relationship with GLYT1 or GLYT2-IR cell processes indicates a non-selective, general role for glycine in all major subdivisions of the BF.

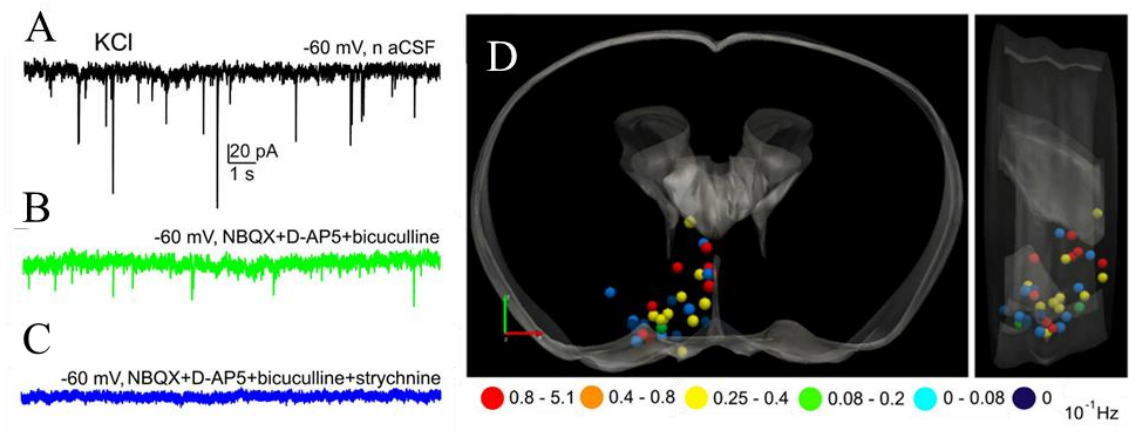

Fig. 14. *Glycinergic IPSCs recorded on cholinergic neurons in the basal forebrain. **(A)**, A 10-s-long representative trace of spontaneous (excitatory and inhibitory) postsynaptic currents recorded in normal aCSF. **(B)**, Inhibitors of ionotropic glutamate receptors (NBQX, D-AP5) and GABAA receptors (bicuculline) did not fully abolish postsynaptic currents. **(C)**, Adding strychnine to the recording cocktail blocked all events. **(E)**, Positions of the recorded neuronal somata in the basal forebrain shown by dots. Differences in the frequency of the strychnine-sensitive events are color coded. The mouse forebrain is reconstructed, and the distribution of recorded cells is shown from two different angles (axial and lateral views; based on the mouse brain atlas (Paxinos, 2013).*

4.2. Characterization of GnRH projections and their target cells in mice and humans

4.2.1. Ultrastructure of GnRH-IR processes in mice

We identified GnRH-IR axon terminals forming asymmetric synaptic contacts on unlabeled dendrites in the RP3V and Arc (**Fig. 15. A-B**). The axon terminals contained small clear vesicles and immunolabeled dense core vesicles and their diameters were about 0.5 μm. In agreement with results of a recently published paper from the Herbison's lab, we also detected GnRH dendron in the Arc with the following diameters i.e. 0.712±0.211 μm and 1.62±0.748 μm. Such dendrons contained both small clear and dense core vesicles (**Fig. 15. C**) and received synaptic inputs (**Fig. 15. D**).

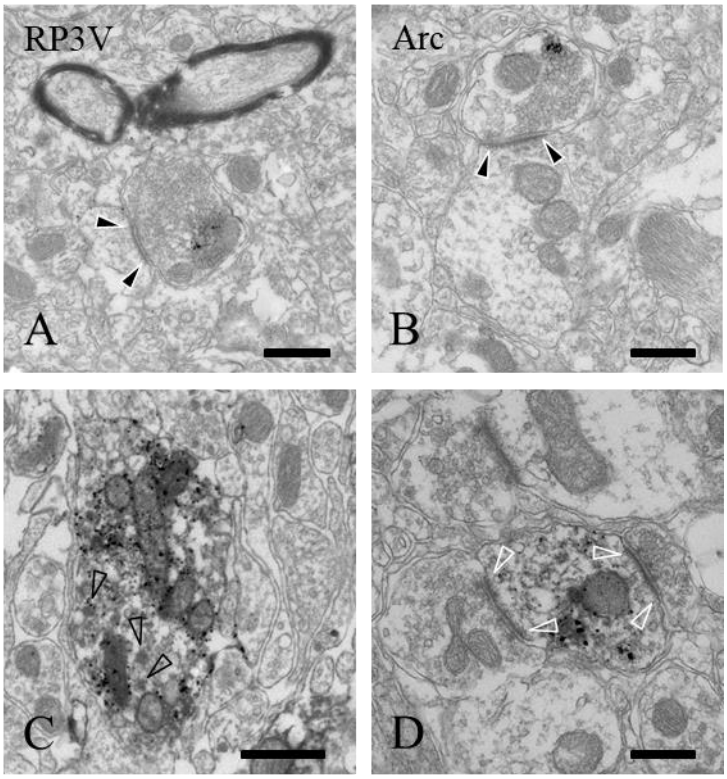

Fig. 15. *Ultrastructures of the GnRH processes in RP3V and Arc. Varying density of silver grains label GnRH-IR processes, which contain dense core and small-clear vesicles. GnRH-IR axon terminals (∅=~0.5 μm) form asymmetric synapses (black arrowheads) on unlabeled dendrites in the RP3V (**A**) and Arc (**B**). The mean diameter of GnRH process are between 0.712±0.211 μm and 1.62±0.748 μm in the Arc. According to its diameter, this GnRH-IR process (∅ =1.62±0.748 μm) is a dendron (**C**),*

*which contains mitochondria and multiple small clear and dense core vesicles (black transparent arrowheads). (**D**) A smaller diameter (∅=0.959±0.253 μm) GnRH-IR process can still be classified as dendron, since it receives synaptic inputs (white transparent arrowheads) in the Arc. Scale bars: A-D, 500 nm.*

4.2.2. Analysis of KP contacts in mice

We observed a dense plexus of KP-IR processes within the RP3V and the Arc by confocal microscopy. The KP-IR varicosities were in close contact with other KP-IR somata both in the RP3V and the Arc. Ultrastructural analysis identified KP-IR axon terminals containing large dense core granules and small clear vesicles in the RP3V and Arc. KP-IR terminals (n=5 in the RP3V; n=3 in the Arc) were found to form symmetric, axo-somatic synapses with KP-IR soma and dendrites (**Fig. 16. C, F).**

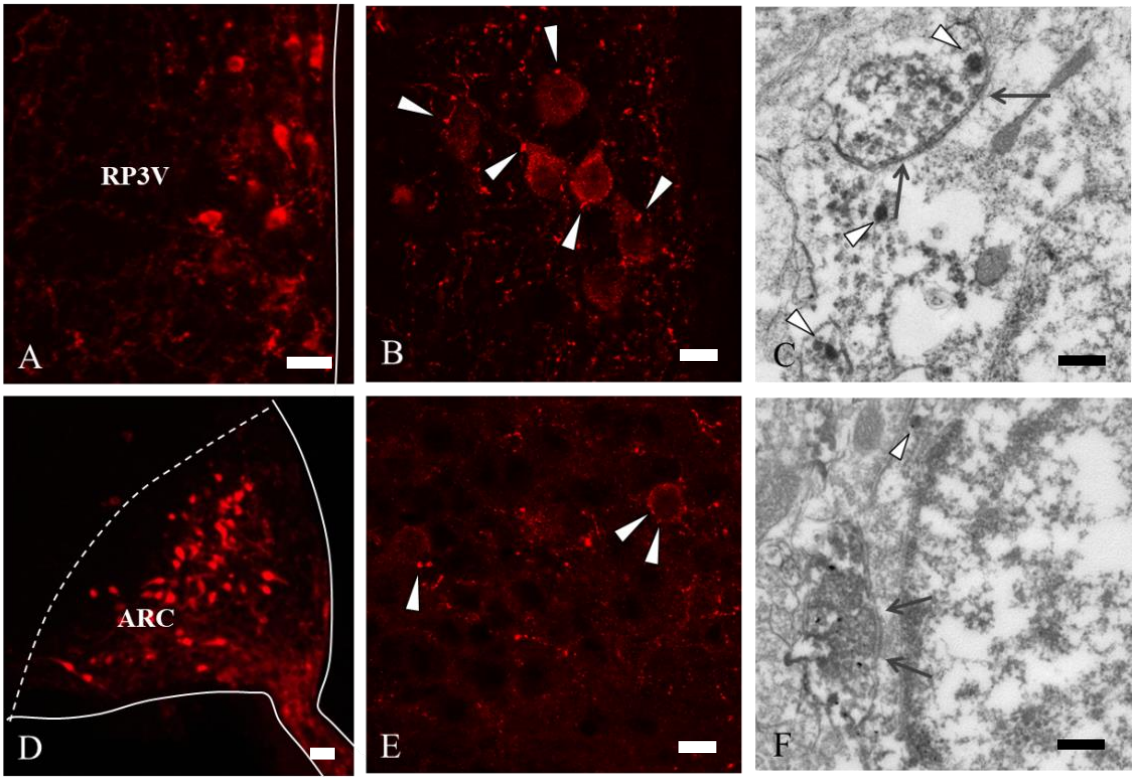

Fig. 16. *Low power confocal images of the (**A**) and Arc (**D**) showing KP-IR somas and fibers. Higher magnification of RP3V (**B**) and Arc (**E**) KP neurons, which are closely apposed by KP-IR fibers (arrowheads). Electron micrographs showing a KP-ir axon terminal in synaptic contact (arrows) with a KP-ir soma in the RP3V (**C**) and Arc (**F**).*

Dense core vesicles (white arrows) are present in both the presynaptic terminal and the postsynaptic soma. Scale bars: A, 25µm; B, 10 µm; C, 500 nm; D, 25 µm, E, 10 µm; F, 500 nm.

4.2.3. Analysis of KP contacts in human

Confocal microscopic study of the human INF revealed that most of the KP-positive cells were localized to the caudal INF and fewer to the infundibular stalk (InfS) (**Fig. 17. A-B**). In these regions, the KP-IR axons often formed axo-somatic and axo-dendritic contacts with the KP neurons (**Fig. 17. C**).

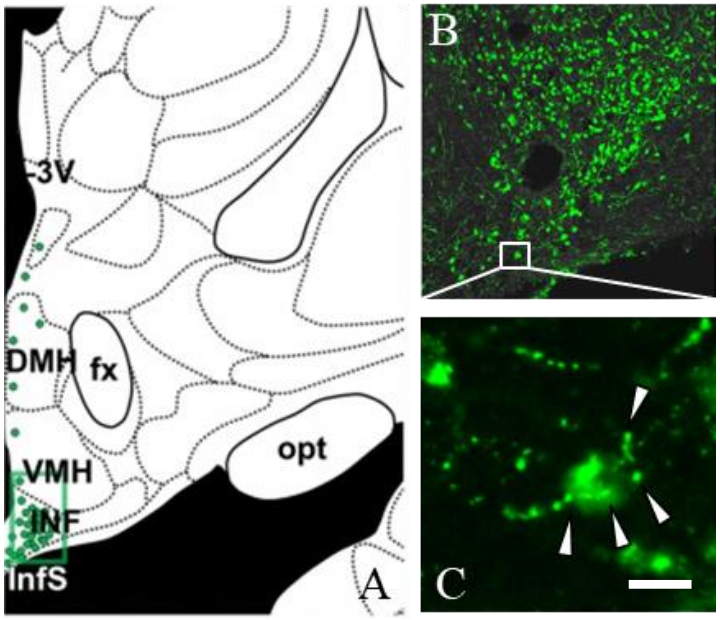

Fig. 17. *The caudal part of the infundibular region contains large numbers of KP-IR neurons. Many KP-IR neurons occur in the caudal infundibular nucleus (INF) and fewer in the infundibular stalk (InfS) in a representative 30-µm-thick section of a post-menopausal woman (case #1367/10; 57-year-old female) (**A-B**). High power image illustrates axo-somatic appositions (arrowheads) between KP-IR soma and fibers (**C**). DMH, dorsomedial nucleus of the hypothalamus; fx, fornix; opt, optic tract; VMH, ventromedial nucleus of the hypothalamus; 3V, third ventricle. Scale bar: C, 10 µm.*

To study the ultrastructure of KP cells and their connections in the human INF, we used hypothalami that were perfused with glutaraldehyde-containing fixative within a 3–4h

time window after death. The relatively good preservation of tissue allowed us to carry out electron microscopic examinations. Analysis of serial ultrathin sections identified classical synapses between KP-IR axons and non-labeled cell bodies and dendrites (**Fig. 18. A, B**). KP axons also contacted other KP-IR profiles including axons (**Fig. 18. C, C1**) and established axo-dendritic (**Fig. 18. D**) and axo-somatic (**Fig. 18. E**) synapses.

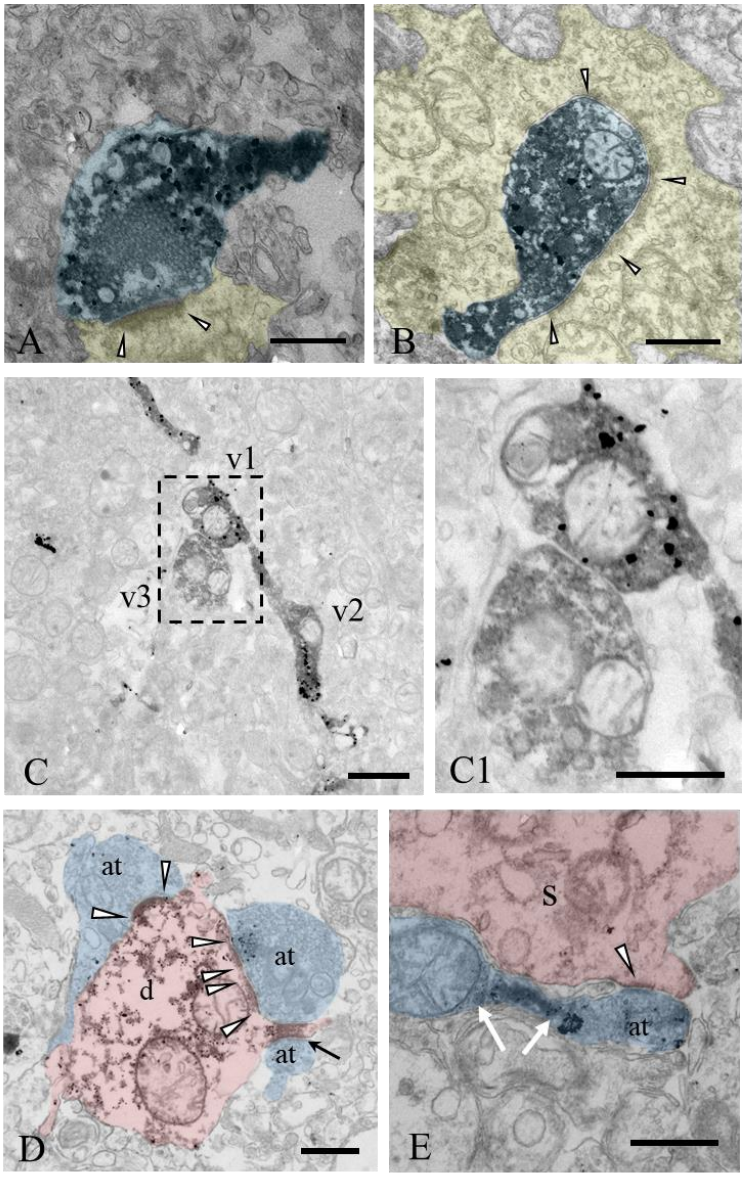

Fig. 18. *KP axons establish contacts and synapses with non-labeled and KP-IR cellular profiles. Neuronal appositions were analyzed in serial ultrathin sections from case SKO7 (55-year-old male). KP-IR axons synapse with unlabeled dendrites (**A**) and soma (**B**) in the infundibular nucleus. The IR terminals (SGI-NiDAB labeling in blue-shaded*

*axon profiles) contain large dense-core (Ø 80–100 nm) and round small clear (Ø 20–30 nm) vesicles. The postsynaptic density (marked by arrowheads in yellow-shaded structures) is relatively thick. (**C**) Heavily labeled KP axon running diagonally exhibits two clear varicosities (v1 and v2) containing mitochondria and numerous vesicles (**C1**). Varicosity v1 forms an immediate axo-axonal contact with a third immuno-labeled axon (v3). Although v3 contains no silver–gold particles, it is labeled clearly with the medium electron-density nickel-diaminobenzidine. High-power images of sequential ultrathin sections reveal that the v1/v3 apposition is devoid of a classic synaptic specialization (**C1**) and raise the possibility that KP axons can communicate with one another via non-synaptic mechanisms. KP-IR axon terminals (at; semi-transparent blue) establish asymmetric synapses (arrowheads) on a KP-IR dendrite (d; semi-transparent pink) (**D**). Black arrow points to a KP/KP synaptic contact on a spine neck. A KP-IR axon (semi-transparent blue) forms an asymmetric synapse (arrowheads) on a KP-IR soma (semi-transparent pink) (**E**). Dense-core vesicles (white arrows) tend to occupy the preterminal zone of the axon, whereas round small clear vesicles mostly accumulate in the vicinity of the presynaptic membrane (**E**). These morphological observations support the notion that KP axons use glutamatergic co-transmission. at, axon terminal; s, soma. Scale bars: A, B, C1, D, 500 nm; C, 1 μm.*

4.2.4. Confocal microscopic analysis of GnRH-IR processes forming appositions on KP- and/or tyrosine hydroxylase (TH)-IR neurons in the RP3V and Arc

GnRH-IR cell bodies were found in the septo-preoptico-hypothalamic continuum, while their processes were seen to course through and form varicosities in the RP3V and MBH (**Fig. 19. A, C**) two regions which contain KP- and TH-IR neurons. Studies using triple-label immunofluorescence identified KP- and TH-IR neurons in the RP3V within a plexus of GnRH-IR processes; some of these processes run close to the ependymal layer of the third ventricle (it is not shown on the pictures) near the most medial KP- and TH-IR neurones. In the Arc, KP- and TH-IR neurones were found in the vicinity of GnRH-IR processes, which were either arching away from the third ventricle or forming a dense ventral bundle coursing towards the median eminence. (**Fig. 19. C.**) Confocal microscopic analysis of the labeled cellular profiles identified GnRH-IR axon varicosities juxtaposed to all three types of labeled neurons (i.e. KP-, TH-, or KP/TH-IR) in the

RP3V (**Fig. 19. A, B1, B2, B3.**) and to both phenotypes (i.e. TH-IR or KP-IR neurones) in the Arc (**Fig. 19. C, D1, D2**).

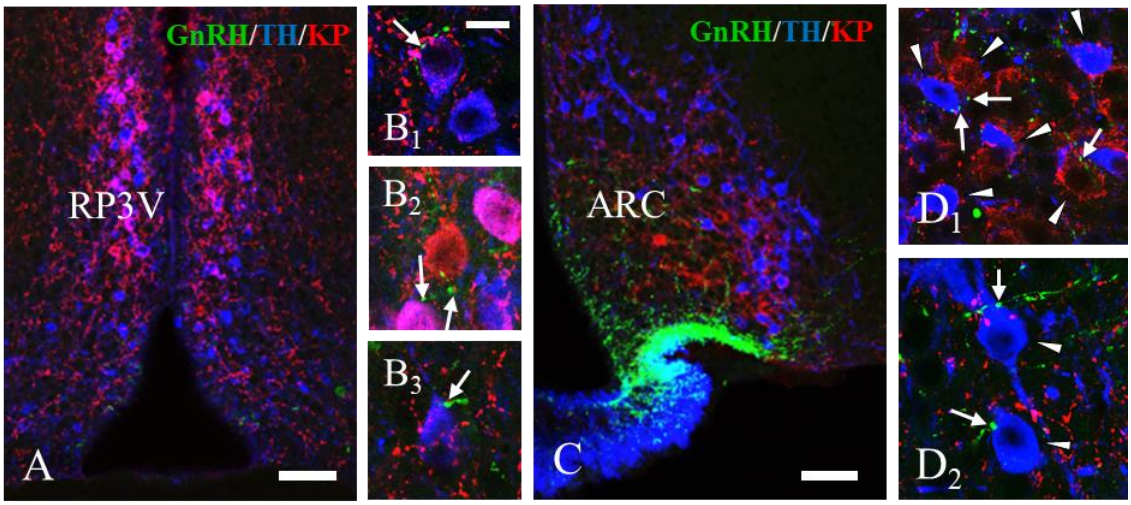

Fig. 19. *Immunohistochemical triple labeling for GnRH (green), TH (blue) and KP (red) in the RP3V) and in the Arc. (**A**) In the RP3V, the majority of TH neurons are also immunoreactive for KP (purple). Besides double-labeled neurons (**B1**), neurons single-labeled for KP (**B2**) or TH (**B3**) are also present. The GnRH-IR varicosities form appositions (arrows) on all three phenotypes of the neurons (**B1-B3**). (**C**) In the Arc, the TH neurons are not immunoreactive for KP; the TH- and KP-IR neurons form two separate populations. The TH- and KP-IR neurons (arrowheads) receive appositions from GnRH-IR fibers (arrows; **D1** and **D2**). Scale bars: A, 50 µm; B1, 10 µm; C, 50 µm.*

4.2.5. Identifying synaptic targets of GnRH axons

The immunofluorescent identification of appositions between GnRH-IR varicosities and KP- and/or TH-IR neurones in the RP3V and Arc prompted an initial investigation for classical synapses at the ultrastructural level. Pre-embedding immunohistochemical double labelling (**Fig. 20.**), employing two distinct electron dense markers, enabled the electron microscopic identification of pre- and postsynaptic elements. This made it possible to select contact sites in flat-embedded sections. Analysis of the selected areas in serial ultrathin sections identified 13 cases of either axo-somatic (**Fig. 20. B1, B2**) or axo-dendritic (**Fig. 20. C1–C6**) synapses between GnRH-IR terminals and KP-IR neurons. In the case of TH-IR neurons, the presence of synaptic specialization has been

proved for 12 appositions. The GnRH-IR presynaptic profiles contained abundant small round clear vesicles and a few dense core granules that were heavily labeled with silver grains. All of the 25 synapses detected in the RP3V (n = 8) and Arc (n = 17) were found to be asymmetric.

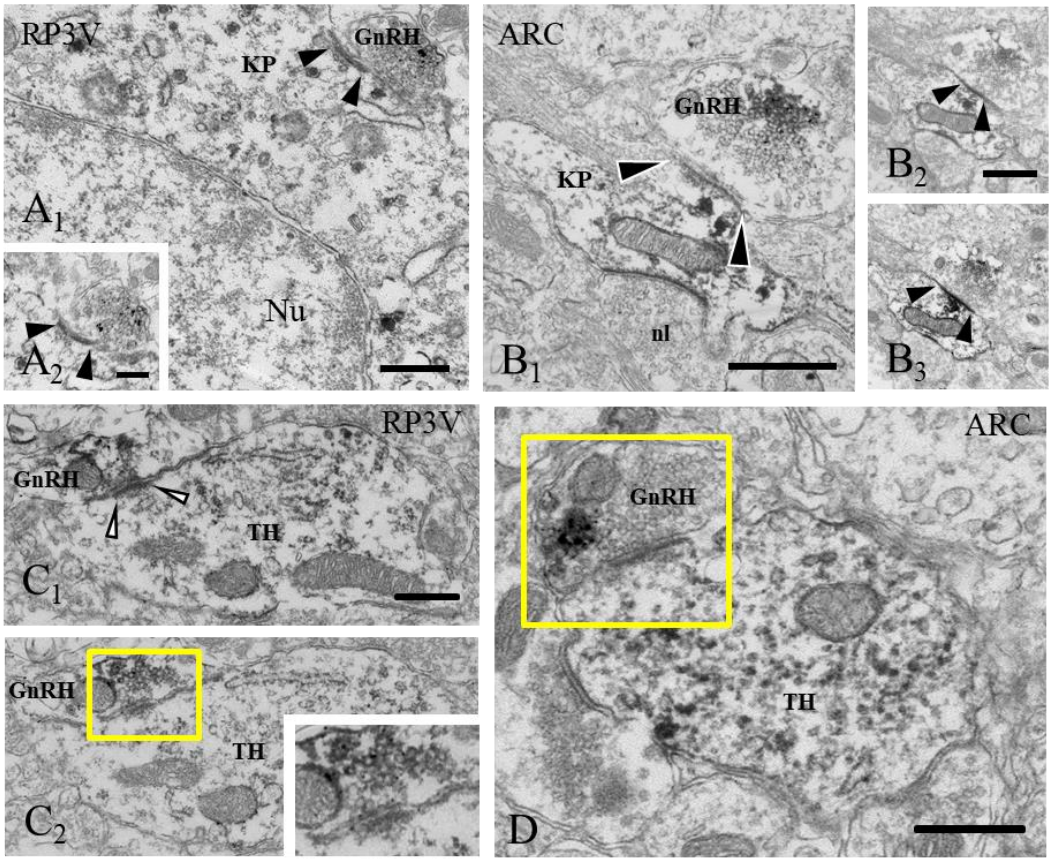

Fig. 20. *Double-label immunohistochemical detection of KP- or TH-IR neurones and GnRH-IR processes visualised with, respectively, the DAB brown reaction product (medium electron dense in the electron microscope) for labeling KP or TH neurons and the SGI-DAB black reaction product (highly electron dense in the electron microscope) for marking GnRH axon terminals in the RP3V (**A1-A2**; **C1-C2** with inset) and in the Arc (**B1-B3**; **D**). Arrowheads indicate axo-somatic, asymmetric synapse between GnRH axon terminal and KP neuron in the RP3V in **A1**, **A2** (showing the same synapse in adjacent ultrathin sections). A representative axodendritic synapse between GnRH axon terminal and KP dendrite is shown in the Arc in **B1-B3** (showing the same synapse in adjacent ultrathin sections). In the RP3V, GnRH axon terminal formed asymmetric syn-*

*apse (arrowheads) on a TH-IR dendrite, which was validated in consecutive ultrathin sections (**C1-C2**). The inset demonstrates a synaptic profile from **C2** at high power. In the Arc, the GnRH-IR axon terminal established asymmetric synaptic contact with TH-IR dendrite (**D**). In the boxed area, the GnRH axon terminal contained both dense-core granules (arrows, heavily labelled with SGI-NiDAB) and round-shaped, small, clear vesicles. Nu = Nucleus; nl = nonlabelled; 3V = third ventricle. Scale bars: A_1, 500 nm; A_2 (inset) 250 nm, B_1-B_2, 500 nm; C_1, D, 500 nm.*

4.2.6. Hormonal and lactation-related effects on the GnRH input to hypothalamic KP- and TH-IR neurons

4.2.6.1 Circadian effect on GnRH input to KP neurons

We tested whether the diurnal changes of estrogen influences the quantity of GnRH inputs to KP neurons in the RP3V and the Arc. In the animal models used for quantifying the innervation patterns in the RP3V (colchicine-treated OVX+E2 mice) and in the Arc (colchicine-treated OVX+Oil mice), GnRH-IR axon varicosities were seen to contact approximately 25% of the RP3V KP-IR neurons [23.79 ± 6.93% at ZT4–5 (n = 5) and 28.19 ± 4.41% at ZT11–12 (n = 7)] and approximately 50% of the Arc KP-IR neurons [45.99 ± 3.02% at ZT4–5 (n = 5) and 55.13 ± 4.62% at ZT11–12 (n = 5)]; the percentage was unaffected by the ZT (**Fig. 21.**). At each of the investigated times there was a significantly greater ($p < 0.003$) percentage of KP-IR neurons with GnRH–IR appositions in the Arc than in the RP3V. At both sites, the mean number of GnRH-IR appositions on their target KP-IR neurons was approximately 3; this number was unaffected by the ZT (**Fig. 21.**).

Percentage of innervated KP neurones (%)		
RP3V	at ZT4-5 (n=5)	at ZT11-12 (n=7)
	23.79±6.93	28.19±4.41
Arc	at ZT4-5 (n=5)	at ZT11-12 (n=5)
	45.99±3.02*	55.13±4.62 *

Fig. 21. *The animals were sacrificed at ZT4 – 5 or at ZT11 – 12. Neither parameter in the RP3V or Arc shows a significant difference between animals sacrificed at the two*

*ZTs. * Significantly greater ($p < 0.003$) percentage of KP-IR neurones with GnRH-IR appositions in the Arc than in the RP3V at the corresponding time.*

4.2.6.2. Effect of lactation on GnRH input to KP- and/or TH-IR neurons

To test for potential plastic changes of the GnRH input to dopaminergic neurons in lactating mothers (postpartum day 11) and in mothers deprived from pups for 24 hours, immunohistochemical triple labeling (for GnRH, TH and KP) and confocal microscopic analyses were conducted. The numbers of GnRH-IR fiber appositions to KP positive as well as KP negative TH-IR neurons (KP+/TH+-IR and KP-/TH+-IR) were analyzed in lactating mothers and compared to the values shown by non-lactating (OVX+E2) mice, and mothers deprived of their pups for 24h.

Lower ratio of TH-IR neurons immunoreactive for KP in the POA of lactating mothers

A relatively high percentage of TH neurons was found to be immunoreactive for KP in OVX-E2 mice (**Fig. 19.**; 57.8±4.3%). This ratio was significantly lower in lactating mice (16.1±5% of all IR cells counted, $F= 28.069$, $p< 0.001$; one-way ANOVA, post hoc Tukey, **Fig. 22.**). The percentage of neurons single-labeled either for TH (KP^-/TH^+-IR) or KP (KP^+/TH^--IR) was in turn significantly elevated in lactating mice (for TH; 39.8±3.7% vs. 72.4±2.9% for all IR cells counted, $F=30.986$, $p< 0.001$; one-way ANOVA, post hoc Tukey, for KP; 2.4±0.8% vs. 15.4±4.1% for all IR cells counted, $F=5.056$, $p= 0.03$; one-way ANOVA, post hoc Tukey, **Fig. 22.**). Removing the pups from the litter for 24 hours did not change the co-localization percentages in the mothers (17.3±4.6% of all IR cells counted; **Fig. 22.**).

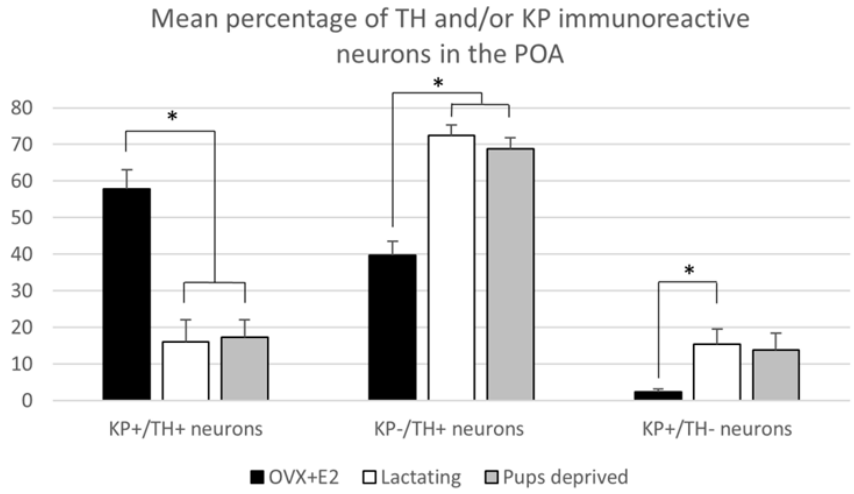

Fig. 22. *Characterization of preoptic and arcuate TH-IR neurons for KP expression. Percentage of neurons immunoreactive for TH and/or KP in the POA.*

Effect of lactation or pup-deprivation on the number of GnRH-IR fiber appositions onto TH-IR neurons

Using confocal microscopic analysis, varicose GnRH-IR fibers were observed in apposition to all the three phenotypes of labeled neurons (i.e. KP^+/TH^+, KP^-/TH^+, or KP^+/TH^-) in the POA (**Fig. 19. A, B1, B2, B3**) and to the TH-IR neurons (i.e. KP^-/TH^+) in the Arc (**Fig. 19. C, D1, D2**). Mothers showed a significantly elevated percentage of GnRH-IR appositions to KP^-/TH^+ neurons in the POA (68.5±4.3% for lactating mice, 72.3±6% for pup-deprived mothers vs. 48.2±3.2% for the OVX+E2 mice, F= 8.834, p=0.006; one-way ANOVA, post hoc Tukey; **Fig. 23. A**). In contrast, KP^+/TH^+ neurons received significantly reduced GnRH innervation in the same groups of animals (13.1±3.8% and 12.4±3.7% vs. 49.3±3.4%, respectively, F=36.225, p< 0.001; one-way ANOVA, post hoc Tukey; **Fig. 23. A**). The net result was a small reduction in the percentage of GnRH appositions on the entire population of preoptic TH-IR neurons of lactating female mice compared to non-lactating animals (F=4.946, p< 0.032; one-way ANOVA, post hoc Tukey; **Fig. 23. A**). Removing the pups from the litter caused no significant changes in the number of contacts. The percentages of GnRH appositions targeting the TH-IR neuron population (KP^+ and KP^-) were high (96.9±1.5%, 81.6 ±4.1%, 84.8±5.9% in the POA of OVX+E2 mice, lactating or pup-deprived mothers, respectively; **Fig. 23. A**). The mean number of GnRH appositions per TH-IR neuron did

not differ among the experimental groups, but its value was significantly lower in the POA than in the Arc for each experimental group ($F=34.043$, $p< 0.001$; two-way ANOVA, post hoc Tukey; **Fig. 23. B**).

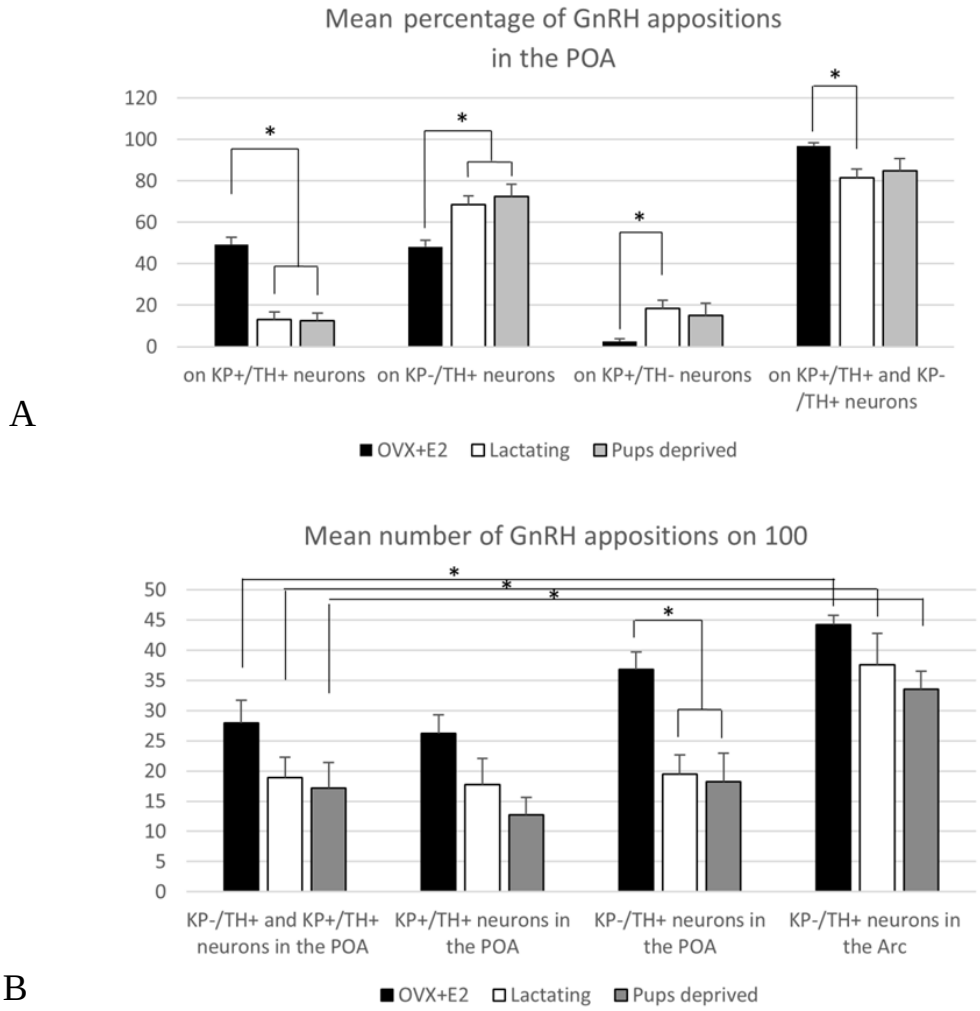

Fig. 23. *Characterization of preoptic and arcuate TH-IR neurons for KP expression and GnRH-IR afferentation. (A) Percentage of the GnRH appositions on each of this neuronal phenotype in the POA. (B) The mean number of GnRH appositions on hundred TH-IR neurons in the POA and arcuate nucleus (Arc).*

5. Discussion

5.1. Glycinergic input of BF neurons

GABA and glycine are the main inhibitory neurotransmitters in the CNS. According to the previously held view, GABA is the predominant inhibitory neurotransmitter of the forebrain, whereas glycine fulfills this function primarily in the brain stem and the spinal cord. The generation of GLYT1- and GLYT2-GFP and GLYT2-Cre mouse lines in 2005 opened a new research area, which enabled the detailed mapping of glycinergic neurons in the brain stem and their projections in the BF. By using these mouse lines and GLYT2 antisera, it has become possible for us to map the glycinergic fibers in the BF areas, where the GnRH and cholinergic neurons are also distributed.

Glycine has a complex role in the central nervous system. Glycine, depending on the target cells physiological conditions (intracellular chloride concentration) and the receptor(s) (glycine or NMDA receptors) involved can exert both excitation and inhibition and consequently, may contribute to activation or silencing the BF neuronal circuit.

5.1.1. GlyRs are distributed throughout the BF

As the alpha subunit is essential for the assembly of functional GlyRs, using a panalpha GlyR antibody allowed us to detect all subunit composition of this receptor in the BF regions. The VP showed the weakest pan-GlyR immunoreactivity; no obvious difference could be observed in the intensity of staining in the MS, VDB/ HDB, SI, basal nucleus Meynert and septal-preoptic area. The receptor immunoreactivity showed a punctate character, which often delineated the shape of neurons in the BF. Using microarray experiments, Vastagh and colleagues have shown alpha 1 GlyR subunit mRNA expression in GnRH neurons, which was downregulated in the proestrous phase compared to the metestrous stage [16]. It was therefore surprising, that the receptor immunoreactivity appearing in the vicinity of GnRH neurons could be rarely associated with the perikarya or the processes. This indicates that the glycine receptor transcript may not be or only rarely translated in GnRH neurons. In contrast, the cholinergic neurons found in the BF regions showed a clear association with GlyR-

immunoreactivity. This suggested that cholinergic neurons contain GlyRs and glycine can directly inhibit BF cholinergic functions via this receptor.

5.1.2. Role of glycinergic (GLYT2-IR) afferents in the BF

GLYT2 is expressed in glycinergic neurons and transported to the membrane of axon terminals. Immunohistochemical detection of GLYT2 makes mapping of the neuronal connections of glycinergic neurons possible.

GLYT2 is localized in the presynaptic plasma membrane of glycinergic neurons and responsible for the uptake of glycine into the terminal, thus enabling the refilling of synaptic vesicles with glycine. GLYT2 is a reliable marker for glycinergic neurotransmission [260]. Using a dual label immunohistochemical approach, we found GLYT2-IR appositions on GnRH neurons. Correlation of the light- and electron microscopic images of these appositions, however, failed to confirm the presence of synaptic contacts between GLYT2-IR axon terminals and GnRH neurons. This observation provides further support that the function of GnRH neurons may not be influenced directly by glycine.

In contrast, using the same correlated approach, we confirmed the existence of both appositions and synapses between GLYT2-IR axon terminals and cholinergic neurons. GLYT2-IR axon terminals were found on ChAT-IR perikarya, as well as smaller- and larger-diameter cholinergic dendrites, including spines. Inhibitory synapses often appeared on the soma and the proximal dendrites of target cells, in a position to block efficiently the generation of action potentials. Their presence on more distal dendritic branches, which was frequently found in the current study, was indicated to exert a less powerful but still significant inhibitory influence on target cells, involving plasticity [294]. It remains to be determined whether glycinergic synapses detected on the spines of the soma and the proximal dendrites counterbalance excitatory inputs impinging on adjacent dendritic segments.

5.1.3. Origin of glycinergic input to the BF

The BF does not contain glycinergic neurons; they are primarily located in the brainstem and spinal cord. Only the axonal projections reach the forebrain areas, as it was shown in transgenic animals expressing GFP under the control of GLYT2 promoter

[257]. In the current study, the same animal model was used to localize the glycinergic neurons projecting to the BF. We injected the retrograde tracer, CTB or Fluoro-Gold, into all major BF areas to find out the origin of glycinergic input to BF cholinergic neurons. Finding the specific glycinergic input of MPA/OVLT regions was not persuaded because there was no indication of direct innervation of GnRH neurons by glycinergic fibers in the preceeding experiments.

After the injection of the tracer, we mapped the GFP and CTB or Fluro-Gold double labeled cells in the brainstem. Relatively few areas were found to exhibit double-labeled cells in the brainstem. The majority of glycine-containing projecting neurons were found in the RMg and the gigantocellular reticular nucleus. These nuclei have been reported to establish a descending pathway responsible for muscle atonia during REM sleep [295, 296]. Although the projection of GABA/glycinergic neurons from these nuclei to the spinal cord has been demonstrated, recent findings emphasize the primary role of glutamatergic neurons in these nuclei in indirectly inhibiting the motoneurons via spinal cord interneurons during REM sleep [297]. Further studies are required to clarify the function of the ascending glycinergic pathways from these REM sleep-active nuclei to the BF. It would be interesting to find out whether bifurcating collaterals of the same cell bodies project to the spinal cord and BF cholinergic neurons, as such a scenario was implicitly suggested by demonstrating bifurcating axons originating from cell bodies in the pontine reticular formation reaching the anterior horn of the spinal cord and the hypothalamus using the classical Golgi technique [298].

5.1.4. Role of the presence of the GLYT1-IR astroglial processes in the BF

GLYT1 is primarily a glial transporter in the CNS, which is responsible for the uptake of glycine from the synaptic cleft, thus causing the termination of glycine's effect at the receptors. Immunohistochemical labeling revealed a very strong immunoreactivity for GLYT1 in the BF regions. At ultrastructural level, the GLYT1 immunoreactivity was observed in thin glial processes, often adjacent to axon terminals establishing asymmetric and symmetric synapse with the GnRH and cholinergic neurons. The high level of GLYT1 in BF [289] suggests a very tight control on the extracellular levels of glycine. Since glycine is a coagonist on NMDA receptors and facilitates the excitatory

neurotransmission, it is important to determine whether glycine can influence the function of GnRH and cholinergic neurons via NMDA receptors.

Microarray data revealed that the subunits (NR1, NR2D and NR3A) of NMDA receptors are present in GnRH neurons and the expression of NR1 and NR3A subunits are upregulated during proestrus [16]. These data highly suggest that the glutamatergic signaling is increased during proestrus, promoting the GnRH surge. However, our collaborative electrophysiological recordings revealed that glycine did not affect the firing of GnRH neurons in proestrous animals. Thus, like the GlyRs, NMDA receptor subunits are either not translated or their expression level may be very low in GnRH neurons.

The NMDA receptor is also expressed in the BF cholinergic neurons [280]. The subunit transcripts aretranslated to functional receptors, since infusion of NMDA into the BF induces cortical ACh release [299]. Previous studies suggest that BF cholinergic neurons are vulnerable to the cytotoxic effects of glutamate analogues [300] which is one of the initiators of AD [301-303]. Overactivation of NMDA receptors could be one of the key mechanisms underlying excitotoxic lesions of BF cholinergic neurons [304].

It still needs to be clarified whether glycine influences NMDA-mediated currents on BF cholinergic neurons and thereby, contributes to the regulation of neuronal plasticity, learning, memory and attention.

5.1.5. Direct glycine responsiveness of BF cholinergic, but not GnRH neurons

Glycine's effects on the glycine receptor evoke chloride currents, which usually hyperpolarize the cell. However, depending on the intracellular concentrations of chloride, the effect can be depolarizing. GnRH neurons have high intracellular Cl^- concentrations, thus the effect of GABA on GnRH neurons is primarily depolarizing [267]. Glycine was expected to have similar effect on the activity of GnRH neurons, but no changes could be detected in whole cell patch clamp conditions using slices from proestrous female mice. The action potential frequency and the resting membrane potential showed no significant alteration in response to glycine (4 μM) by none of the current steps (-30, 0, +30 pA) applied. However, glycine's effect, cannot be excluded in other phases of the cycle or in male animals.

In case of cholinergic neurons, approximately 80% of the cells selected randomly from the medial septal nucleus, HDB, VP, Si, and the lateral nucleus of the diagonal band, displayed bicuculline-resistant, strychnine-sensitive spontaneous IPSCs. Thus, these inhibitory events suggest that glycine evokes Cl^- influx from the cholinergic neurons.
The frequent appearance of cholinergic neurons showing pan-GlyR immunoreactivity or a close relationship with GLYT1 or GLYT2-IR cell processes indicates a region-independent, general role for glycine in all major subdivisions of the BF. This does not exclude the possibility that the glycinergic input to specific cholinergic cell populations is heterogenous. For example, EF and LF cholinergic neurons were distinguished [29] with putative functional consequences. It was suggested, that the EF neurons are more suitable for phasic changes in ACh release associated with attention, and the late firing neurons could support general arousal by maintaining tonic ACh levels. Comparison of the glycinergic sIPSCs of these subtypes in our study revealed a significantly higher amplitude and longer decay time in EF than in LF neurons, indicating a potential difference in the somatodendritic, proximodistal location of their glycinergic synapses or in the general membrane properties determining propagation characteristics of IPSCs. The responses of EF and LF cholinergic neurons to glycine raise a possibility for the involvement of this inhibitory neurotransmitter in both attention regulation and arousal.

5.2. Characterizing GnRH efferents and their target cells in mice and humans

5.2.1. Ultrastructural features of GnRH processes in mice

The GnRH neurons have long processes, which terminate primarily in the median eminence. These processes receive abundant synaptic inputs and propagate the action potentials. Thus, they possess both dendritic and axonal characteristics. Therefore, recently they have been renamed dendrons [115]. The dendron projects to long distances and branches extensively in the median eminence. At the ultrastructure level, it is difficult to distuinguish the dendrites (dendrons) and axon varicosities and terminals because mitochondria, small clear vesicles and dense core vesicles can equally be detected in these processes. The diameter of the processes may help in the distinction, since processes below 1 μm were classified as axons [305]. We identified dendrons with the same diameters (0.712±0.211 μm) which received synaptic inputs from non-labeled axons (**Fig 15. D**). Our finding is in agreement with recent new data,

reporting rich afferentation to distal segments of the dendron [105]. Furthermore, we have identified GnRH-IR axon terminals (with about 0.5 μm diameter) in the RP3V and Arc forming synapses on unknown target cells (**Fig. 15. A-B**). The phenotypes of these target neuron are discussed in the next chapters (6.2.3., 6.2.4.)

Thus, in addition to the GnRH dendrons identified in the Arc, we detected several axon teminals forming synapses in both the RP3V and Arc, which lead us to examine the phenotype of target cells.

5.2.2. The importance of KP-KP contacts in mice and human

Light- and electron microscopic studies provide morphological evidence for the existence of synaptic interaction between KP neurons in both mice and humans. In mice, we identified axo-somatic, symmetric synapses in both the rostral periventricular area and the Arc. In these nuclei, expression of the G-protein-coupled receptor (GPR54) to which KP binds is fairly abundant, suggesting an intranuclear communication mediated by this receptor. Surprisingly, GPR54 mRNA was detected by real-time PCR neither in the preoptic nor in the arcuate KP neurons, suggesting that KP itself may not contribute to the intranuclear communication of KP neurons. Consequently, the KP-KP neuronal communication in the RP3V and Arc may be mediated by alternative neurotransmitter(s) and/or neuropeptide(s).

In the RP3V, it has been shown that about 75% of KP neurons are GABAergic, whereas 20% of them are glutamatergic [306]. Furthermore, the RP3V KP neurons also contain tyrosine-hydroxylase, galanin and met-enkephalin [215, 307, 308] but they express receptors only for GABA and glutamate. These observation indicate that the RP3V KP neurons use GABA and/or glutamate in the communications among them. Thus, based on the previous studies showing the majority of KP neurons to be GABAergic [306] and our results in which we found symmetric synapses between KP neurons, it is highly possible that the preoptic KP neurons use primarily GABA for interneuronal communication.

KP neurons have been shown to directly innervate GnRH cell bodies and implicated in the estrogen-induced preovulatory LH surge. The intra RP3V connections might have a significance in generating synchronous activity of KP neurons; which is most likely

necessary for triggering the preovulatory LH surge. However the exact role of the connection remains to be elucidated.

In the Arc 50% of the KP neurons are GABAergic, whereas 90% of them are glutamatergic [306] and they coexpress NKB and Dyn (thus they are termed as KNDy neurons in rodents, sheep, but not in human). A series of morphological and functional studies on various laboratory animals provided evidence that KNDy neurons communicate substantially with each other also in the Arc [225, 226, 309-312]. Since KP itself does not influence the electric activity of KNDy neurons [310], and they don't express Kiss1R local communication of KNDy neurons appears to take place mostly via NKB/NK3R and Dyn/κ-opioid receptor signaling in rat, mouse and sheep; KP, in turn, seems to provide the main output signal of KNDy neurons toward the GnRH neuronal system, and thus, plays a crucial role in the generation of episodic GnRH/LH pulses [163, 313, 314]. Indeed, the pulsatile KP output and GnRH secretory pulses are temporally correlated in the median eminence of the female rhesus monkey [315]. However, these KNDy neurons are not only connected in the Arc, but connectivity between Arc KNDy and RP3V KP neurons also exists [316]. As KNDy neurons synchronize their own activity, at the same time they also excite the RP3V KP neurons via glutamate that, in turn, robustly excites GnRH functions [317].

In the case of studies of the human INF and InfS, we found that KP-IR neurons form a compact cell mass. High-power confocal and electron microscopic images revealed that these cells establish axo-somatic and axo-dendritic contacts and synapses among one another. Furthermore, we have also found ultrastructural evidence for direct axo-axonal appositions without synaptic specializations between KP axons. Electron microscopic observations can contribute to a better understanding of neurotransmitter storage and release. While analyzing the fine structure of KP axon terminals, we observed not only neuropeptide-containing, large, electron dense-core vesicles but also small, round clear synaptic vesicles known to accumulate classical neurotransmitters [318]. KP terminals formed asymmetric synapses in which the thickened postsynaptic membrane is caused by the conglomerations of membrane receptors, scaffolding proteins and second messenger effectors [319]. Although exceptions exist, this asymmetric morphology usually reflects excitatory neurotransmission [320]. The identity of neurotransmitters whereby human KP cells communicate with each other requires clarification. It is

noteworthy that neuropeptides co-contained with KP are not necessarily the same in humans and in laboratory species [321] Furthermore, many of the KP-IR and NKB-IR axons in the human hypothalamus are single-labeled and devoid of Dyn [322] suggesting that the 'KNDy neuron' terminology and the recent models of the GnRH/LH pulse generator which are based on results of animal experiments, should be applied with great caution to humans. Results of our ultrastructural studies suggest that, in addition to different neuropeptides, endogenous glutamate may also play a co-transmitter role in the communication among human KP neurons.

5.2.3. GnRH axons target KP-IR neurons in both the RP3V and the Arc

In rodents, RP3V KP neurons provide a direct input to GnRH neurons [214, 215, 323]; this is of critical importance in generating the GnRH surge during estrogen's positive feedback phase [190, 191, 216-218]. The population of KP neurons in the Arc has been implicated in the generation of GnRH pulses and in the negative feedback effects of gonadal steroids on the reproductive neuroendocrine axis [313, 324]. Our studies provided evidence for connections in the opposite direction, i.e. GnRH neurons also innervate KP neurons in the RP3V and Arc.

Our study identified exclusively asymmetric synapses between GnRH-IR processes and KP-IR neurons in the RP3V and Arc. These findings and the presence of the glutamatergic marker, VGLUT2, in most GnRH neurons in rats and mice [325, 326] are consistent with the putative excitatory glutamatergic transmission from GnRH neurons at the synapses. Furthermore, the abundant small round clear vesicles that were seen also in rodents (rats and mice) in the presynaptic profiles may indicate the presence of glutamate [318].

The GnRH projections to KP neurons may supplement the ultrashort feedback onto GnRH neurons with indirect autoregulatory mechanisms established through the RP3V and Arc KP neurons. Thus, these GnRH-IR terminals may provide substrates for the final common pathway neurons to influence signals from the estrogen-responsive KP neuronal populations that contribute to the surge and/or pulsatile release of GnRH. The functional significance of the GnRH-IR input to KP neurons and the existence of the regulatory loop we propose based on our new neuroanatomical data will need to be addressed in electrophysiological experiments.

5.2.4. TH-IR neurons represent the second major neuronal population targeted by GnRH afferents

We have also demonstrated GnRH afferents to TH-IR neurons located in the mouse periventricular POA, as well as the Arc. This supplements our previous data showing a similar connection of GnRH axon varicosities with preoptic and arcuate KP-IR cells (see above) [117]. Considering that almost all preoptic KP neurons express TH [307] (more than 90% in the current study) the question has emerged whether only KP-expressing TH neurons are targets of GnRH afferents. Although the percentage of preoptic KP-/TH+ neurons varied in the different animal models, they represented nearly half of all immunoreactive neurons in the OVX+E2 animals, and more than two-third of all immunoreactive neurons in lactating and pup-deprived mothers (**Fig. 22.**). Relatively high percentages of these neurons received GnRH-IR fiber appositions in all experimental models (**Fig. 23. A**), indicating that the KP immunonegative TH-IR neurons represent the second major neuronal population in the POA targeted by GnRH afferents. The TH-IR neurons in the Arc, where they form a completely separate cell population from KP neurons [307, 321, 327], were also found to receive input from GnRH axon terminals.

As GnRH neurons are phenotypically heterogeneous, the question arises which subpopulation of GnRH neurons innervates the dopaminergic neurons. Dumalska and colleagues reported [230] that in VGLUT2-GFP mice 84% of GnRH-IR neurons expressed GFP; moreover, the cytoplasmic extract of each GnRH-GFP cell recorded also contained mRNA for VGLUT2. The asymmetric type of synapses found exclusively between GnRH axons and TH-IR neurons in the current study suggests that the GnRH neurons innervating the TH-IR neurons use glutamate, and very likely exert excitatory effects on these dopaminergic neurons. Nevertheless, the possibility for GABA to appear in the GnRH axon terminals synapsing on TH-IR neurons cannot be excluded.

5.3. Hormonal- and lactation-related effects on the GnRH input of KP- and TH-IR neurons

5.3.1. Possible plasticity of GnRH input to KP-and TH-IR neurons in lactating animals

In my PhD investigations, we focused on the GnRH neuronal projections to the preoptic (A14-15) and the arcuate (A12) subgroups of the dopaminergic neurons. These subpopulations of dopaminergic neurons establish local connections, as well as projections to the median eminence (TIDA cells), or to the posterior and intermediate lobes of the pituitary gland (THDA and PHDA), where they access the short portal vessels to transport dopamine to the anterior pituitary gland [328]. As far as the GnRH afferents to these dopaminergic neurons are concerned, we found no preferential targeting of GnRH axons to any one of these three subpopulations. This is reminiscent of the prolactin receptor expression in all three subgroups of dopaminergic cells [329], which indicates that these neurons may contribute similarly to the regulation of prolactin secretion.

Based on the asymmetric type of the synapses established, it is reasonable to think that the GnRH neuronal afferents stimulate the dopaminergic cells under certain conditions and facilitate dopamine secretion; consequently, they inhibit prolactin secretion from the pituitary gland. This effect would be in congruence with the biological need of the normal estrous cycle to keep the inhibitory effect of prolactin low on GnRH secretion. However, secretion of prolactin is far more complicated, showing proestrus- and lactation related surges, the regulation of which cannot be directly associated with the transmitter-release of GnRH neurons.

Mitchell et al. reported an estrous cycle dependent variation in the number of contacts between GnRH processes and TH-IR neurons in the Arc, suggesting a hormone-dependent plasticity in this communication [330]. A profound suppression of TH mRNA expression [331, 332] and phosphorylation [333, 334] of this enzyme with activity reduction have been shown during lactation. This might have contributed to the lower levels of preoptic neurons immunoreactive for both TH and KP, as well as the lower percentage of GnRH appositions on the entire population of TH-IR neurons in lactating vs. OVX+E2 mice. Furthermore, NPY, ENK and NT-immunoreactivities are enhanced in TIDA neurons during lactation, while removing the pups from the litter

resulted in a marked depletion of the immunoreactivity for these peptides from the median eminence TH-IR endings [335] with a concurrent elevation of TH mRNA expression in the Arc [331]. These observations prompted us to study whether lactation, when the pulsatile secretion of GnRH is suspended, or removal of the pups and consequently the stimulus of breast-feeding reflexes for 24h, induce plastic changes in the GnRH-TH connection. We found a significant increase in the percentage of GnRH apposition on single-labeled TH-IR ($KP^{-/}TH^{+}$) neurons in the POA of mothers, which was accompanied by the significantly reduced percentage of these afferents to KP^{+}/TH^{+} neurons in the same groups of animals. However, when the mean number of GnRH-IR appositions was investigated on the full population of preoptic (KP^{-} and KP^{+}) and arcuate TH-IR neurons, no significant group difference could be observed (**Fig. 23. B**). This indicates, that the GnRH input to TH-IR neurons is maintained in the POA during lactation, while a subpopulation of the neurons shows a reduced KP expression, as reported earlier [336, 337]. Similarly, no significant difference could be observed in the GnRH input of Arc neurons among the different experimental groups. However, the possibility cannot be excluded that plastic changes may occur at ultrastructural and/or molecular levels, at different time points of lactation or following a longer pup-deprivation.

5.3.2. Possible plastic change of the GnRH afferents to KP neurons at different circadian stages

To study the circadian effect on connection between GnRH axon terminals and KP neurons in the RP3V and Arc, we used ovariectomized and oil treated or ovariectomized and Estrogen treated animals. The RP3V KP neurons mediate the positive effect of estrogen and the estrogen treatment increases KP expression in the RP3V KP cells. However, in the Arc estrogen negatively regulates the KP neurons and thus, the absence of estrogen increases KP expression at this site. Taken together, depending on whether or not the animals were treated with estrogen, we could examine the negative and positive feedback phases of estrogen's effects on LH release. Furthermore, we used OVX+E2 treatment mouse model which mimicked the sustained high levels of estradiol in proestrus. The constant high level of estrogen induces LH surge which is timed to the late afternoon in nocturnal rodents [125, 174]. Thus, we examined whether the presence

or absence of estrogen at different zeitgeber timepoints may have affected the connections between GnRH and KP neurons. Finally, during the confocal microscopic analysis, we have not observed differences between the experimental animal groups. GnRH-IR axon varicosities were seen to contact approximately 25% of the RP3V KP-IR neurons [23.79 ± 6.93% at ZT4–5 (n = 5) and 28.19 ± 4.41% at ZT11–12 (n = 7)] and approximately 50% of the Arc KP-IR neurons [45.99 ± 3.02% at ZT4–5 (n = 5) and 55.13 ± 4.62% at ZT11–12 (n = 5)].

6. Conclusions

In the first part of my PhD work, we examined the potential target cells of glycine in the BF. Thus, we carried out morphological and functional examinations to identify the glycine target cells and areas in the BF. We investigated the presence of GlyR in GnRH and cholinergic neurons and we found that all of the BF regions contain GlyRs, including the areas where the GnRH and cholinergic neurons are located. Immunofluorescence labeling provided no clear evidence for the presence of this receptor in GnRH neurons, whereas the cholinergic neurons were positive for GlyR in all BF regions.

Furthermore, we tested the presence of GLYT's in the vicinity of GnRH and cholinergic neurons. Using double immunostaining, we were not able to confirm the presence of synaptic specializations between GLYT2-IR axon terminals and GnRH neurons. In contrast to GnRH neurons, cholinergic neurons received GLYT2-IR axon terminals with both axo-somatic and axo-dendritic arrangement. These synapses belonged to the symmetric category. We found the synapses frequently on more distal branches, indicating less powerful but still significant inhibitory influence on target cells, involving plasticity.

To identify the source of glycinergic afferents to BF, we used tract tracing examinations. We injected CTB or Fluoro-Gold into different BF regions and analyzed the distribution of double labelled cells in the brainstem of transgenic mice expressing GFP in GLYT2-eypressing cells (i.e. glycinergic neurons). We found that the glycinergic cell bodies were located mainly in the RMg, Periaquaductal grey and the Gigantocellular formation of the brain stem.

We also tested the distribution of the GLYT1-IR astrocytic processes in the vicinity of GnRH and cholinergic neurons. Double immunostaining confirmed that the GnRH and cholinergic neurons were embedded in rich networks of GLYT1-IR glial processes. At the ultrastructural level, these glial processes were in the vicinity of asymmetric and symmetric synapses onto GnRH or cholinergic neurons, suggesting that the glycine concentration is highly controlled in the extracellular space at these synapses.

Finally, we tested the potential effects of glycine on the membrane properties of the GnRH and cholinergic neurons in collaboration with other laboratories. At whole cell patch clamp recording conditions, we could not detect any effect of glycine on the firing

of GnRH neurons. As opposed to GnRH neurons, cholinergic neurons were inhibited by glycine. These findings are summarized in **Fig. 24.**

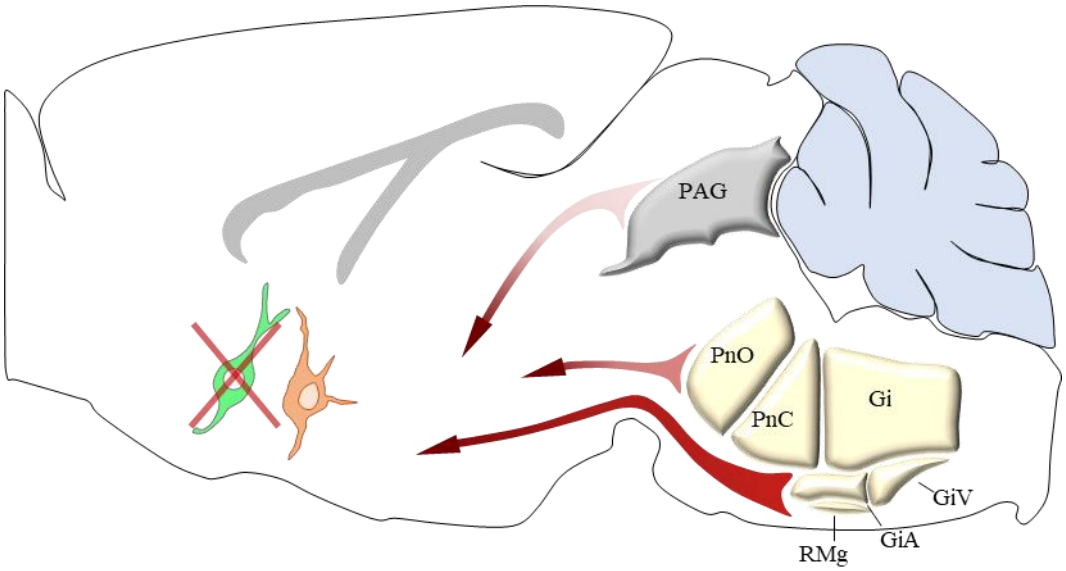

Fig. 24. *Schematic overview of glycinergic projections from the brainstem to basal forebrain cholinergic neurons but not to GnRH neurons. The most abundant input from the raphe magnus (RMg) and its neighboring nuclei (red arrow) and the lowest number of retrogradely labeled cells located in the periaqueductal gray matter (PAG; light red arrow). Modified from [338].*

In the second part of my PhD studies, we characterized the GnRH efferents and their target cells in mice and humans. First, we have studied the ultrastructure of the GnRH-IR processes identified at light microscopic level in the MBH and in the Arc. GnRH-IR processes could be identified with varying diameters (0.712±0.211 µm-1.62±0.748 µm); these processes often established synaptic specializations with axon terminals, as well as somata and dendritic processes. Thus, some of these processes clearly function in a post-synaptic arrangement, while others fulfill a pre-synaptic position in the neuronal connections established. The KP neurons play an important role in the regulation of GnRH neurons in both mice and human. We investigated the KP-KP interactions at ultrastructural level in the mouse RP3V and Arc and in the human INF. In mice, we found axo-somatic synapses between KP neurons in both regions. These interactions seem to be phylogenetically conserved, since studies support their existence in rats [309], sheep

[226], and also in humans. Our observations revealed axo-somatic and axo-dendritic synapses, as well as axo-axonic connections between KP neurons. Our findings indicate that the operation of the KP neurons could be highly synchronized also in humans. The neurotransmitters/neuromodulators used by these connections might show certain species-difference, e.g. Dyn immunoreactivity in the human KP neurons is fairly low. However, the full repertoire of neurotransmitters and receptors used for communication between KP neurons in mice and human remain to be elucidated. Besides forming the final common pathway in the neuroendocrine regulation of reproduction by releasing GnRH into the hypothalamo-hypophyseal circulation, GnRH neurons innervate hypothalamic areas including the RP3V and Arc nucleus. In my Ph.D. work, we examined putative synaptic targets of the GnRH neurons in the RP3V and Arc. We demonstrated for the first time synaptic contacts between GnRH and KP- or TH-IR neurons by electron microscopy (see for summary diagram in **Fig. 25.**). Furthermore, we also investigated a potential effect of circadian stages and and lactation on the GnRH afferents to KP- and TH-IR neurons. Using triple labeling immunohistochemistry, we quantified the GnRH appositions on the KP-, TH- and KP/TH neurons at different circadian time points, during lactation and in lactating animals following pup-removal in both areas. KP and TH co-localization levels were influenced significantly by the altered hormonal conditions. We observed a reduced ratio of TH-IR neurons that were also immunoreactive for KP in the POA in lactating mothers. However, the circadian and hormonal changes did not influence the interaction between GnRH neurons and KP or TH-IR neurons at the studied intercellular connection, time points and subcellular levels. Taken together, the number of appositions were maintained. We note that that plastic changes may still be present at other post partum time points and/or at ultrastructural and/or molecular levels. It is possible, that there is a change in the synaptic strength or composition of neurotransmitters and/or neuropeptides used in the communications.

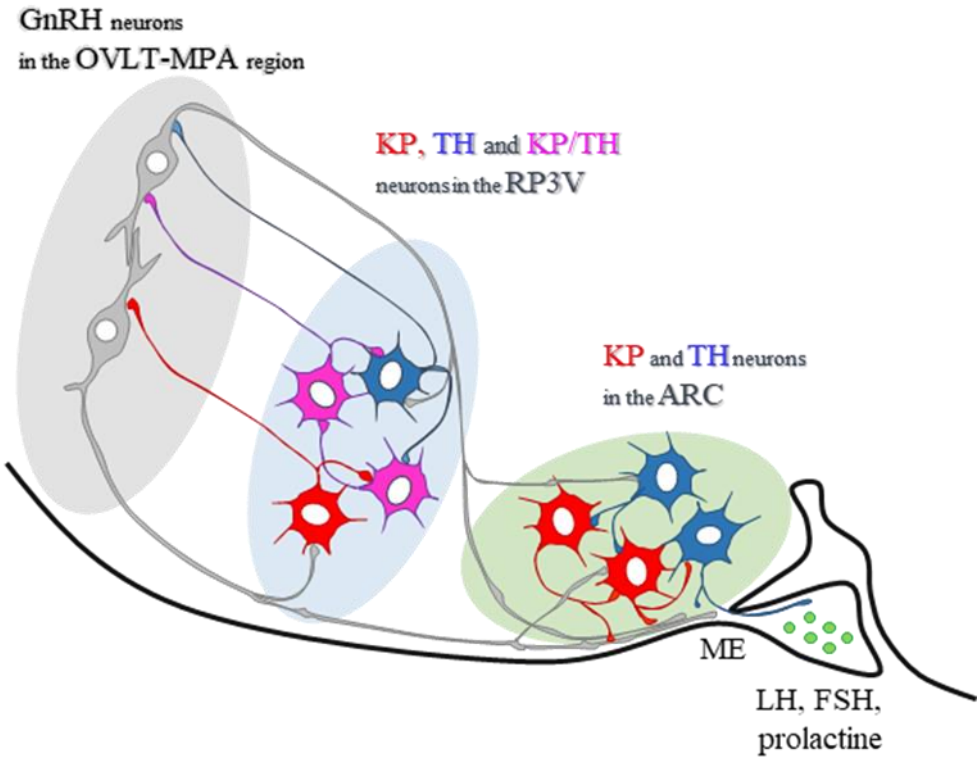

Fig. 25. *Summary scheme illustrating neuronal interactions between GnRH and KP- and TH-IR neurons in mice. In the mouse preoptic area, about two-thirds of TH-IR neurons are also immunoreactive for KP. One-third of them, similarly to the Arc TH-IR, are distinct from KP-IR neurons. Axonal branches of GnRH processes establish synaptic connections with the KP- and TH-IR cell populations in both the preoptic area and arcuate nucleus. Modified from [247].*

7. Summary

We identified the putative targets of the glycinergic projection in the BF. One of the possible cellular targets was the GnRH neuronal population. Using light- and electron microscopic studies, we have shown that GLYT1-IR astrocytes are present in the vicinity of the GnRH neurons. However, we failed to find convincing evidence for the GlyR subunit transcripts that may be translated to functional proteins in GnRH neurons. Furthermore, no synaptic connections could be detected between GLYT2-IR axon terminals and GnRH neurons and we did not record membrane potential changes *in vitro* in response to bath-application of glycine. Thus, we can conclude that glycine is unlikely to influence directly the function of GnRH neurons in mice, at least in the proestrus phase of the estrous cycle. The other putative target of the glycinergic fibers was the cholinergic neuron in the BF. Our observations that the BF cholinergic neurons (1) contain GlyR subunits; (2) are in connection with a rich network of glycinergic axons; (3) symmetric glycinergic synapses are established; (4) show bicuculline-resistant, strychnine-sensitive postsynaptic events; (5) furthermore, GLYT1 are present in the vicinity of the cholinergic neurons, strongly support our hypothesis [338]. In summary, these results also indicate a general inhibitory role for glycine in the regulation of BF cholinergic functions and a tight control of extracellular glycine concentrations in the BF. KP neurons are the main afferent regulators of GnRH neurons. We tested whether connections exist between KP neurons in the human INF. Similarly to the mouse RP3V and Arc, synaptic contacts between KP neurons were observed in the human INF [339]. These findings suggest that these contacts are phylogenetically conserved and the activity of KP neurons could be synchronized also in humans. Besides the projection to the ME, GnRH-IR varicosities and axon terminals could be observed in other hypothalamic areas i.e. RP3V and Arc, which contain the KP and TH neurons. Synaptic connections were demonstrated between GnRH to KP or TH neurons in both regions. The presence of the projections in the opposite direction may supplement the ultrashort feedback onto GnRH neurons with indirect autoregulatory mechanisms established through the RP3V and Arc KP and TH neurons. Furthermore, we have revealed that hormonal changes (in different circadian timepoints, in lactation and in lactating mice following pup-removal) did not influence the number of contacts between GnRH and KP and TH neurons [247].

8. Összefoglalás

PhD tanulmányaim során a glicin lehetséges célsejtjeit tártuk fel a bazális előagyban. Az egyik célsejt-populácó, a GnRH sejtek voltak. Fény- és elektronmikroszkópos vizsgálatokkal kimutattuk, hogy a GLYT1-IR asztrociták jelen vannak a GnRH sejtek közelében, azonban nem sikerült egyértelműen kimutatni, hogy GlyR alegység transzkriptumok átíródnak-e a GnRH sejtekben. Továbbá szinaptikus kapcsolatokat sem sikerült találni a GLYT2-IR axon terminálisok és a GnRH idegsejtek között és az elektrofiziológiai mérések során nem lehetett direkt glicin hatást kimutatni a GnRH sejtekben. Összességében tehát a GnRH idegsejtek direkt glicinerg beidegzésére nem találtunk meggyőző bizonyítékot, legalábbis nem az ösztrusz ciklus proösztrus fázisában. A glicinerg rostok másik célpontja a bazális előagyi kolinerg sejtek voltak. Megfigyeléseink szerint, hogy (1) a kolinerg idegsejtek tartalmazzák GlyR alegységeket; (2) bőséges glicinerg rost található a kolinerg idegsejtek közelében; (3) szinapszisok detektálhatók a GLYT2-IR axon terminálisok és kolinerg sejtek között; (4) a kolinerg idegsejtek sztrichnin szenzitív és bicuculline rezisztens áramokat mutattak; (5) a GLYT1-IR asztrocita nyúlványok a kolinerg sejtek közelében kimutathatóak, feltételezésünk alátámasztást nyert [338]. Összességében tehát a glicin egy általános gátló szerepet tölt be a bazális előagyi kolinerg idegsejtek működésében, illetve a glicin koncentrációja az extracelluláris térben nagy valószínűséggel szigorúan szabályozott folyamat. A GnRH sejtek működésének fő afferens szabályozói a KP sejtek. Kimutattuk, hogy a KP sejtek szinaptizálnak egymással az emberi INF mag területén, hasonlóan az egér RP3V és Arc régiójában [339]. Ezen eredmények azt sugallják, hogy a KP sejtek egymás közötti kapcsolata filogenetikailag megőrzött és működésük szinkronizált. A GnRH sejtek fő vetítési területe az eminentia mediana, azonban varikozitásokat és axon terminálisokat figyelhetünk meg más hipotalamikus régiókban is, úgy mint a RP3V és Arc területén, ahol a KP és TH sejtek is megtalálhatóak. A GnRH axon terminálisok és KP vagy TH sejtek között szinaptikus kapcsolatokat mutattunk ki, mindkét régióban. Mindez egy ultrashort feedback rendszer jelenlétére utal, mellyel a GnRH sejtek afferenseiken (KP, TH sejtek) keresztül befolyásolhatják saját működésüket. Továbbá kimutattuk, hogy ezen kapcsolatrendszerek nem mutatnak plaszticitást különböző hormonális változásokra (eltérő circadián időpontokban, szoptatás és szoptató, de kölyök-elvont körülmények között) [247].

9. References

1. Zaborszky L, van den Pol A, Gyengesi E, The Basal Forebrain Cholinergic Projection System in Mice, in The Mouse Nervous System. 2012. p. 684-718.

2. Unal CT, Pare D, Zaborszky L. (2015) Impact of basal forebrain cholinergic inputs on basolateral amygdala neurons. J Neurosci. 35(2): 853-863.

3. Blanco-Centurion C, Gerashchenko D, Shiromani PJ. (2007) Effects of saporin-induced lesions of three arousal populations on daily levels of sleep and wake. J Neurosci. 27(51): 14041-14048.

4. Conner JM, Culberson A, Packowski C, Chiba AA, Tuszynski MH. (2003) Lesions of the Basal forebrain cholinergic system impair task acquisition and abolish cortical plasticity associated with motor skill learning. Neuron. 38(5): 819-829.

5. Détári L. (2000) Tonic and phasic influence of basal forebrain unit activity on the cortical EEG. Behavioural Brain Research. 115(2): 159-170.

6. Goard M, Dan Y. (2009) Basal forebrain activation enhances cortical coding of natural scenes. Nat Neurosci. 12(11): 1444-1449.

7. Jones BE. (2008) Modulation of cortical activation and behavioral arousal by cholinergic and orexinergic systems. Ann N Y Acad Sci. 1129: 26-34.

8. Kaur S, Junek A, Black MA, Semba K. (2008) Effects of ibotenate and 192IgG-saporin lesions of the nucleus basalis magnocellularis/substantia innominata on spontaneous sleep and wake states and on recovery sleep after sleep deprivation in rats. J Neurosci. 28(2): 491-504.

9. Lin SC, Nicolelis MA. (2008) Neuronal ensemble bursting in the basal forebrain encodes salience irrespective of valence. Neuron. 59(1): 138-149.

10. Parikh V, Sarter M. (2008) Cholinergic mediation of attention: contributions of phasic and tonic increases in prefrontal cholinergic activity. Ann N Y Acad Sci. 1129: 225-235.

11. Weinberger NM. (2007) Associative representational plasticity in the auditory cortex: a synthesis of two disciplines. Learn Mem. 14(1-2): 1-16.

12. Constantin S. (2011) Physiology of the gonadotrophin-releasing hormone (GnRH) neurone: studies from embryonic GnRH neurones. J Neuroendocrinol. 23(6): 542-553.

13. Allaway KC, Machold R. (2017) Developmental specification of forebrain cholinergic neurons. Dev Biol. 421(1): 1-7.

14. Nauta WJH, Kuypers HGJM, Some ascending pathways in the brain stem reticular formation. Reticular formation of the brain. 1957, Boston: Little, Brown and Co.

15. Bardóczi Z, Watanabe M, Zaborszky L, Liposits Z, Kalló I, Morphological evidence for direct glycinergic input to cholinergic neurons in the mouse basal forebrain, in 43rd annual meeting of the Society for Neuroscience,San Diego, CA. 2013, Society for Neuroscience, 2013. Online. : San Diego, CA.

16. Vastagh C, Rodolosse A, Solymosi N, Liposits Z. (2016) Altered Expression of Genes Encoding Neurotransmitter Receptors in GnRH Neurons of Proestrous Mice. Front Cell Neurosci. 10: 230.

17. Seminara SB, Messager S, Chatzidaki EE, Thresher RR, Acierno JS, Shagoury JK, Bo-Abbas Y, Kuohung W, Schwinof KM, Hendrick AG, Zahn D, Dixon J, Kaiser UB, Slaugenhaupt SA, Gusella JF, O'Rahilly S, Carlton MBL, Crowley WF, Aparicio SAJR, Colledge WH. (2004) The GPR54 Gene as a Regulator of Puberty. Obstetrical & Gynecological Survey. 59(5): 351-353.

18. Arvidsson U, Riedl M, Elde R, Meister B. (1997) Vesicular acetylcholine transporter (VAChT) protein: A novel and unique marker for cholinergic neurons in the central and peripheral nervous systems. Journal of Comparative Neurology. 378(4): 454-467.

19. Lauterborn JC, Isackson PJ, Montalvo R, Gall CM. (1993) In situ hybridization localization of choline acetyltransferase mRNA in adult rat brain and spinal cord. Molecular Brain Research. 17: 59-69.

20. Woolf NJ. (1991) Cholinergic systems in mammalian brain and spinal cord. Progress in Neurobiology. 37: 475-524.

21. Mesulam MM, Mufson EJ, Wainer BH, Levey AI. (1983) Central cholinergic pathways in the rat: an overview based on an alternative nomenclature (Ch1-Ch6). Neuroscience. 10(4): 1185-1201.

22. Hernandes MS, de Magalhaes L, Troncone LR. (2007) Glycine stimulates the release of labeled acetylcholine but not dopamine nor glutamate from superfused rat striatal tissue. Brain Res. 1168: 32-37.

23. Sakurai T, Nagata R, Yamanaka A, Kawamura H, Tsujino N, Muraki Y, Kageyama H, Kunita S, Takahashi S, Goto K, Koyama Y, Shioda S, Yanagisawa M. (2005) Input of orexin/hypocretin neurons revealed by a genetically encoded tracer in mice. Neuron. 46(2): 297-308.

24. Dani JA, Bertrand D. (2007) Nicotinic acetylcholine receptors and nicotinic cholinergic mechanisms of the central nervous system. Annu Rev Pharmacol Toxicol. 47: 699-729.

25. Descarries L, Gisiger V, Steriade M. (1997) Diffuse transmission by acetylcholine in the CNS. Progress in Neurobiology. 53(5): 603-625.

26. Sarter M, Lustig C, Howe WM, Gritton H, Berry AS. (2014) Deterministic functions of cortical acetylcholine. Eur J Neurosci. 39(11): 1912-1920.

27. Munoz W, Rudy B. (2014) Spatiotemporal specificity in cholinergic control of neocortical function. Curr Opin Neurobiol. 26: 149-160.

28. Sarter M, Kim Y. (2015) Interpreting chemical neurotransmission in vivo: techniques, time scales, and theories. ACS Chem Neurosci. 6(1): 8-10.

29. Unal CT, Golowasch JP, Zaborszky L. (2012) Adult mouse basal forebrain harbors two distinct cholinergic populations defined by their electrophysiology. Front Behav Neurosci. 6: 21.

30. Picciotto MR, Higley MJ, Mineur YS. (2012) Acetylcholine as a neuromodulator: cholinergic signaling shapes nervous system function and behavior. Neuron. 76(1): 116-129.

31. Zaborszky L, Duque A. (2003) Sleep-wake mechanisms and basal forebrain circuitry. Front Biosci. 8: d1146-1169.

32. Buzsaki G, Bickford RG, Ponomareff G, Thal LJ, Mandel R, Gage FH. (1988) Nucleus basalis and thalamic control of neocortical activity in the freely moving rat. J Neurosci. 8(11): 4007-4026.

33. Datta S, Maclean RR. (2007) Neurobiological mechanisms for the regulation of mammalian sleep-wake behavior: reinterpretation of historical evidence and inclusion of contemporary cellular and molecular evidence. Neurosci Biobehav Rev. 31(5): 775-824.

34. Fuller P, Sherman D, Pedersen NP, Saper CB, Lu J. (2011) Reassessment of the structural basis of the ascending arousal system. Journal of Comparative Neurology. 519(5): 933-956.

35. Luppi PH, Clement O, Valencia Garcia S, Brischoux F, Fort P. (2013) New aspects in the pathophysiology of rapid eye movement sleep behavior disorder: the potential role of glutamate, gamma-aminobutyric acid, and glycine. Sleep Med. 14(8): 714-718.

36. Saper CB, Cano G, Scammell TE. (2005) Homeostatic, circadian, and emotional regulation of sleep. J Comp Neurol. 493(1): 92-98.

37. Steriade M, Timofeev I. (2002) Generators of ictal and interictal electroencephalograms associated with infantile spasms: intracellular studies of cortical and thalamic neurons. Int Rev Neurobiol. 49: 77-98.

38. Sutcliffe JG, de Lecea L. (2002) The hypocretins: setting the arousal threshold. Nat Rev Neurosci. 3(5): 339-349.

39. Moruzzi G, Magoun HW. (1949) Brain stem reticular formation and activation of the EEG. Electroencephalogr Clin Neurophysiol. 1(4): 455-473.

40. Strecker RE, Morairty S, Thakkar MM, Porkka-Heiskanen T, Basheer R, Dauphin LJ, Rainnie DG, Portas CM, Greene RW, McCarley RW. (2000) Adenosinergic modulation of basal forebrain and preoptic/anterior hypothalamic neuronal activity in the control of behavioral state. Behavioural Brain Research. 115(2): 183-204.

41. Aston-Jones G, Bloom FE. (1981) Activity of norepinephrine-containing locus coeruleus neurons in behaving rats anticipates fluctuations in the sleep-waking cycle. The Journal of neuroscience : the official journal of the Society for Neuroscience. 1(8): 876-886.

42. Fornal C, Auerbach S, Jacobs BL. (1985) Activity of serotonin-containing neurons in nucleus raphe magnus in freely moving cats. Experimental Neurology. 88(3): 590-608.

43. Steininger TL, Gong H, Szymusiak R, McGinty D. (1999) Sleep – waking discharge of neurons in the posterior lateral hypothalamus of the albino rat. Brain Research. 840: 138-147.

44. Estabrooke IV, McCarthy MT, Ko E, Chou TC, Chemelli RM, Yanagisawa M, Saper CB, Scammell TE. (2001) Fos Expression in Orexin Neurons Varies with Behavioral State. Journal of Neuroscience. 21(5): 1656-1662.

45. Lee MG. (2005) Discharge of Identified Orexin/Hypocretin Neurons across the Sleep-Waking Cycle. Journal of Neuroscience. 25(28): 6716-6720.

46. Mileykovskiy BY, Kiyashchenko LI, Siegel JM. (2005) Behavioral correlates of activity in identified hypocretin/orexin neurons. Neuron. 46(5): 787-798.

47. Verret L, Goutagny R, Fort P, Cagnon L, Salvert D, Léger L, Boissard R, Salin P, Peyron C, Luppi P-h. (2003) Central Regulation of Paradoxical Sleep. 10: 1-10.

48. Lee MG. (2005) Cholinergic Basal Forebrain Neurons Burst with Theta during Waking and Paradoxical Sleep. Journal of Neuroscience. 25(17): 4365-4369.

49. Sherin JE, Shiromani PJ, McCarley RW, Saper CB. (1996) Activation of ventrolateral preoptic neurons during sleep. Science. 271(5246): 216-219.

50. Gaus SE, Strecker RE, Tate BA, Parker RA, Saper CB. (2002) Ventrolateral preoptic nucleus contains sleep-active, galaninergic neurons in multiple mammalian species. Neuroscience. 115(1): 285-294.

51. Sherin JE, Elmquist JK, Torrealba F, Saper CB. (1998) Innervation of histaminergic tuberomammillary neurons by GABAergic and galaninergic neurons in the ventrolateral preoptic nucleus of the rat. Journal of neuroscience. 18(12): 4705-4721.

52. Szymusiak R, Alam N, Steininger TL, McGinty D. (1998) Sleep-waking discharge patterns of ventrolateral preoptic/anterior hypothalamic neurons in rats. Brain Res. 803(1-2): 178-188.

53. Lu J, Bjorkum Aa, Xu M, Gaus SE, Shiromani PJ, Saper CB. (2002) Selective activation of the extended ventrolateral preoptic nucleus during rapid eye movement sleep. The Journal of neuroscience : the official journal of the Society for Neuroscience. 22(11): 4568-4576.

54. John J, Wu MF, Boehmer LN, Siegel JM. (2004) Cataplexy-active neurons in the hypothalamus: Implications for the role of histamine in sleep and waking behavior. Neuron. 42(4): 619-634.

55. Ko EM, Estabrooke IV, McCarthy M, Scammell TE. (2003) Wake-related activity of tuberomammillary neurons in rats. Brain Research. 992(2): 220-226.

56. Bentley P, Driver J, Dolan RJ. (2011) Cholinergic modulation of cognition: Insights from human pharmacological functional neuroimaging. Progress in Neurobiology. 94(4): 360-388.

57. Klinkenberg I, Sambeth A, Blokland A. (2011) Acetylcholine and attention. Behav Brain Res. 221(2): 430-442.

58. Détári L, Rasmusson DD, Semba K. (1999) The role of basal forebrain neurons in tonic and phasic activation of the cerebral cortex. Progress in Neurobiology. 58: 249-277.

59. Metherate R, Cox CL, Ashe JH. (1992) Cellular bases of neocortical activation: modulation of neural oscillations by the nucleus basalis and endogenous acetylcholine. The Journal of neuroscience : the official journal of the Society for Neuroscience. 12(12): 4701-4711.

60. Platt B, Riedel G. (2011) The cholinergic system, EEG and sleep. Behav Brain Res. 221(2): 499-504.

61. Gu Z, Lamb PW, Yakel JL. (2012) Cholinergic coordination of presynaptic and postsynaptic activity induces timing-dependent hippocampal synaptic plasticity. J Neurosci. 32(36): 12337-12348.

62. Hasselmo ME. (2006) The role of acetylcholine in learning and memory. Curr Opin Neurobiol. 16(6): 710-715.

63. Deurveilher S, Semba K. (2011) Basal forebrain regulation of cortical activity and sleep-wake states: Roles of cholinergic and non-cholinergic neurons. Sleep and Biological Rhythms. 9: 65-70.

64. Lin JS, Anaclet C, Sergeeva OA, Haas HL. (2011) The waking brain: an update. Cell Mol Life Sci. 68(15): 2499-2512.

65. Everitt BJ, Robbins TW. (1997) Central Cholinergic Systems. Annu. Rev. Psychol. 48: 649-684.

66. Gritti I, Mainville L, Jones BE. (1993) Codistribution of GABA- with acetylcholine-synthesizing neurons in the basal forebrain of the rat. Journal of Comparative Neurology. 329(4): 438-457.

67. Rye DB, Wainer BH, Mesulam MM, Mufson EJ, Saper CB. (1984) Cortical projections arising from the basal forebrain: a study\nof cholinergic and noncholinergic components employing\ncombined retrograde tracing and immunohistochemical\nlocalization of choline acetyltransferase. Neuroscience. 13(3): 627-643.

68. Starzl TE, Taylor CW, Magoun HW. (1951) Ascending conduction in reticular activating system, with special reference to the diencephalon. J Neurophysiol. 14(6): 461-477.

69. Krnjević K, Schwartz S. (1967) The action of gamma-aminobutyric acid on cortical neurones. Experimental brain research. 3(4): 320-336.

70. McCormick DA, Prince DA. (1986) Mechanisms of action of acetylcholine in the guinea-pig cerebral cortex in vitro. The Journal of Physiology. 375(1): 169-194.

71. McCormick DA. (1992) Neurotransmitter actions in the thalamus and cerebral cortex. Journal of Clinical Neurophysiology. 9(2): 212-223.

72. Celesia GG, Jasper HH. (1966) Acetylcholine released from cerebral cortex in relation to state of activation. Neurology. 16(11): 1053-1063.

73. Jasper HH, Tessier J. (1971) Acetylcholine liberation from cerebral cortex during paradoxical (REM) sleep. Science. 172(3983): 601-602.

74. Jones BE, Activity, modulation and role of basal forebrain cholinergic neurons innervating the cerebral cortex, in Acetylcholine in the Cerebral Cortex. 2004, Elsevier Science. p. 157-169.

75. Marrosu F, Portas C, Mascia MS, Casu MA, Fà M, Giagheddu M, Imperato A, Gessa GL. (1995) Microdialysis measurement of cortical and hippocampal acetylcholine release during sleep-wake cycle in freely moving cats. Brain Research. 671(2): 329-332.

76. Xu M. (2015) Basal forebrain circuit for brain state control. Society for Neuroscience Abstracts. 18(11): Program No. 642.606-Program No. 642.606.

77. Anaclet C, Pedersen NP, Ferrari LL, Venner A, Bass CE, Arrigoni E, Fuller PM. (2015) Basal forebrain control of wakefulness and cortical rhythms. Nat Commun. 6: 8744.

78. Bloem B, Schoppink L, Rotaru DC, Faiz A, Hendriks P, Mansvelder HD, van de Berg WD, Wouterlood FG. (2014) Topographic mapping between basal forebrain cholinergic neurons and the medial prefrontal cortex in mice. J Neurosci. 34(49): 16234-16246.

79. Chandler DJ, Lamperski CS, Waterhouse BD. (2013) Identification and distribution of projections from monoaminergic and cholinergic nuclei to functionally differentiated subregions of prefrontal cortex. Brain Res. 1522: 38-58.

80. Chandler D, Waterhouse BD. (2012) Evidence for broad versus segregated projections from cholinergic and noradrenergic nuclei to functionally and anatomically discrete subregions of prefrontal cortex. Front Behav Neurosci. 6: 20.

81. Katsuki F, Qi XL, Meyer T, Kostelic PM, Salinas E, Constantinidis C. (2014) Differences in intrinsic functional organization between dorsolateral prefrontal and posterior parietal cortex. Cereb Cortex. 24(9): 2334-2349.

82. Sarter M, Lustig C, Blakely RD, Koshy Cherian A. (2016) Cholinergic genetics of visual attention: Human and mouse choline transporter capacity variants influence distractibility. J Physiol Paris. 110(1-2): 10-18.

83. Howe WM, Berry AS, Francois J, Gilmour G, Carp JM, Tricklebank M, Lustig C, Sarter M. (2013) Prefrontal cholinergic mechanisms instigating shifts from monitoring for cues to cue-guided performance: converging electrochemical and fMRI evidence from rats and humans. J Neurosci. 33(20): 8742-8752.

84. Parikh V, Kozak R, Martinez V, Sarter M. (2007) Prefrontal acetylcholine release controls cue detection on multiple timescales. Neuron. 56(1): 141-154.

85. Cohen MR, Maunsell JH. (2009) Attention improves performance primarily by reducing interneuronal correlations. Nat Neurosci. 12(12): 1594-1600.

86. Mitchell JF, Sundberg KA, Reynolds JH. (2009) Spatial attention decorrelates intrinsic activity fluctuations in macaque area V4. Neuron. 63(6): 879-888.

87. Mitsushima D, Sano A, Takahashi T. (2013) A cholinergic trigger drives learning-induced plasticity at hippocampal synapses. Nat Commun. 4: 2760.

88. Roland JJ, Stewart AL, Janke KL, Gielow MR, Kostek JA, Savage LM, Servatius RJ, Pang KC. (2014) Medial septum-diagonal band of Broca (MSDB) GABAergic regulation of hippocampal acetylcholine efflux is dependent on cognitive demands. J Neurosci. 34(2): 506-514.

89. Stanley EM, Wilson MA, Fadel JR. (2013) Object Recognition in Rats. 511(1): 38-42.

90. Hasselmo ME, Stern CE. (2014) Theta rhythm and the encoding and retrieval of space and time. Neuroimage. 85 Pt 2: 656-666.

91. Backus AR, Schoffelen JM, Szebenyi S, Hanslmayr S, Doeller CF. (2016) Hippocampal-Prefrontal Theta Oscillations Support Memory Integration. Curr Biol. 26(4): 450-457.

92. Brazhnik E, Muller RU, Fox SE. (2003) Muscarinic blockade slows and degrades the location-specific firing of hippocampal pyramidal cells. The Journal of neuroscience : the official journal of the Society for Neuroscience. 23(2): 611-621.

93. Lee MG, Chrobak JJ, Sik A, Wiley RG, Buzsáki G. (1994) Hippocampal theta activity following selective lesion of the septal cholinergic systeM. Neuroscience. 62(4): 1033-1047.

94. Vandecasteele M, Varga V, Berenyi A, Papp E, Bartho P, Venance L, Freund TF, Buzsaki G. (2014) Optogenetic activation of septal cholinergic neurons suppresses sharp wave ripples and enhances theta oscillations in the hippocampus. Proc Natl Acad Sci U S A. 111(37): 13535-13540.

95. Dannenberg H, Pabst M, Braganza O, Schoch S, Niediek J, Bayraktar M, Mormann F, Beck H. (2015) Synergy of direct and indirect cholinergic septo-hippocampal pathways coordinates firing in hippocampal networks. J Neurosci. 35(22): 8394-8410.

96. Janak PH, Tye KM. (2015) From circuits to behaviour in the amygdala. Nature. 517(7534): 284-292.

97. Jiang L, Kundu S, Lederman JD, Lopez-Hernandez GY, Ballinger EC, Wang S, Talmage DA, Role LW. (2016) Cholinergic Signaling Controls Conditioned Fear Behaviors and Enhances Plasticity of Cortical-Amygdala Circuits. Neuron. 90(5): 1057-1070.

98. Senut MC, Menetrey D, Lamour Y. (1989) Cholinergic and peptidergic projections from the medial septum and the nucleus of the diagonal band of broca to dorsal hippocampus, cingulate cortex and olfactory bulb: A combined wheatgerm agglutinin-apohorseradish peroxidase-gold immunohistochemical stu. Neuroscience. 30(2): 385-403.

99. Wenk H, Bigl V, Meyer U. (1980) Cholinergic projections from magnocellular nuclei of the basal forebrain to cortical areas in rats. Brain Research Reviews. 2(3): 295-316.

100. D'Souza RD, Vijayaraghavan S. (2014) Paying attention to smell: cholinergic signaling in the olfactory bulb. Front Synaptic Neurosci. 6: 21.

101. Hoffman GE, Finch CE. (1986) LHRH neurons in the female C57BL/6J mouse brain during reproductive aging: No loss up to middle age. Neurobiology of Aging. 7(1): 45-48.

102. Campbell RE, Han SK, Herbison AE. (2005) Biocytin filling of adult gonadotropin-releasing hormone neurons in situ reveals extensive, spiny, dendritic processes. Endocrinology. 146(3): 1163-1169.

103. Cottrell EC, Campbell RE, Han SK, Herbison AE. (2006) Postnatal remodeling of dendritic structure and spine density in gonadotropin-releasing hormone neurons. Endocrinology. 147(8): 3652-3661.

104. Fiala JC, Spacek J, Harris KM. (2002) Dendritic spine pathology: Cause or consequence of neurological disorders? Brain Research Reviews. 39(1): 29-54.

105. Moore AM, Prescott M, Czieselsky K, Desroziers E, Yip SH, Campbell RE, Herbison AE. (2018) Synaptic Innervation of the GnRH Neuron Distal Dendron in Female Mice. Endocrinology. 159(9): 3200-3208.

106. Fiala JC, Feinberg M, Popov V, Harris KM. (1998) Synaptogenesis via dendritic filopodia in developing hippocampal area CA1. J Neurosci. 18(21): 8900-8911.

107. Maletic-Savatic M, Malinow R, Svoboda K. (1999) Rapid dendritic morphogenesis in CA1 hippocampal dendrites induced by synaptic activity. Science. 283(5409): 1923-1927.

108. Wong WT, Wong ROL. (2001) Changing specificity of neurotransmitter regulation of rapid dendritic remodeling during synaptogenesis. Nature Neuroscience. 4(4): 351-352.

109. Silverman A-J LI, Witkin JW., The gonadortophin-releasing hormone (GnRH) neural systems: immunocytochemistry and in situ hybridization., in The Physiology of Reproduction., E. Knobil, Editor. 1994, Raven Press: New York. p. 1683-1709.

110. Witkin JW, O'Sullivan H, Ferin M. (1995) Glial Ensheathment of GnRH Neurons in Pubertal Female Rhesus Macaques. Journal of Neuroendocrinology. 7(9): 665-671.

111. Koemeter-Cox AI, Sherwood TW, Green JA, Steiner RA, Berbari NF, Yoder BK, Kauffman AS, Monsma PC, Brown A, Askwith CC, Mykytyn K. (2014) Primary cilia enhance kisspeptin receptor signaling on gonadotropin-releasing hormone neurons. Proc Natl Acad Sci U S A. 111(28): 10335-10340.

112. Goldsmith PC, Thind KK, Song T, Kim EJ, Boggant JE. (1990) Location of the Neuroendocrine Gonadotropin-Releasing Hormone Neurons in the Monkey Hypothalamus by Retrograde Tracing and Immunostaining. Journal of Neuroendocrinology. 2(2): 157-168.

113. Merchenthaler I, Setalo G, Csontos C, Petrusz P, Flerko B, Vilar AN. (1989) Combined Retrograde Tracing and Immunocytochemical Identification of Luteinizing Hormone-Releasing Hormone- and Somatostatin-Containing Neurons Projecting to the Median Eminence of the Rat*. Endocrinology. 125(6): 2812-2821.

114. Silverman aJ, Jhamandas J, Renaud LP. (1987) Localization of luteinizing hormone-releasing hormone (LHRH) neurons that project to the median eminence. The Journal of neuroscience : the official journal of the Society for Neuroscience. 7(8): 2312-2319.

115. Herde MK, Iremonger KJ, Constantin S, Herbison AE. (2013) GnRH neurons elaborate a long-range projection with shared axonal and dendritic functions. J Neurosci. 33(31): 12689-12697.

116. Liposits Z, Sétáló G, Flerkó B. (1984) Application of the Silver-Gold Intensified Chromogen To the Light and Electron Microscopic Detection of the Luteinizing Hormone-Releasing Hormone System of the Rat Brain. Neuroscience. 13(2): 513-525.

117. Kallo I, Vida B, Bardoczi Z, Szilvasy-Szabo A, Rabi F, Molnar T, Farkas I, Caraty A, Mikkelsen J, Coen CW, Hrabovszky E, Liposits Z. (2013) Gonadotropin-releasing hormone neurones innervate kisspeptin neurones in the female mouse brain. Neuroendocrinology. 98(4): 281-289.

118. King JC, Anthony ELP. (1984) LHRH neurons and their projections in humans and other mammals: Species comparisons. Peptides. 5: 195-207.

119. Hall JE, Reproductive and Hormonal Functions of the Male (and Function of the Pineal Gland), in Guyton and Hall Textbook of Medical Physiology, R. Gruliow, Editor. 2011, Saunders Elsevier: Philadelphia. p. 973-986.

120. Dalkin AC, Haisenleder DJ, Ortolano GA, Ellis TR, Marshall JC. (1989) The frequency of gonadotropin-releasing-hormone stimulation differentially regulates gonadotropin subunit messenger ribonucleic acid expression. Endocrinology. 125(2): 917-923.

121. Craig A. McArdle MSR, Gonadotropes and Gonadotropin-Releasing Hormone Signaling, in Knobil and Neill's Physiology of Reproduction, A.J.Z. Tony M. Plant, Editor. 2015, Elsevier: United States of America. p. 335-399.

122. Caligioni CS. (2009) Assessing reproductive status/stages in mice. Curr Protoc Neurosci. Appendix 4: Appendix 4I.

123. Collins J. (1982) Plasma and Pituitary Concentrations of LH , FSH , and Prolactin in Aging C57BL / 6 Mice at Various Times of the Estrous Cycle. Neurobiology of Aging. 3: 31-35.

124. Terasawa E. (1998) Cellular mechanism of pulsatile LHRH release. General and Comparative Endocrinology. 112: 283-295.

125. Christian CA, Mobley JL, Moenter SM. (2005) Diurnal and estradiol-dependent changes in gonadotropin-releasing hormone neuron firing activity. Proc Natl Acad Sci U S A. 102(43): 15682-15687.

126. Moenter SM, Caraty A, Locatelli A, Karsch FJ. (1991) Pattern of Gonadotropin-Releasing Hormone (GnRH) Secretion Leading up to Ovulation in the Ewe: Existence of a Preovulatory GnRH Surge*. Endocrinology. 129(3): 1175-1182.

127. Pau KY, Berria M, Hess DL, Spies HG. (1993) Preovulatory gonadotropin-releasing hormone surge in ovarian-intact rhesus macaques. Endocrinology. 133(4): 1650-1656.

128. Sarkar DK, Chiappa SA, Fink G, Sherwood NM. (1976) Gonadotropin-releasing hormone surge in pro-oestrous rats. Nature. 264: 461-461.

129. Carmel PW, Arak S, Ferin M. (1976) Pituitary stalk portal blood collection in rhesus monkeys: Evidence for pulsatile release of gonadotropin-releasing hormone (GnRH). Endocrinology. 99(1): 243-248.

130. Levine JE, Ramirez VD. (1980) In vivo release of luteinizing hormone-releasing hormone estimated with push-pull cannulae from the mediobasal hypothalami of ovariectomized, steroid- primed rats. Endocrinology. 107(6): 1782-1790.

131. Van Vugt DA, Diefenbach WD, Alston E, Ferin M, Van Vugt DA. (1985) Gonadotropin-releasing hormone pulses in third ventricular cerebrospinal fluid of ovariectomized rhesus monkeys: Correlation with luteinizing hormone pulses. Endocrinology. 117(4): 1550-1558.

132. Clarke IJ, Cummins JT. (1982) The temporal relationship between gonadotropin releasing hormone (GnRH) and luteinizing hormone (LH) secretion in ovariectomized ewes. Endocrinology. 111(5): 1737-1739.

133. Constantin S, Piet R, Iremonger K, Hwa Yeo S, Clarkson J, Porteous R, Herbison AE. (2012) GnRH neuron firing and response to GABA in vitro depend on acute brain slice thickness and orientation. Endocrinology. 153(8): 3758-3769.

134. Lee K, Duan W, Sneyd J, Herbison AE. (2010) Two slow calcium-activated afterhyperpolarization currents control burst firing dynamics in gonadotropin-releasing hormone neurons. J Neurosci. 30(18): 6214-6224.

135. Abe H, Terasawa E. (2005) Firing pattern and rapid modulation of activity by estrogen in primate luteinizing hormone releasing hormone-1 neurons. Endocrinology. 146(10): 4312-4320.

136. Kuehl-Kovarik MC, Pouliot WA, Halterman GL, Handa RJ, Dudek FE, Partin KM. (2002) Episodic bursting activity and response to excitatory amino acids in acutely dissociated gonadotropin-releasing hormone neurons genetically targeted with green fluorescent protein. The Journal of Neuroscience. 22(6): 2313-2322.

137. Nunemaker CS, Straume M, DeFazio RA, Moenter SM. (2003) Gonadotropin-releasing hormone neurons generate interacting rhythms in multiple time domains. Endocrinology. 144(3): 823-831.

138. Suter KJ, Wuarin J-p, Smith BN, Dudek FE, Moenter SM, Neurobiology KJS, Reproduction A. (2000) Whole-Cell Recordings from Preoptic / Hypothalamic Slices Reveal Burst Firing in Gonadotropin-Releasing Hormone Neurons Identified with Green Fluorescent Protein in Transgenic Mice *. 141(10): 3731-3736.

139. Constantin S, Iremonger KJ, Herbison AE. (2013) In vivo recordings of GnRH neuron firing reveal heterogeneity and dependence upon GABAA receptor signaling. J Neurosci. 33(22): 9394-9401.

140. Liu X, Lee K, Herbison AE. (2008) Kisspeptin excites gonadotropin-releasing hormone neurons through a phospholipase C/calcium-dependent pathway regulating multiple ion channels. Endocrinology. 149(9): 4605-4614.

141. Perez-reyes E, Perez-reyes E. (2003) Molecular Physiology of Low-Voltage-Activated T-type Calcium Channels. Physiol Rev. 83: 117-161.

142. Pielecka J, Moenter SM. (2006) Effect of steroid milieu on gonadotropin-releasing hormone-1 neuron firing pattern and luteinizing hormone levels in male mice. Biol Reprod. 74(5): 931-937.

143. Christian CA, Moenter SM. (2007) Estradiol induces diurnal shifts in GABA transmission to gonadotropin-releasing hormone neurons to provide a neural signal for ovulation. J Neurosci. 27(8): 1913-1921.

144. Christian CA, Pielecka-Fortuna J, Moenter SM. (2009) Estradiol Suppresses Glutamatergic Transmission to Gonadotropin-Releasing Hormone Neurons in a Model of Negative Feedback in Mice1. Biology of Reproduction. 80(6): 1128-1135.

145. Sun J, Chu Z, Moenter SM. (2010) Diurnal in vivo and rapid in vitro effects of estradiol on voltage-gated calcium channels in gonadotropin-releasing hormone neurons. J Neurosci. 30(11): 3912-3923.

146. Duittoz aH, Batailler M. (2000) Pulsatile GnRH secretion from primary cultures of sheep olfactory placode explants. Journal of reproduction and fertility. 120(2): 391-396.

147. Funabashi T, Daikoku S, Shinohara K, Kimura F. (2000) Pulsatile gonadotuopin-releasing hormone (GnRH) secretion is an inherent function of GnRH neurons, as revealed by the culture of medial olfactory placode obtained from embryonic rats. Neuroendocrinology. 71(2): 138-144.

148. Terasawa E, Keen KL, Mogi K, Claude P. (1999) Pulsatile release of luteinizing hormone-releasing hormone (LHRH) in cultured LHRH neurons derived from the embryonic olfactory placode of the rhesus monkey. Endocrinology. 140(3): 1432-1441.

149. Bosma MM. (1993) Ion channel properties and episodic activity in isolated immortalized gonadotropin-releasing hormone (GnRH) neurons. J. Membrane Biol. 136: 85-96.

150. De GM, Escalera L, Choi ALH, Weiner RI. (1992) Generation and synchronization of gonadotropin-releasing hormone (GnRH) pulses: Intrinsic properties of the GT1-1 GnRH neuronal cell line. Physiology. 89(March): 1852-1855.

151. Hiruma H, Uemura T, Kimura F. (1997) Neuronal synchronization and ionic mechanisms for propagation of excitation in the functional network of immortalized GT1-7 neurons: Optical imaging with a voltage-sensitive dye. Journal of Neuroendocrinology J. Neuroendocrinol. 9: 835-840.

152. Krsmanovic LZ, Stojilkovic SS, Merelli F, Dufour SM, Virmani MA, Catt KJ. (1992) Calcium signaling and episodic secretion of gonadotropin-releasing hormone in hypothalamic neurons. Proceedings of the National Academy of Sciences. 89(18): 8462-8466.

153. Nunez L, Villalobos C, Boockfor FR, Frawley LS. (2000) The relationship between pulsatile secretion and calcium dynamics in single, living gonadotropin-releasing hormone neurons. Endocrinology. 141(6): 2012-2017.

154. Sun W, Jarry H, Wuttke W, Kim K. (1997) Gonadotropin releasing hormone modulates gamma-aminobutyric acid-evoked intracellular calcium increase in immortalized hypothalamic gonadotropin releasing hormone neurons. Brain research. 747(1): 70-77.

155. Blake CA, Sawyer CH. (1974) Effects of hypothalamic deafferentation on the pulsatile rhythm in plasma concentrations of luteinizing hormone in ovariectomized rats. Endocrinology. 94(3): 730-736.

156. Halász B, Pupp L. (1965) Hormone secretion of the anterior pituitary gland after physical interruption of all nervous pathways to the hypophysiotrophic area. Endocrinology. 77(3): 553-562.

157. Krey LC, Lu KH, Butler WR, Hotchkiss J, Piva F, Knobil E. (1975) Surgical disconnection of the medial basal hypothalamus and pituitary function in the rhesus monkey. II. GH and cortisol secretion. Endocrinology. 96(5): 1088-1093.

158. Plant TM, Krey LC, Moossy J, McCormack JT, Hess DL, Knobil E. (1978) The Arcuate Nucleus and the Control of Gonadotropin and Prolactin Secretion in the Female Rhesus Monkey (Macaca mulatta)*. Endocrinology. 102(1): 52-62.

159. Ohkura S, Tsukamura H, Maeda Kii. (1991) Effects of Various Types of Hypothalamic Deafferentation on Luteinizing Hormone Pulses in Ovariectomized Rats. Journal of Neuroendocrinology. 3(5): 503-508.

160. de Roux N, Genin E, Carel JC, Matsuda F, Chaussain JL, Milgrom E. (2003) Hypogonadotropic hypogonadism due to loss of function of the KiSS1-derived peptide receptor GPR54. Proceedings of the National Academy of Sciences. 100(19): 10972-10976.

161. Li XF, Kinsey-Jones JS, Cheng Y, Knox AM, Lin Y, Petrou NA, Roseweir A, Lightman SL, Milligan SR, Millar RP, O'Byrne KT. (2009) Kisspeptin signalling in the hypothalamic arcuate nucleus regulates GnRH pulse generator frequency in the rat. PLoS One. 4(12): e8334.

162. Grachev P, Goodman RL. (2016) The GnRH Pulse Generator. AIMS Medical Science. 3: 359-385.

163. Wakabayashi Y, Nakada T, Murata K, Ohkura S, Mogi K, Navarro VM, Clifton DK, Mori Y, Tsukamura H, Maeda K, Steiner RA, Okamura H. (2010) Neurokinin B and dynorphin A in kisspeptin neurons of the arcuate nucleus participate in generation of periodic oscillation of neural activity driving pulsatile gonadotropin-releasing hormone secretion in the goat. J Neurosci. 30(8): 3124-3132.

164. Legan SJ, Karsch FJ. (1975) A Daily Signal for the LH Surge in the Rat. Endocrinology. 96(1): 57-62.

165. Norman RL, Blake CA, Sawyer CH. (1973) Estrogen-Dependent Twenty-four-Hour Periodicity in Pituitary LH Release in the Female Hamster1. Endocrinology. 93(4): 965-970.

166. Kerdelhué B, Brown S, Lenoir V, Queenan JT, Jones GS, Scholler R, Jones HW. (2002) Timing of initiation of the preovulatory luteinizing hormone surge and its relationship with the circadian cortisol rhythm in the human. Neuroendocrinology. 75(3): 158-163.

167. de la Iglesia HO, Blaustein JD, Bittman EL. (1995) The suprachiasmatic area in the female hamster projects to neurons containing estrogen receptors and GnRH. Neuroreport. 6(13): 1715-1722.

168. Van der Beek EM, Horvath TL, Wiegant VM, Van den Hurk R, Buijs RM. (1997) Evidence for a direct neuronal pathway from the suprachiasmatic nucleus to the gonadotropin-releasing hormone system: combined tracing and light and electron microscopic immunocytochemical studies. J Comp Neurol. 384(4): 569-579.

169. van der Beek EM, Wiegant VM, van der Donk HA, van den Hurk R, Buijs RM. (1993) Lesions of the Suprachiasmatic Nucleus Indicate the Presence of a Direct Vasoactive Intestinal Polypeptide-Containing Projection to Gonadotrophin-Releasing Hormone Neurons in the Female Rat. Journal of Neuroendocrinology. 5(2): 137-144.

170. Smith MJ, Jiennes L, Wise PM. (2000) Localization of the VIP2 receptor protein on GnRH neurons in the female rat. Endocrinology. 141(11): 4317-4320.

171. Christian CA, Moenter SM. (2008) Vasoactive intestinal polypeptide can excite gonadotropin-releasing hormone neurons in a manner dependent on estradiol and gated by time of day. Endocrinology. 149(6): 3130-3136.

172. Ward DR, Dear FM, Ward IA, Anderson SI, Spergel DJ, Smith PA, Ebling FJ. (2009) Innervation of gonadotropin-releasing hormone neurons by peptidergic neurons conveying circadian or energy balance information in the mouse. PLoS One. 4(4): e5322.

173. Chappell PE, Lee J, Levine JE. (2000) Stimulation of Gonadotropin-Releasing Hormone Surges by Estrogen. II. Role of Cyclic Adenosine 3',5'-Monophosphate. Endocrinology. 141(4): 1486-1492.

174. Vida B, Deli L, Hrabovszky E, Kalamatianos T, Caraty A, Coen CW, Liposits Z, Kallo I. (2010) Evidence for suprachiasmatic vasopressin neurones innervating kisspeptin neurones in the rostral periventricular area of the mouse brain: regulation by oestrogen. J Neuroendocrinol. 22(9): 1032-1039.

175. Couse JF, Yates MM, Walker VR, Korach KS. (2003) Characterization of the Hypothalamic-Pituitary-Gonadal Axis in Estrogen Receptor (ER) Null Mice Reveals Hypergonadism and Endocrine Sex Reversal in Females Lacking ERα But Not ERβ. Molecular Endocrinology. 17(6): 1039-1053.

176. Dorling AA, Todman MG, Korach KS, Herbison AE. (2003) Critical role for estrogen receptor alpha in negative feedback regulation of gonadotropin-releasing hormone mRNA expression in the female mouse. Neuroendocrinology. 78(4): 204-209.

177. Herbison AE. (1998) Multimodal Influence of Estrogen upon Gonadotropin-Releasing Hormone Neurons. Endocrine reviews. 19(3): 302-330.

178. Hewitt SC, Korach KS. (2002) Estrogen receptors: structure, mechanisms and function. Reviews in endocrine & metabolic disorders. 3(3): 193-200.

179. Lindzey J, Jayes FL, Yates MM, Couse JF, Korach KS. (2006) The bi-modal effects of estradiol on gonadotropin synthesis and secretion in female mice are dependent on estrogen receptor-alpha. J Endocrinol. 191(1): 309-317.

180. Wintermantel TM, Campbell RE, Porteous R, Bock D, Grone HJ, Todman MG, Korach KS, Greiner E, Perez CA, Schutz G, Herbison AE. (2006) Definition of estrogen receptor pathway critical for estrogen positive feedback to gonadotropin-releasing hormone neurons and fertility. Neuron. 52(2): 271-280.

181. Couse JF, Korach KS. (1999) Reproductive phenotypes in the estrogen receptor-alpha knockout mouse. Annales d'endocrinologie. 60(2): 143-148.

182. Christian CA, Glidewell-Kenney C, Jameson JL, Moenter SM. (2008) Classical estrogen receptor alpha signaling mediates negative and positive feedback on gonadotropin-releasing hormone neuron firing. Endocrinology. 149(11): 5328-5334.

183. Herbison AE, Pape JR. (2001) New evidence for estrogen receptors in gonadotropin-releasing hormone neurons. Front Neuroendocrinol. 22(4): 292-308.

184. Herbison AE. (2008) Estrogen positive feedback to gonadotropin-releasing hormone (GnRH) neurons in the rodent: the case for the rostral periventricular area of the third ventricle (RP3V). Brain Res Rev. 57(2): 277-287.

185. Flügge G, Oertel WH, Wuttke W. (1986) Evidence for Estrogen-Receptive GABAergic Neurons in the Preoptic/Anterior Hypothalamic Area of the Rat Brain. Neuroendocrinology. 43(1): 1-5.

186. Herbison AE. (1997) Estrogen regulation of GABA transmission in rat preoptic area. Brain Research Bulletin. 44(4): 321-326.

187. Eyigor O, Lin W, Jennes L. (2004) Identification of neurones in the female rat hypothalamus that express oestrogen receptor-alpha and vesicular glutamate transporter-2. Journal of Neuroendocrinology. 16(1): 26-31.

188. Ottem EN. (2004) Dual-Phenotype GABA/Glutamate Neurons in Adult Preoptic Area: Sexual Dimorphism and Function. Journal of Neuroscience. 24(37): 8097-8105.

189. Herbison AE, Theodosis DT. (1992) Localization of oestrogen receptors in preoptic neurons containing neurotensin but not tyrosine hydroxylase, cholecystokinin or luteinizing hormone-releasing hormone in the male and female rat. Neuroscience. 50(2): 283-298.

190. Adachi S, Yamada S, Takatsu Y, Matsui H, Kinoshita M, Takase K, Sugiura H, Ohtaki T, Matsumoto H, Uenoyama Y, Tsukamura H, Inoue K, Maeda K-I. (2007) Involvement of anteroventral periventricular metastin/kisspeptin neurons in estrogen positive feedback action on luteinizing hormone release in female rats. Journal of reproduction and development. 53(2): 367-378.

191. Clarkson J, d'Anglemont de Tassigny X, Moreno AS, Colledge WH, Herbison AE. (2008) Kisspeptin-GPR54 signaling is essential for preovulatory gonadotropin-releasing hormone neuron activation and the luteinizing hormone surge. J Neurosci. 28(35): 8691-8697.

192. Smith JT, Popa SM, Clifton DK, Hoffman GE, Steiner RA. (2006) Kiss1 neurons in the forebrain as central processors for generating the preovulatory luteinizing hormone surge. J Neurosci. 26(25): 6687-6694.

193. Hrabovszky E, Shughrue PJ, Merchenthaler I, Hajszan T, Carpenter CD, Liposits Z, Petersen SL. (2000) Detection of estrogen receptor-beta messenger

ribonucleic acid and 125I-estrogen binding sites in luteinizing hormone-releasing hormone neurons of the rat brain. Endocrinology. 141(9): 3506-3509.

194. Skynner MJ, Sim Ja, Herbison aE. (1999) Detection of estrogen receptor alpha and beta messenger ribonucleic acids in adult gonadotropin-releasing hormone neurons. Endocrinology. 140(11): 5195-5201.

195. Hrabovszky E, Steinhauser A, Barabas K, Shughrue PJ, Petersen SL, Merchenthaler I, Liposits Z. (2001) Estrogen receptor-beta immunoreactivity in luteinizing hormone-releasing hormone neurons of the rat brain. Endocrinology. 142(7): 3261-3264.

196. Kallo I, Butler JA, Barkovics-Kallo M, Goubillon ML, Coen CW. (2001) Oestrogen receptor beta-immunoreactivity in gonadotropin releasing hormone-expressing neurones: regulation by oestrogen. J Neuroendocrinol. 13(9): 741-748.

197. Herbison AE. (2009) Rapid actions of oestrogen on gonadotropin-releasing hormone neurons; from fantasy to physiology? J Physiol. 587(Pt 21): 5025-5030.

198. Kelly MJ, Qiu J. (2010) Estrogen signaling in hypothalamic circuits controlling reproduction. Brain Res. 1364: 44-52.

199. Moenter SM, Chu Z. (2012) Rapid nongenomic effects of oestradiol on gonadotrophin-releasing hormone neurones. J Neuroendocrinol. 24(1): 117-121.

200. Abraham IM, Han SK, Todman MG, Korach KS, Herbison AE. (2003) Estrogen receptor beta mediates rapid estrogen actions on gonadotropin-releasing hormone neurons in vivo. J Neurosci. 23(1529-2401): 5771-5777.

201. Romano N, Lee K, Abraham IM, Jasoni CL, Herbison AE. (2008) Nonclassical estrogen modulation of presynaptic GABA terminals modulates calcium dynamics in gonadotropin-releasing hormone neurons. Endocrinology. 149(11): 5335-5344.

202. Chu Z, Andrade J, Shupnik MA, Moenter SM. (2009) Differential regulation of gonadotropin-releasing hormone neuron activity and membrane properties by acutely applied estradiol: dependence on dose and estrogen receptor subtype. J Neurosci. 29(17): 5616-5627.

203. Romano N, Herbison AE. (2012) Activity-dependent modulation of gonadotrophin-releasing hormone neurone activity by acute oestradiol. J Neuroendocrinol. 24(10): 1296-1303.

204. Chan YM, Broder-Fingert S, Wong KM, Seminara SB. (2009) Kisspeptin/Gpr54-independent gonadotrophin-releasing hormone activity in Kiss1 and Gpr54 mutant mice. J Neuroendocrinol. 21(12): 1015-1023.

205. Colledge WH. (2009) Transgenic mouse models to study Gpr54/kisspeptin physiology. Peptides. 30(1): 34-41.

206. Lapatto R, Pallais JC, Zhang D, Chan YM, Mahan A, Cerrato F, Wei WL, Hoffman GE, Seminara SB. (2007) Kiss1-/-mice exhibit more variable hypogonadism than Gpr54-/-mice. Endocrinology. 148(10): 4927-4936.

207. Lehman MN, Merkley CM, Coolen LM, Goodman RL. (2010) Anatomy of the kisspeptin neural network in mammals. Brain Res. 1364: 90-102.

208. Garcia-Galiano D, Pinilla L, Tena-Sempere M. (2012) Sex steroids and the control of the Kiss1 system: developmental roles and major regulatory actions. J Neuroendocrinol. 24(1): 22-33.

209. Gottsch ML, Navarro VM, Zhao Z, Glidewell-Kenney C, Weiss J, Jameson JL, Clifton DK, Levine JE, Steiner RA. (2009) Regulation of Kiss1 and dynorphin gene expression in the murine brain by classical and nonclassical estrogen receptor pathways. J Neurosci. 29(29): 9390-9395.

210. Khan AR, Kauffman AS. (2012) The role of kisspeptin and RFamide-related peptide-3 neurones in the circadian-timed preovulatory luteinising hormone surge. J Neuroendocrinol. 24(1): 131-143.

211. Oakley AE, Clifton DK, Steiner RA. (2009) Kisspeptin signaling in the brain. Endocr Rev. 30(6): 713-743.

212. Tsukamura H, Homma T, Tomikawa J, Uenoyama Y, Maeda K. (2010) Sexual differentiation of kisspeptin neurons responsible for sex difference in gonadotropin release in rats. Ann N Y Acad Sci. 1200: 95-103.

213. Piet R, Boehm U, Herbison AE. (2013) Estrous Cycle Plasticity in the Hyperpolarization-Activated Current Ih Is Mediated by Circulating 17 -Estradiol in Preoptic Area Kisspeptin Neurons. Journal of Neuroscience. 33(26): 10828-10839.

214. Clarkson J, Herbison AE. (2006) Postnatal development of kisspeptin neurons in mouse hypothalamus; sexual dimorphism and projections to gonadotropin-releasing hormone neurons. Endocrinology. 147(12): 5817-5825.

215. Kallo I, Vida B, Deli L, Molnar CS, Hrabovszky E, Caraty A, Ciofi P, Coen CW, Liposits Z. (2012) Co-localisation of kisspeptin with galanin or neurokinin B in afferents to mouse GnRH neurones. J Neuroendocrinol. 24(3): 464-476.

216. Kinoshita M, Tsukamura H, Adachi S, Matsui H, Uenoyama Y, Iwata K, Yamada S, Inoue K, Ohtaki T, Matsumoto H, Maeda K. (2005) Involvement of central metastin in the regulation of preovulatory luteinizing hormone surge and estrous cyclicity in female rats. Endocrinology. 146(10): 4431-4436.

217. Pineda R, Garcia-Galiano D, Roseweir A, Romero M, Sanchez-Garrido MA, Ruiz-Pino F, Morgan K, Pinilla L, Millar RP, Tena-Sempere M. (2010) Critical

roles of kisspeptins in female puberty and preovulatory gonadotropin surges as revealed by a novel antagonist. Endocrinology. 151(2): 722-730.

218. Roseweir AK, Kauffman AS, Smith JT, Guerriero KA, Morgan K, Pielecka-Fortuna J, Pineda R, Gottsch ML, Tena-Sempere M, Moenter SM, Terasawa E, Clarke IJ, Steiner RA, Millar RP. (2009) Discovery of potent kisspeptin antagonists delineate physiological mechanisms of gonadotropin regulation. J Neurosci. 29(12): 3920-3929.

219. Contini M, Lin B, Kobayashi K, Okano H, Masland RH, Raviola E. (2010) Synaptic input of ON-bipolar cells onto the dopaminergic neurons of the mouse retina. J Comp Neurol. 518(11): 2035-2050.

220. Wulle I, Schnitzer J. (1989) Distribution and morphology of tyrosine hydroxylase-immunoreactive neurons in the developing mouse retina. Developmental brain research. 48(1): 59-72.

221. Zhang Y, Granholm AC, Huh K, Shan L, Diaz-Ruiz O, Malik N, Olson L, Hoffer BJ, Lupica CR, Hoffman AF, Backman CM. (2012) PTEN deletion enhances survival, neurite outgrowth and function of dopamine neuron grafts to MitoPark mice. Brain. 135(Pt 9): 2736-2749.

222. Dungan HM, Gottsch ML, Zeng H, Gragerov A, Bergmann JE, Vassilatis DK, Clifton DK, Steiner RA. (2007) The role of kisspeptin-GPR54 signaling in the tonic regulation and surge release of gonadotropin-releasing hormone/luteinizing hormone. J Neurosci. 27(44): 12088-12095.

223. Mittelman-Smith MA, Williams H, Krajewski-Hall SJ, Lai J, Ciofi P, McMullen NT, Rance NE. (2012) Arcuate kisspeptin/neurokinin B/dynorphin (KNDy) neurons mediate the estrogen suppression of gonadotropin secretion and body weight. Endocrinology. 153(6): 2800-2812.

224. Cheng G, Coolen LM, Padmanabhan V, Goodman RL, Lehman MN. (2010) The kisspeptin/neurokinin B/dynorphin (KNDy) cell population of the arcuate nucleus: sex differences and effects of prenatal testosterone in sheep. Endocrinology. 151(1): 301-311.

225. Goodman RL, Lehman MN, Smith JT, Coolen LM, de Oliveira CV, Jafarzadehshirazi MR, Pereira A, Iqbal J, Caraty A, Ciofi P, Clarke IJ. (2007) Kisspeptin neurons in the arcuate nucleus of the ewe express both dynorphin A and neurokinin B. Endocrinology. 148(12): 5752-5760.

226. Foradori CD, Amstalden M, Goodman RL, Lehman MN. (2006) Colocalisation of dynorphin a and neurokinin B immunoreactivity in the arcuate nucleus and median eminence of the sheep. J Neuroendocrinol. 18(7): 534-541.

227. Han SK, Gottsch ML, Lee KJ, Popa SM, Smith JT, Jakawich SK, Clifton DK, Steiner RA, Herbison AE. (2005) Activation of gonadotropin-releasing hormone

neurons by kisspeptin as a neuroendocrine switch for the onset of puberty. J Neurosci. 25(49): 11349-11356.

228. Herbison AE, de Tassigny X, Doran J, Colledge WH. (2010) Distribution and postnatal development of Gpr54 gene expression in mouse brain and gonadotropin-releasing hormone neurons. Endocrinology. 151(1): 312-321.

229. Irwig MS, Fraley GS, Smith JT, Acohido BV, Popa SM, Cunningham MJ, Gottsch ML, Clifton DK, Steiner RA. (2004) Kisspeptin activation of gonadotropin releasing hormone neurons and regulation of KiSS-1 mRNA in the male rat. Neuroendocrinology. 80(4): 264-272.

230. Dumalska I, Wu M, Morozova E, Liu R, van den Pol A, Alreja M. (2008) Excitatory effects of the puberty-initiating peptide kisspeptin and group I metabotropic glutamate receptor agonists differentiate two distinct subpopulations of gonadotropin-releasing hormone neurons. J Neurosci. 28(32): 8003-8013.

231. Han SY, McLennan T, Czieselsky K, Herbison AE. (2015) Selective optogenetic activation of arcuate kisspeptin neurons generates pulsatile luteinizing hormone secretion. Proc Natl Acad Sci U S A. 112(42): 13109-13114.

232. Lyons DJ, Broberger C. (2014) TIDAL WAVES: Network mechanisms in the neuroendocrine control of prolactin release. Front Neuroendocrinol. 35(4): 420-438.

233. Grattan DR. (2001) The actions of prolactin in the brain during pregnancy and lactation. Progress in Brain Research. 133: 153-171.

234. McNeilly AS. (2001) Lactational control of reproduction. Reproduction, Fertility and Development. 13(8): 583-583.

235. Goodman RL, Maltby MJ, Millar RP, Hileman SM, Nestor CC, Whited B, Tseng AS, Coolen LM, Lehman MN. (2012) Evidence that dopamine acts via kisspeptin to hold GnRH pulse frequency in check in anestrous ewes. Endocrinology. 153(12): 5918-5927.

236. Iwata K, Ikehara M, Kunimura Y, Ozawa H. (2016) Interactions between Kisspeptin Neurons and Hypothalamic Tuberoinfundibular Dopaminergic Neurons in Aged Female Rats. Acta Histochem Cytochem. 49(6): 191-196.

237. Ogawa S, Kow LM, Pfaff DW. (1992) Effects of lordosis-relevant neuropeptides on midbrain periaqueductal gray neuronal activity in vitro. Peptides. 13(5): 965-975.

238. Herde MK, Geist K, Campbell RE, Herbison AE. (2011) Gonadotropin-releasing hormone neurons extend complex highly branched dendritic trees outside the blood-brain barrier. Endocrinology. 152(10): 3832-3841.

239. Levin BE, Magnan C, Dunn-Meynell A, Le Foll C. (2011) Metabolic sensing and the brain: who, what, where, and how? Endocrinology. 152(7): 2552-2557.

240. Cone R LJ, Elmquist KJ, Cameron LJ., Neuroendocrinology, in Williams textbook of endocrinology, W.R. Kronenberg H, Editor. 2003, Saunders: Philadelphia. p. 81-176.

241. Furman M, Wade GN. (2007) Animal models in the study of nutritional infertility. Current Opinion in Endocrinology, Diabetes and Obesity. 14(6): 475-481.

242. Prevot V. (2011) GnRH neurons directly listen to the periphery. Endocrinology. 152(10): 3589-3591.

243. Johnson AK, Zardetto-Smith AM, Edwards GL, Chapter 50: Integrative mechanisms and the maintenance of cardiovascular and body fluid homeostasis: the central processing of sensory input derived from the circumventricular organs of the lamina terminalis, in Circumventricular Organs and Brain Fluid Environment - Molecular and Functional Aspects. 1992, Elsevier Science. p. 381-393.

244. McKinley MJ, Allen AM, Burns P, Colvill LM, Oldfield BJ. (1998) Interaction of circulating hormones with the brain: the roles of the subfornical organ and the organum vasculosum of the lamina terminalis. Clinical and experimental pharmacology {&} physiology. Supplement. 25(June): S61--67.

245. Ferguson AV, Bains JS. (1996) Electrophysiology of the circumventricular organs. Front Neuroendocrinol. 17(4): 440-475.

246. Sharma HC, Pampapathy G, Dhillon MK, Ridsdill-Smith JT. (2005) Detached leaf assay to screen for host plant resistance to Helicoverpa armigera. J Econ Entomol. 98(2): 568-576.

247. Bardoczi Z, Wilheim T, Skrapits K, Hrabovszky E, Racz G, Matolcsy A, Liposits Z, Sliwowska JH, Dobolyi A, Kallo I. (2018) GnRH Neurons Provide Direct Input to Hypothalamic Tyrosine Hydroxylase Immunoreactive Neurons Which Is Maintained During Lactation. Front Endocrinol (Lausanne). 9: 685.

248. Merchenthaler I, Gorcs T, Setalo G, Petrusz P, Flerko B. (1984) Gonadotropin-releasing hormone (GnRH) neurons and pathways in the rat brain. Cell Tissue Res. 237(1): 15-29.

249. Herman ME, Adams TE. (1990) Gonadotropin secretion in ovariectomized ewes: effect of passive immunization against gonadotropin-releasing hormone (GnRH) and infusion of a GnRH agonist and estradiol. Biology of reproduction. 42(2): 273-280.

250. Naylor AM, Porter DWF, Lincoln DW. (1989) Inhibitory effect of central LHRH on LH secretion in the ovariectomized ewe. Neuroendocrinology. 49(5): 531-536.

251. Bedran de Castro JC, Khorram O, McCann SM. (1985) Possible negative ultra-short loop feedback of luteinizing hormone releasing hormone (LHRH) in the ovariectomized rat. Proc Soc Exp Biol Med. 179(1): 132-135.

252. DePaolo LV KR, Carrillo AJ. (1987) In vivo and in vitro examination of an autoregulatory mechanism for luteinizing hormone-releasing hormone. Endocrinology. 120(1): 272-279.

253. Herbison AE, Hubbard JI, Sirett NE. (1984) LH-RH in picomole concentrations evokes excitation and inhibition of rat arcuate neurones in vitro. Neuroscience Letters. 46: 311-315.

254. Burchanowski BJ, Sternberger LA. (1980) Improved visualization of luteinizing hormone releasing hormone pathways by immunocytochemical staining of thick vibratome sections. Journal of Histochemistry and Cytochemistry. 28(4): 361-363.

255. Legendre P. (2001) The glycinergic inhibitory synapse. Cellular and molecular life sciences : CMLS. 58(5-6): 760-793.

256. Zafra F, Aragon C, Gimenez C. (1997) Molecular biology of glycinergic neurotransmission. Molecular neurobiology. 14(3): 117-142.

257. Zeilhofer HU, Studler B, Arabadzisz D, Schweizer C, Ahmadi S, Layh B, Bosl MR, Fritschy JM. (2005) Glycinergic neurons expressing enhanced green fluorescent protein in bacterial artificial chromosome transgenic mice. J Comp Neurol. 482(2): 123-141.

258. Gomeza J, Ohno K, Betz H. (2003) Glycine transporter isoforms in the mammalian central nervous system: structures, functions and therapeutic promises. Curr Opin Drug Discov Devel. 6(5): 675-682.

259. Eulenburg V, Armsen W, Betz H, Gomeza J. (2005) Glycine transporters: essential regulators of neurotransmission. Trends Biochem Sci. 30(6): 325-333.

260. Poyatos I, Ponce J, Aragón C, Giménez C, Zafra F. (1997) The glycine transporter GLYT2 is a reliable marker for glycine-immunoreactive neurons. Molecular Brain Research. 49(1-2): 63-70.

261. Ben-Ari Y. (2002) Excitatory actions of gaba during development: the nature of the nurture. Nat Rev Neurosci. 3(9): 728-739.

262. Sanchez JT, Gans D, Wenstrup JJ. (2008) to combinations of sounds. 28(1): 80-90.

263. Lynch JW. (2004) Molecular Structure and Function of the Glycine Receptor Chloride Channel. Physiological Reviews. 84(4): 1051-1095.

264. Johnson JW, Ascher P. (1987) Glycine potentiates the NMDA response in cultured mouse brain neurons. Nature. 325: 529-531.

265. DeFazio RA, Heger S, Ojeda SR, Moenter SM. (2002) Activation of A-type gamma-aminobutyric acid receptors excites gonadotropin-releasing hormone neurons. Mol Endocrinol. 16(12): 2872-2891.

266. Han SK, Todman MG, Herbison AE. (2004) Endogenous GABA release inhibits the firing of adult gonadotropin-releasing hormone neurons. Endocrinology. 145(2): 495-499.

267. Moenter SM, DeFazio RA. (2005) Endogenous gamma-aminobutyric acid can excite gonadotropin-releasing hormone neurons. Endocrinology. 146(12): 5374-5379.

268. Spergel DJ, Kruth U, Hanley DF, Sprengel R, Seeburg PH. (1999) GABA- and glutamate-activated channels in green fluorescent protein-tagged gonadotropin-releasing hormone neurons in transgenic mice. J Neurosci. 19(6): 2037-2050.

269. Han SK, Abraham Im Fau - Herbison AE, Herbison AE. Effect of GABA on GnRH neurons switches from depolarization to hyperpolarization at puberty in the female mouse. (0013-7227 (Print)).

270. Zhang C, Bosch MA, Ronnekleiv OK, Kelly MJ. (2009) Gamma-aminobutyric acid B receptor mediated inhibition of gonadotropin-releasing hormone neurons is suppressed by kisspeptin-G protein-coupled receptor 54 signaling. Endocrinology. 150(5): 2388-2394.

271. Watanabe M, Sakuma Y, Kato M. (2009) GABAA receptors mediate excitation in adult rat GnRH neurons. Biol Reprod. 81(2): 327-332.

272. Yin C, Ishii H, Tanaka N, Sakuma Y, Kato M. (2008) Activation of A-type gamma-amino butyric acid receptors excites gonadotrophin-releasing hormone neurones isolated from adult rats. J Neuroendocrinol. 20(5): 566-575.

273. Leonhardt S, Seong JY, Kim K, Thorun Y, Wuttke W, Jarry H. (1995) Activation of central GABAA-but not of GABAB-receptors rapidly reduces pituitary LH release and GnRH gene expression in the preoptic/anterior hypothalamic area of ovariectomized rats. Neuroendocrinology. 61(6): 655-662.

274. Herbison AE, Chapman C, Dyer RG. (1991) Role of medial preoptic GABA neurones in regulating luteinising hormone secretion in the ovariectomised rat. Experimental Brain Research. 87(2): 345-352.

275. Scott CJ, Clarke IJ. (1993) Inhibition of luteinizing hormone secretion in ovariectomized ewes during the breeding season by gamma-aminobutyric acid (GABA) is mediated by GABA-A receptors, but not GABA-B receptors. Endocrinology. 132(4): 1789-1796.

276. Constantin S, Jasoni CL, Wadas B, Herbison AE. (2010) Gamma-aminobutyric acid and glutamate differentially regulate intracellular calcium concentrations in mouse gonadotropin-releasing hormone neurons. Endocrinology. 151(1): 262-270.

277. Suter KJ. (2004) Control of firing by small (S)-alpha-amino-3-hydroxy-5-methyl-isoxazolepropionic acid-like inputs in hypothalamic gonadotropin releasing-hormone (GnRH) neurons. Neuroscience. 128(2): 443-450.

278. Zaborszky L, Heimer L, Eckenstein F, Leranth C. (1986) GABAergic input to cholinergic forebrain neurons: an ultrastructural study using retrograde tracing of HRP and double immunolabeling. J Comp Neurol. 250(3): 282-295.

279. Dudchenko P, Sarter M. (1991) GABAergic control of basal forebrain cholinergic neurons and memory. Behavioural Brain Research. 42(1): 33-41.

280. De Souza Silva MA, Dolga A, Pieri I, Marchetti L, Eisel UL, Huston JP, Dere E. (2006) Cholinergic cells in the nucleus basalis of mice express the N-methyl-D-aspartate-receptor subunit NR2C and its replacement by the NR2B subunit enhances frontal and amygdaloid acetylcholine levels. Genes Brain Behav. 5(7): 552-560.

281. Kellermayer R, Halvax L, Czako M, Shahid M, Dhillon VS, Husain SA, Sule N, Gomori E, Mammel M, Kosztolanyi G. (2005) A novel frame shift mutation in the HMG box of the SRY gene in a patient with complete 46,XY pure gonadal dysgenesis. Diagn Mol Pathol. 14(3): 159-163.

282. Molnar CS, Vida B, Sipos MT, Ciofi P, Borsay BA, Racz K, Herczeg L, Bloom SR, Ghatei MA, Dhillo WS, Liposits Z, Hrabovszky E. (2012) Morphological evidence for enhanced kisspeptin and neurokinin B signaling in the infundibular nucleus of the aging man. Endocrinology. 153(11): 5428-5439.

283. Schmolke C. (1993) Effects of mounting media on fading of toluidine blue and pyronin g staining in epoxy sections. Biotechnic and Histochemistry. 68(3): 132-136.

284. Dhillo WS, Chaudhri OB, Patterson M, Thompson EL, Murphy KG, Badman MK, McGowan BM, Amber V, Patel S, Ghatei MA, Bloom SR. (2005) Kisspeptin-54 stimulates the hypothalamic-pituitary gonadal axis in human males. J Clin Endocrinol Metab. 90(12): 6609-6615.

285. Franceschini I, Lomet D, Cateau M, Delsol G, Tillet Y, Caraty A. (2006) Kisspeptin immunoreactive cells of the ovine preoptic area and arcuate nucleus co-express estrogen receptor alpha. Neurosci Lett. 401(3): 225-230.

286. Hrabovszky E, Molnar CS, Sipos MT, Vida B, Ciofi P, Borsay BA, Sarkadi L, Herczeg L, Bloom SR, Ghatei MA, Dhillo WS, Kallo I, Liposits Z. (2011) Sexual dimorphism of kisspeptin and neurokinin B immunoreactive neurons in the infundibular nucleus of aged men and women. Front Endocrinol (Lausanne). 2: 80.

287. Hondo M, Furutani N, Yamasaki M, Watanabe M, Sakurai T. (2011) Orexin neurons receive glycinergic innervations. PLoS One. 6(9): e25076.

288. Motts SD, Slusarczyk AS, Sowick CS, Schofield BR. (2008) Distribution of cholinergic cells in guinea pig brainstem. Neuroscience. 154(1): 186-195.

289. Kallo I, Jekkel C, Hrabovszky E, Juranyi Z, Vida B, Jarasi A, Wilheim T, Harsing LG, Jr., Liposits Z. (2008) Immunohistochemical and in situ hybridization studies on glycine transporter 1 after transient ischemia in the rat forebrain. Neurochem Int. 52(4-5): 799-808.

290. Hrabovszky E, Ciofi P, Vida B, Horvath MC, Keller E, Caraty A, Bloom SR, Ghatei MA, Dhillo WS, Liposits Z, Kallo I. (2010) The kisspeptin system of the human hypothalamus: sexual dimorphism and relationship with gonadotropin-releasing hormone and neurokinin B neurons. Eur J Neurosci. 31(11): 1984-1998.

291. Hrabovszky E, Molnar CS, Borsay BA, Gergely P, Herczeg L, Liposits Z. (2013) Orexinergic input to dopaminergic neurons of the human ventral tegmental area. PLoS One. 8(12): e83029.

292. Ramaswamy S, Guerriero KA, Gibbs RB, Plant TM. (2008) Structural interactions between kisspeptin and GnRH neurons in the mediobasal hypothalamus of the male rhesus monkey (Macaca mulatta) as revealed by double immunofluorescence and confocal microscopy. Endocrinology. 149(9): 4387-4395.

293. Borsay BA, Skrapits K, Herczeg L, Ciofi P, Bloom SR, Ghatei MA, Dhillo WS, Liposits Z, Hrabovszky E. (2014) Hypophysiotropic gonadotropin-releasing hormone projections are exposed to dense plexuses of kisspeptin, neurokinin B and substance p immunoreactive fibers in the human: a study on tissues from postmenopausal women. Neuroendocrinology. 100(2-3): 141-152.

294. Chiu CQ, Lur G, Morse TM, Carnevale NT, Ellis-Davies GC, Higley MJ. (2013) Compartmentalization of GABAergic inhibition by dendritic spines. Science. 340(6133): 759-762.

295. Holstege JC, Bongers CM. (1991) A glycinergic projection from the ventromedial lower brainstem to spinal motoneurons. An ultrastructural double labeling study in rat. Brain Res. 566(1-2): 308-315.

296. Kato G, Yasaka T, Katafuchi T, Furue H, Mizuno M, Iwamoto Y, Yoshimura M. (2006) Direct GABAergic and glycinergic inhibition of the substantia gelatinosa from the rostral ventromedial medulla revealed by in vivo patch-clamp analysis in rats. J Neurosci. 26(6): 1787-1794.

297. Vetrivelan R, Fuller PM, Tong Q, Lu J. (2009) Medullary circuitry regulating rapid eye movement sleep and motor atonia. J Neurosci. 29(29): 9361-9369.

298. Scheibel MES, A.B., Structural substrates for integrative patterns in the brain stem reticular core., in Reticular formation of the brain, H.H.P. Jasper, L.D.;

Knighton,R.S.; Noshay,W.C.;Costello,R.T.;, Editor. 1958, Little, Brown: Oxford, England. p. 31-55.

299. Fournier GN, Materi Lm Fau - Semba K, Semba K Fau - Rasmusson DD, Rasmusson DD. (2004) Cortical acetylcholine release and electroencephalogram activation evoked by ionotropic glutamate receptor agonists in the rat basal forebrain. Neuroscience. 123(3): 785-792.

300. Wenk GL, Willard LB. (1998) The neural mechanisms underlying cholinergic cell death within the basal forebrain. Int J Dev Neurosci. 16(7-8): 729-735.

301. Doble A. (1999) The role of excitotoxicity in neurodegenerative disease: implications for therapy. Pharmacol Ther. 81(3): 163-221.

302. Bordji K, Becerril-Ortega J, Buisson A. (2011) Synapses, NMDA receptor activity and neuronal Abeta production in Alzheimer's disease. Rev Neurosci. 22(3): 285-294.

303. Gu Z, Cheng J, Zhong P, Qin L, Liu W, Yan Z. (2014) Aβ Selectively Impairs mGluR7 Modulation of NMDA Signaling in Basal Forebrain Cholinergic Neurons: Implication in Alzheimer's Disease. The Journal of Neuroscience. 34(41): 13614-13628.

304. Choi DW. (1992) Excitotoxic cell death. J. Neurobiol. 23(9): 1261-1276.

305. Herde MK, Herbison AE. (2015) Morphological Characterization of the Action Potential Initiation Segment in GnRH Neuron Dendrites and Axons of Male Mice. Endocrinology. 156(11): 4174-4186.

306. Cravo RM, Margatho LO, Osborne-Lawrence S, Donato J, Jr., Atkin S, Bookout AL, Rovinsky S, Frazao R, Lee CE, Gautron L, Zigman JM, Elias CF. (2011) Characterization of Kiss1 neurons using transgenic mouse models. Neuroscience. 173: 37-56.

307. Clarkson J, Herbison AE. (2011) Dual phenotype kisspeptin-dopamine neurones of the rostral periventricular area of the third ventricle project to gonadotrophin-releasing hormone neurones. J Neuroendocrinol. 23(4): 293-301.

308. Porteous R, Petersen SL, Yeo SH, Bhattarai JP, Ciofi P, D'Anglemont de Tassigny X, Colledge WH, Caraty A, Herbison AE. (2011) Kisspeptin neurons co-express met-enkephalin and galanin in the rostral periventricular region of the female mouse hypothalamus. Journal of Comparative Neurology. 519(17): 3456-3469.

309. Burke MC, Letts PA, Krajewski SJ, Rance NE. (2006) Coexpression of dynorphin and neurokinin B immunoreactivity in the rat hypothalamus: Morphologic evidence of interrelated function within the arcuate nucleus. J Comp Neurol. 498(5): 712-726.

310. de Croft S, Boehm U, Herbison AE. (2013) Neurokinin B Activates Arcuate Kisspeptin Neurons Through Multiple Tachykinin Receptors in the Male Mouse. Endocrinology. 154(8): 2750-2760.

311. Navarro VM, Gottsch Ml Fau - Wu M, Wu M Fau - Garcia-Galiano D, Garcia-Galiano D Fau - Hobbs SJ, Hobbs Sj Fau - Bosch MA, Bosch Ma Fau - Pinilla L, Pinilla L Fau - Clifton DK, Clifton Dk Fau - Dearth A, Dearth A Fau - Ronnekleiv OK, Ronnekleiv Ok Fau - Braun RE, Braun Re Fau - Palmiter RD, Palmiter Rd Fau - Tena-Sempere M, Tena-Sempere M Fau - Alreja M, Alreja M Fau - Steiner RA, Steiner RA. (2011) Regulation of NKB pathways and their roles in the control of Kiss1 neurons in the arcuate nucleus of the male mouse. Endocrinology. 152(11): 4265-4275.

312. Ruka KA, Burger Ll Fau - Moenter SM, Moenter SM. (2013) Regulation of arcuate neurons coexpressing kisspeptin, neurokinin B, and dynorphin by modulators of neurokinin 3 and kappa-opioid receptors in adult male mice. Endocrinology. 154(8): 2761-2771.

313. Navarro VM, Gottsch ML, Chavkin C, Okamura H, Clifton DK, Steiner RA. (2009) Regulation of gonadotropin-releasing hormone secretion by kisspeptin/dynorphin/neurokinin B neurons in the arcuate nucleus of the mouse. J Neurosci. 29(38): 11859-11866.

314. Ohkura S, Takase K Fau - Matsuyama S, Matsuyama S Fau - Mogi K, Mogi K Fau - Ichimaru T, Ichimaru T Fau - Wakabayashi Y, Wakabayashi Y Fau - Uenoyama Y, Uenoyama Y Fau - Mori Y, Mori Y Fau - Steiner RA, Steiner Ra Fau - Tsukamura H, Tsukamura H Fau - Maeda KI, Maeda Ki Fau - Okamura H, Okamura H. (2009) Gonadotrophin-releasing hormone pulse generator activity in the hypothalamus of the goat. J. Neuroendocrinol. 21(10): 813-821.

315. Keen KL, Wegner Fh Fau - Bloom SR, Bloom Sr Fau - Ghatei MA, Ghatei Ma Fau - Terasawa E, Terasawa E. (2008) An increase in kisspeptin-54 release occurs with the pubertal increase in luteinizing hormone-releasing hormone-1 release in the stalk-median eminence of female rhesus monkeys in vivo. Endocrinology. 149(8): 4151-4157.

316. Yip SH, Boehm U, Herbison AE, Campbell RE. (2015) Conditional Viral Tract Tracing Delineates the Projections of the Distinct Kisspeptin Neuron Populations to Gonadotropin-Releasing Hormone (GnRH) Neurons in the Mouse. Endocrinology. 156(7): 2582-2594.

317. Qiu J, Nestor CC, Zhang C, Padilla SL, Palmiter RD, Kelly MJ, Ronnekleiv OK. (2016) High-frequency stimulation-induced peptide release synchronizes arcuate kisspeptin neurons and excites GnRH neurons. Elife. 5: pii: e16246.

318. El Mestikawy S, Wallen-Mackenzie A, Fortin GM, Descarries L, Trudeau LE. (2011) From glutamate co-release to vesicular synergy: vesicular glutamate transporters. Nat Rev Neurosci. 12(4): 204-216.

319. Niciu MJ, Kelmendi B Fau - Sanacora G, Sanacora G. (2012) Overview of glutamatergic neurotransmission in the nervous system. Pharmacol Biochem Behav. 100(4): 656-664.

320. Klemann CJ, Roubos EW. (2011) The gray area between synapse structure and function-Gray's synapse types I and II revisited. Synapse. 65(11): 1222-1230.

321. Skrapits K, Borsay BA, Herczeg L, Ciofi P, Liposits Z, Hrabovszky E. (2015) Neuropeptide co-expression in hypothalamic kisspeptin neurons of laboratory animals and the human. Front Neurosci. 9: 29.

322. Hrabovszky E, Sipos Mt Fau - Molnar CS, Molnar Cs Fau - Ciofi P, Ciofi P Fau - Borsay BA, Borsay Ba Fau - Gergely P, Gergely P Fau - Herczeg L, Herczeg L Fau - Bloom SR, Bloom Sr Fau - Ghatei MA, Ghatei Ma Fau - Dhillo WS, Dhillo Ws Fau - Liposits Z, Liposits Z. (2012) Low degree of overlap between kisspeptin, neurokinin B, and dynorphin immunoreactivities in the infundibular nucleus of young male human subjects challenges the KNDy neuron concept. Endocrinology. 153(10): 4978-4989.

323. Pielecka-Fortuna J, Chu Z, Moenter SM. (2008) Kisspeptin acts directly and indirectly to increase gonadotropin-releasing hormone neuron activity and its effects are modulated by estradiol. Endocrinology. 149(4): 1979-1986.

324. Smith MA, Williams H, Krajewski SJ, McMullen NT, Rance NE, Arcuate NK3 receptor-expressing KNDy neurons are essential for estrogen modulation of LH secretion and body weight in the female rat, in Society for Neuroscience, 2011. 2011, Society for Neuroscience: Washington, DC.

325. Hrabovszky E, Turi GF, Kallo I, Liposits Z. (2004) Expression of vesicular glutamate transporter-2 in gonadotropin-releasing hormone neurons of the adult male rat. Endocrinology. 145(9): 4018-4021.

326. Wu M, Dumalska I, Morozova E, van den Pol AN, Alreja M. (2009) Gonadotropin inhibitory hormone inhibits basal forebrain vGluT2-gonadotropin-releasing hormone neurons via a direct postsynaptic mechanism. J Physiol. 587(Pt 7): 1401-1411.

327. Kauffman AS, Gottsch ML, Roa J, Byquist AC, Crown A, Clifton DK, Hoffman GE, Steiner RA, Tena-Sempere M. (2007) Sexual differentiation of Kiss1 gene expression in the brain of the rat. Endocrinology. 148(4): 1774-1783.

328. Luanne L. Peters MTH, Nira Ben-Jonathan. (1981) The Posterior Pituitary: Regulation of Anterior Pituitary Prolactin Secretion. Science. 213(August): 659-661.

329. Demaria JE, Lerant AA, Freeman ME. (1999) Prolactin activates all three populations of hypothalamic neuroendocrine dopaminergic neurons in ovariectomized rats. Brain Research. 837(1-2): 236-241.

330. Mitchell V, Loyens A, Spergel DJ, Flactif M, Poulain P, Tramu G, Beauvillain JC. (2003) A confocal microscopic study of gonadotropin-releasing hormone (GnRH) neuron inputs to dopaminergic neurons containing estrogen receptor alpha in the arcuate nucleus of GnRH-green fluorescent protein transgenic mice. Neuroendocrinology. 77(3): 198-207.

331. Berghorn KA, Le WW, Sherman TG, Hoffman GE. (2001) Suckling stimulus suppresses messenger RNA for tyrosine hydroxylase in arcuate neurons during lactation. Journal of Comparative Neurology. 438(4): 423-432.

332. Wang HJ, Hoffman GE, Smith MS. (1993) Suppressed tyrosine hydroxylase gene expression in the tuberoinfundibular dopaminergic system during lactation. Endocrinology. 133(4): 1657-1663.

333. Feher P, Olah M, Bodnar I, Hechtl D, Bacskay I, Juhasz B, Nagy GM, Vecsernyes M. (2010) Dephosphorylation/inactivation of tyrosine hydroxylase at the median eminence of the hypothalamus is required for suckling-induced prolactin and adrenocorticotrop hormone responses. Brain Res Bull. 82(1-2): 141-145.

334. Romano N, Yip SH, Hodson DJ, Guillou A, Parnaudeau S, Kirk S, Tronche F, Bonnefont X, Le Tissier P, Bunn SJ, Grattan DR, Mollard P, Martin AO. (2013) Plasticity of hypothalamic dopamine neurons during lactation results in dissociation of electrical activity and release. J Neurosci. 33(10): 4424-4433.

335. Ciofi P, Crowley WR, Pillez A, Schmued LL, Tramu G, Mazzuca M. (1993) Plasticity in Expression of Immunoreactivity for Neuropeptide Y, Enkephalins and Neurotensin in the Hypothalamic Tubero-lnfundibular Dopaminergic System during Lactation in Mice. Journal of Neuroendocrinology. 5(6): 599-602.

336. Brown RS, Herbison AE, Grattan DR. (2014) Prolactin regulation of kisspeptin neurones in the mouse brain and its role in the lactation-induced suppression of kisspeptin expression. J Neuroendocrinol. 26(12): 898-908.

337. Yamada S, Uenoyama Y, Deura C, Minabe S, Naniwa Y, Iwata K, Kawata M, Maeda KI, Tsukamura H. (2012) Oestrogen-dependent suppression of pulsatile luteinising hormone secretion and kiss1 mRNA expression in the arcuate nucleus during late lactation in rats. J Neuroendocrinol. 24(9): 1234-1242.

338. Bardoczi Z, Pal B, Koszeghy A, Wilheim T, Watanabe M, Zaborszky L, Liposits Z, Kallo I. (2017) Glycinergic Input to the Mouse Basal Forebrain Cholinergic Neurons. J Neurosci. 37(39): 9534-9549.

339. Takacs S, Bardoczi Z, Skrapits K, Gocz B, Vaczi V, Magloczky Z, Szucs I, Racz G, Matolcsy A, Dhillo WS, Watanabe M, Kadar A, Fekete C, Kallo I, Hrabovszky E. (2018) Post mortem single-cell labeling with DiI and immunoelectron microscopy unveil the fine structure of kisspeptin neurons in humans. Brain Struct Funct. 223(5): 2143-2156.

10. List of publications

10.1. List of publications underlying the thesis

1. Szabolcs Takács[1] , Zsuzsanna Bardóczi[1] , Katalin Skrapits , Balázs Göcz , Viktória Váczi , Zsófia Maglóczky , Iván Szűcs , Gergely Rácz , András Matolcsy , Waljit S Dhillo , Masahiko Watanabe , Andrea Kádár , Csaba Fekete , Imre Kalló , Erik Hrabovszky
   Post mortem single-cell labeling with DiI and immunoelectron microscopy unveil the fine structure of kisspeptin neurons in humans
   BRAIN STRUCTURE & FUNCTION 223:(5) pp. 2143-2156. (2018)
   [1] Authors have contributed equally to this work.

2. Zsuzsanna Bardóczi , Tamás Wilheim , Katalin Skrapits , Erik Hrabovszky , Gergely Rácz , András Matolcsy , Zsolt Liposits , Joanna H. Sliwowska , Árpád Dobolyi and Imre Kalló
   GnRH neurons provide direct input to hypothalamic tyrosine hydroxylase immunoreactive neurons which is maintained during lactation
   FRONTIERS IN ENDOCRINOLOGY DOI: 10.3389/fendo.2018.00685 11 p. (2018)

3. Bardóczi Z , Pál B , Kőszeghy Á , Wilheim T , Watanabe M , Záborszky L , Liposits Z , Kalló I
   Glycinergic input to the mouse basal forebrain cholinergic neurons
   JOURNAL OF NEUROSCIENCE 37:(39) pp. 9534-9549. (2017)

4. Kallo I , Vida B , Bardoczi Z , Szilvasy-Szabo A , Rabi F , Molnar T , Farkas I , Caraty A , Mikkelsen J , Coen CW , Hrabovszky E , Liposits Z
   Gonadotropin-Releasing Hormone Neurones Innervate Kisspeptin Neurones in the Female Mouse Brain.
   NEUROENDOCRINOLOGY 98:(4) pp. 281-289. (2013)

10.2. List of other publications

1. Hollo K , Ducza L , Hegyi Z , Docs K , Hegedus K , Bakk E , Papp I , Kis G , Meszar Z , Bardoczi Z , Antal M
   Interleukin-1 receptor type 1 is overexpressed in neurons but not in glial cells within the rat superficial spinal dorsal horn in complete Freund adjuvant-induced inflammatory pain.
   JOURNAL OF NEUROINFLAMMATION 14: Paper 125. (2017)

2. Jo S , Kallo I , Bardoczi Z , Arrejo e Drigo R , Zeold A , Liposits Z , Oliva A , Lemmon VP , Bixby JL , Gereben B , Bianco AC
   Neuronal Hypoxia Induces Hsp40-Mediated Nuclear Import of Type 3 Deiodinase As an Adaptive Mechanism to Reduce Cellular Metabolism
   JOURNAL OF NEUROSCIENCE 32:(25) pp. 8491-8500. (2012)

3. Kallo I , Mohacsik P , Vida B , Zeold A , Bardoczi Z , Zavacki AM , Farkas E , Kadar A , Hrabovszky E , Arrojo e Drigo R , Dong L , Barna L , Palkovits M , Borsay BA , Herczeg L , Lechan RM , Bianco AC , Liposits Z , Fekete C , Gereben B
   A Novel Pathway Regulates Thyroid Hormone Availability in Rat and Human Hypothalamic Neurosecretory Neurons
   PLOS ONE 7:(6) Paper e37860. 16 p. (2012)

11. Acknowledgements

First of all, I'm grateful to my supervisor, Dr. Imre Kalló, for the professional advices and ideas. His patient guidance enabled me to complete my Ph.D. work.

I'm very thankful to Professor Zsolt Liposits, Head of the Department of Endocrine Neurobiology for the opportunity to do my Ph.D. work in his research team.

I would like to thank Dr. Erik Hrabovszky and Dr. Imre Farkas for the collaborative studies and the helpful advices.

I am thankful to Barna László for his technical assistance during many years.

I thank to all members of the Laboratory of Endocrine Neurobiology, Reproductive Neurobiology, Integrative Neuroendocrinology and Molecular Cell Metabolism; especially to Tamás Wilheim, Dr. Csaba Vastagh, Veronika Csillag, Dr. Miklós Sárvári, Dr. Szabolcs Takács, Balázs Gergő Göcz, Viktória Váczi; Dr. Csaba Fekete, Dr. Erzsébet Farkas, Dr. Andrea Kádár, Dr. Zoltán Attila Péterfi, Dr. Edina Varga, Ágnes Simon, Dr. Balázs Gereben, Petra Mohácsik, Andrea Juhász for the advices, scientific discussions, technical supports and the joyful, friendly atmosphere. Special thanks to my friends Dr. Flóra Bálint, Dr. Katalin Skrapits, Anett Szilvásy-Szabó and Dr. Barbara Vida. I could always turn to them with my questions and problems and they helped my work.

I would like to express my heartfelt gratitude for my mother, Zsuzsanna Bardócziné Sass, and my aunt Piroska Bardóczi for their understanding and unceasing support. Last but not least, I thank my fiancé, Tibor Bűcs for his love and spiritually support throughout writing my Ph.D. thesis.

In memoriam of my father, Antal Bardóczi.